

**STUDY OF THE EFFECTS OF AGEING TEMPERATURE AND
AGEING TIME ON THE MICROSTRUCTURE AND SOME
MECHANICAL PROPERTIES OF SAND CAST AL-SI-CU AND
AL-SI-MG ALLOYS**

by

Ebenezer Donkoh, BSc. (Hons.) Materials Engineering

A Thesis submitted to the Department of Physics,

Kwame Nkrumah University of Science and Technology,

Kumasi.

in partial fulfillment of the requirements for the degree of

MASTER OF PHILOSOPHY

College of Science

October, 2016

DECLARATION

I hereby declare that this thesis is my original work towards the Master of Philosophy and that, to the best of my knowledge, has not been presented for a degree in any other University, except where due acknowledgement has been made in the text.

Ebenezer Donkoh

PG1056213

Student

.....
Signature

.....
Date

This thesis has been certified by;

1) Mr. Oswald A. Nunoo

.....

Supervisor

.....
Signature

.....
Date

2) Prof. S.K. Danuor

.....

Head of Department

.....
Signature

.....
Date

ACKNOWLEDGEMENT

My foremost thanks go to the Living God for seeing me through this work. His grace and mercies have brought me this far.

My sincere thanks go to my research supervisor, Mr. Oswald Nunoo, who offered valuable criticisms, suggestions and guidance throughout my work.

Sincere thanks go to Valco Ghana and Aluworks Ghana limited for providing me with all the raw materials like Aluminium, magnesium and silicon needed for my research, and special thanks goes to Madam Elizabeth Essilfie of the learning and development section of Valco Ghana for her undying support for me in acquiring the materials, and to Mr. Edward Arthur for performing Chemical analysis on the samples produced.

Thanks to Mr. Amoah, a technician at the physics department, for his assistance during mechanical testing of the samples; to Mr. Clifford and Uncle Ato all of the mechanical engineering department for their support during preparation of the samples.

I thank the technicians at Great Kosa foundry, Mr. Edward Kwadwo Adusei and Nana Ama Nkunim Safoah for their undying support during casting of the samples. And thanks to my friend and colleague Joseph Asare Awuah from the physics department for his support for me throughout my research.

My heartfelt thanks go to my special one Priscilla Nana Yaa Sarfowaah for her support, encouragement and care for me throughout my research work.

Thanks to all my guardians for their support for me to pursue this MPhil programme.

KNUST



TABLE OF CONTENTS

ACKNOWLEDGEMENT.....	iii
TABLE OF CONTENTS	iv
LIST OF TABLES.....	viii
LIST OF FIGURES	ix
ABSTRACT	xiv
INTRODUCTION	1
1.1 Industrial Applications of Aluminium Alloys.....	1
1.2 Aluminium Castings classification.....	2
1.3 Aluminium Castings defect.....	3
1.4 Mechanical properties	3
1.5 Aluminium alloying elements	6
1.6 Research Objectives	8
1.7 Justification of the Study.....	9
CHAPTER 2.....	10
LITERATURE REVIEW	10
2.1 Aluminium and its Alloys	10
2.2 Aluminium Casting Methods	13
2.2.1 Green sand moulding process	13

2.3 Methods of Strengthening Metals	14
2.3.1 Strengthening by alloying	14
2.3.2 Dispersion strengthening	15
2.3.3 Cold working.....	16
2.3.4 Precipitation strengthening	16
2.3.4.1 Ageing of Al-Si-Cu alloys.....	18
2.3.4.2 Ageing of Al-Si-Mg alloys.....	21
2.4 Grain Size Reduction Strengthening	22
2.5 Impact Properties of Materials	23
CHAPTER 3	24
RESEARCH METHODOLOGY	24
3.1 Sand Casting Aluminium Alloys.....	24
3.1.1 Mould design and Preparation	24
3.1.2 Casting Operation for Al-Si-Mg alloy	24
3.1.3 Casting Operation for Al-Si-Cu alloy	25
3.2 Chemical Analysis of Samples.....	28
3.3 Solution Heat Treatment	29
3.3.1 Artificial ageing of Al-Si-Cu and Al-Si-Mg alloys	30
3.4 Tensile Testing	30

3.4.1 Sample preparation	30
3.4.2 Tensile test	31
3.5 Charpy Impact Test	31
3.6 Impact Test.....	32
3.7 Microstructural Analysis	33
3.7.1 Specimen preparation.....	33
3.7.2 Microscopic examination.....	34
CHAPTER 4	35
RESULTS AND DISCUSSION.....	35
4.1 Chemical Analysis of Al-Si-Mg and Al-Si-Cu Alloys.....	35
4.2 Microstructural Evaluation.....	36
4.2.1 Microstructure evaluation of Al-Si-Mg alloys.....	36
4.2.2 Microstructural evaluation of Al-Si-Cu alloy	37
4.3 Mechanical Properties	39
4.3.1 Tensile properties of Al-14%Si-0.288Mg.....	39
4.3.2 Impact Properties of Al-14%Si-0.288Mg alloys	58
4.3.3 Tensile Properties of Al-14%Si-2.688Cu	63
4.3.4 Impact properties of Al-14%-2.688Cu alloys	78
CHAPTER 5	83

CONCLUSIONS AND RECOMMENDATION	83
5.1 CONCLUSIONS	83
5.2 RECOMMENDATIONS	84
REFERENCES	85
APPENDICES	88
Appendix A.....	88
Appendix B.....	99
Appendix C.....	101
 LIST OF TABLES	
Table 1-1 Mechanical properties of Sand and Chill cast test bars EN 1706	5
Table 2-1 Main alloying elements in the wrought alloy designation system	11
Table 2-2 Main alloying elements in the cast alloy designation systems	12
Table 2-3 Temper Designation for Heat Treatment of Aluminium Alloys	13
Table 4-1 Elemental Compositions of Sand Cast Al-Si-Mg alloy (wt. %)	35
Table 4-2 Elemental Compositions of Sand Cast Al-Si-Cu alloy (wt. %).....	35
Table 4-3 Tensile properties of Al-14%Si-0.288Mg as cast, SHT, Peaked aged at 160 °C and 170 °C respectively	50
Table 4-4 Summary of ultimate tensile strength values for Al-Si-Mg alloys	55
Table 4-5 Ultimate tensile strength values versus impact energy values of Al-Si-Mg alloys at ageing temperatures of 160°C and 170°C	60

Table 4-6 Tensile properties of as cast, SHT, Peaked aged at 155 °C and 165 °C Al-Si-Cu alloys respectively	70
Table 4-7 Summary of ultimate tensile strength values for Al-Si-Cu alloys	74
Table 4-8 Ultimate tensile strength values versus impact energy values of Al-Si-Cu alloys at 155 °C and 165 °C	79

LIST OF FIGURES

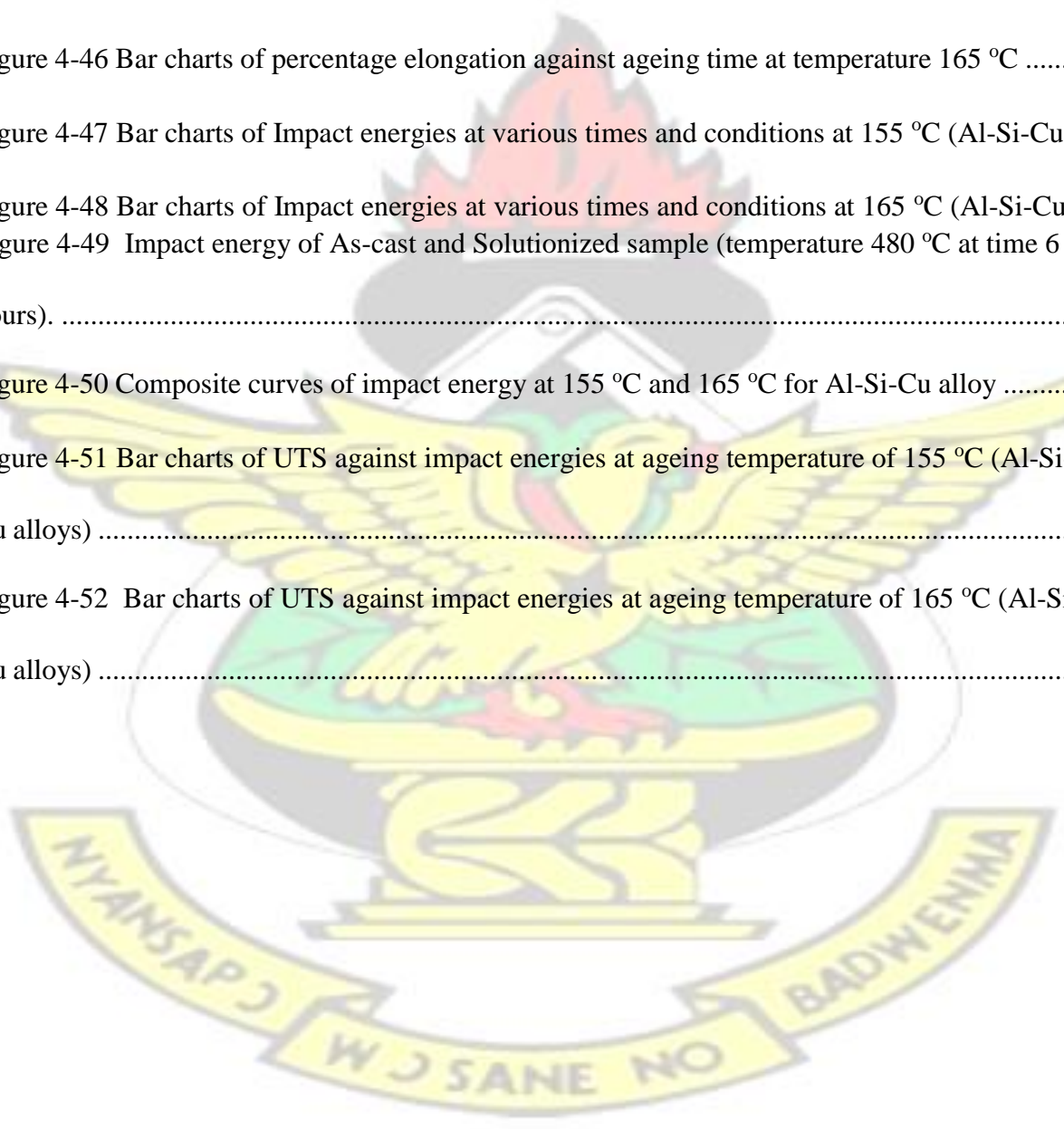
Figure 2-1 Variation of nickel content on tensile strength for copper-nickel alloy, showing strengthening (Callister and Rethwisch, 2009).	15
Figure 2-2 The aluminum rich end of the Al-Cu phase diagram showing the three steps in the age-hardening heat treatment and the microstructures that are produced (Askeland and Wright, 2009).	17
Figure 2-3 dislocations can get pass precipitates by (a) cutting (b) bowing (Ashby and Jones, 2005)	18
Figure 2-4 Correlation of structures and hardness for Al-4%Cu alloy (Callister and Rethwisch, 2009)..	20
Figure 2-5 Aluminium rich end of Al-Cu phase diagram (Bacon and Hull, 2001)....	19
Figure 2-6 Graph of Yield strength against small Mg content for a peak-aged Al-7Si-Mg alloy (Taylor, St John, Barresi, and Couper, 2000).	22
Figure 3-1 Fuel fired lift out crucible furnace used for the melting operation	26
Figure 3-2 Shows (A) Pure aluminium and (B) shows pure magnesium which 0.3g was used ...	26
Figure 3-3 Shows (C) Pure silicon used and (D) shows copper coil, 300g was used	27
Figure 3-4 Picture of (E) Moulds and (F) samples cooling in moulds after casting operation.....	27

Figure 3-5 Picture of (G) samples fresh out of mould and (H) machined samples with good finish	27
Figure 3-6 Picture of sample in quantometer to be tested	28
Figure 3-7 Picture of (A) Al-Si-Cu and (B) Al-Si-Mg discs used for the chemical analysis	29
Figure 3-8 Schematic diagram of tensile test sample	30
Figure 3-9 Picture of sample in the tensile testing machine	31
Figure 3-10 Schematic of impact test sample	32
Figure 3-11 Picture of (a) The Impact testing machine and (b) loading of sample	32
Figure 3-12 LEICA Microscope with computer interface	33
Figure 4-1 Optical microstructures of Al-Si-Mg (a) as cast (b) SHT for 6 hours (c) aged 2 hours and (d) aged 3hours at 170 °C (x200).	36
Figure 4-2 Optical microstructures of Al-Si-Mg alloy (e) 1 hour (f) 4 hours (g) 5 hours (h) 6 hours (i) 7 hours and (j) 8 hours at 160 °C (x100)	37
Figure 4-3 Optical microstructures of Al-Si-Cu (a) as cast (b) SHT for 6 hours (c) aged for 4 hours (d) aged for 6 hours at 165 °C (x200)	38
Figure 4-4 Optical microstructures of Al-Si-Cu (e) 1 hour (f) 2 hours, (g) 3 hours, (h) 5 hours, (i)7 hours and (j) 8 hours at 155 °C (x100)	39
Figure 4-5 Stress-strain curve for Al-Si-Mg as it is sample showing the stresses in the range of the strain.	40
Figure 4-6 Stress-strain curve of Al-Si-Mg alloy Solution Heat treated at 530 °C for 6 hours sample, showing the stresses in the range of the strain.	41
Figure 4-7 (a) Stress-strain graph for Al-Si-Mg alloy at 170 °C artificially aged for 1 hour	42
Figure 4-8 Stress-Strain plot of Al-Si-Mg alloy at 170 °C artificially aged for 2 hours	43

Figure 4-9 Stress-strain plot of Al-Si-Mg alloy at 170 °C artificially aged for 3 hours	43
Figure 4-10 Stress-strain plot of Al-Si-Mg alloy at 170 °C artificially aged for 4 hours	44
Figure 4-11 Stress-strain plot of Al-Si-Mg alloy at 170 °C artificially aged for 5 hours.	44
Figure 4-12 Stress-strain plot of Al-Si-Mg alloy at 160 °C artificially aged for 1 hour	45
Figure 4-13 Stress-strain plot of Al-Si-Mg alloy at 160 °C artificially aged for 2 hours	46
Figure 4-14 Stress-strain plot of Al-Si-Mg alloy at 160 °C artificially aged for 3 hours	46
Figure 4-15 Stress-strain plot of Al-Si-Mg alloy at 160 °C artificially aged for 4 hours	47
Figure 4-16 Stress-strain plot of Al-Si-Mg alloy at 160 °C artificially aged for 7 hours	47
Figure 4-17 Composite bar charts of UTS of as cast, solutionized and ageing time between 1 and 8 hours for Al-Si-Mg alloy at 170 °C.....	48
Figure 4-18 Composite bar charts of UTS of as cast, solutionized and ageing time between 1 and 8 hours for Al-Si-Mg alloy at 160 °C.....	49
Figure 4-19 Tensile strengths of Al-14%Si-0.288Mg as cast, SHT, Peak-aged at 160 °C and Peak-aged at 170 °C.	50
Figure 4-20 Composite curves for Al-14%Si-0.288Mg at 160 °C and 170 °C for 8 hours	52
Figure 4-21 Microstructures of Al-14%Si-0.288Mg peak-aged (a) at 170 °C for 5 hours and (b) at 160 °C for 7 hours. (x200).	53
Figure 4-22 Bar charts of percentage elongation against ageing time at temperature at 160 °C ..	54
Figure 4-23 Bar charts of percentage elongation against ageing time at temperature 170 °C	54
Figure 4-24 Bar charts of Impact energies at various times and conditions at 160 °C	56
Figure 4-25 Bar charts of Impact energies at various times and conditions at 170 °C	56
Figure 4-26 Impact energy of As-cast and Solutionized sample	57

Figure 4-27 Composite curves for impact energies at 160 °C and 170 °C for Al-Si-Mg alloy. ...	58
Figure 4-28 Bar charts of UTS against impact energies at ageing at 160 °C (Al-Si-Mg alloys) ..	59
Figure 4-29 Bar charts of UTS against impact energies at ageing temperature of 170 °C (Al-Si-Mg alloys)	59
Figure 4-30 Stress-strain curve for Al-Si-Cu as it is, sample showing the stresses in the range of the strain.	61
Figure 4-31 Stress-strain curves for Al-Si-Cu solution heat treated at 480 °C for 6 hours ageing time, sample showing the stresses in the range of the strain	62
Figure 4-32 Stress-strain graphs for Al-Si-Cu alloy at 165 °C artificially aged for 1 hour	63
Figure 4-33 Stress-strain graphs for Al-Si-Cu alloy at 165 °C artificially aged for 2 hours	63
Figure 4-34 Stress-strain graphs for Al-Si-Cu alloy at 165 °C artificially aged for 4 hours	64
Figure 4-35 Stress-strain graphs for Al-Si-Cu alloy at 165 °C artificially aged for 6 hours	64
Figure 4-36 Stress-strain graphs for Al-Si-Cu alloy at 155 °C artificially aged for 1 hour	65
Figure 4-37 Stress-strain graphs for Al-Si-Cu alloy at 155 °C artificially aged for 2 hours	66
Figure 4-38 Stress-strain graphs for Al-Si-Cu alloy at 155 °C artificially aged for 7 hours	66
Figure 4-39 Stress-strain graphs for Al-Si-Cu alloy at 155 °C artificially aged for 8 hours	67
Figure 4-40 Composite bar charts of UTS of as cast, solutionized and ageing time between 1 and 8 hours for Al-Si-Cu alloy at 165 °C.	68
Figure 4-41 Composite bar charts of UTS of as cast, solutionized and ageing time between 1 and 8 hours for Al-Si-Cu alloy at 155 °C.	69
Figure 4-42 Tensile strengths of Al-14%Si-2.688Cu: as cast, solutionized, peak-aged at 155 °C	

for 7 hours and the same alloy peak-aged at 165 °C for 6 hours.	70
Figure 4-43 Composite curves for Al-14%Si-2.688Cu at temperatures of 155 °C and 165 °C	71
Figure 4-44 Microstructures of peak aged Al-14%Si-2.688Cu (c) at time 6 hours at 165 °C and (d) 155 °C at time 7 hours. (x500).	72
Figure 4-45 Bar charts of percentage elongation against ageing time at temperature 155 °C	73
Figure 4-46 Bar charts of percentage elongation against ageing time at temperature 165 °C	73
Figure 4-47 Bar charts of Impact energies at various times and conditions at 155 °C (Al-Si-Cu)75	
Figure 4-48 Bar charts of Impact energies at various times and conditions at 165 °C (Al-Si-Cu)75	
Figure 4-49 Impact energy of As-cast and Solutionized sample (temperature 480 °C at time 6 hours).	76
Figure 4-50 Composite curves of impact energy at 155 °C and 165 °C for Al-Si-Cu alloy	76
Figure 4-51 Bar charts of UTS against impact energies at ageing temperature of 155 °C (Al-Si- Cu alloys)	78
Figure 4-52 Bar charts of UTS against impact energies at ageing temperature of 165 °C (Al-Si- Cu alloys)	78



KNUST

ABSTRACT

This research work studied the effect of heat treatment on some mechanical properties of locally produced sand cast Al-Si-Mg and Al-Si-Cu alloys. The T6 heat treatment method was used for the heat treatment. The results show that solution heat treatment of Al-14%Si-2.66Cu at 480 °C produced an ultimate tensile strength of (126.72±0.51 MPa) with impact energy of (18.00±0.58 J) and the as-cast ultimate tensile strength was (129.94±0.66 MPa) with impact energy of (13.33±1.15 J). The peak ultimate tensile strength for the Al-14%Si-2.66Cu, artificially aged at 155°C for 7 hours was (143.46±0.33 MPa) with impact energy of (17.33±0.58 J) and (150.70±1.20 MPa) with impact energy of (14.67±1.53 J) when artificially aged at 165 °C for 6 hours. The solution heat treatment of Al-14%Si-0.288Mg at 530 °C for 6 hours resulted in an ultimate tensile strength of (120.00±0.70 MPa) with impact energy of (20.00±2.65 J) and the ascast ultimate tensile strength was (122.00±0.70 MPa) with impact energy of (12.33±0.58 J). The peak ultimate tensile strength was (228.32±0.93 MPa) with impact energy (14.00±0.58 J) when artificially aged at 170 °C for 5 hours. The peak strength at 160 °C for 7 hours was (200.40±0.98 MPa) with impact energy (13.67±0.58 J). These values obtained for the ultimate tensile strength were within the European standards for the ultimate tensile strength of sand cast Al-Si-Mg and Al-Si-Cu alloys (ISO Al Si7Mg, ISO AlSi10Mg and ISO Al Si12Cu in the T6

conditions are 260, 260 and 170 MPa) respectively. Also the Al-Si-Mg alloy responded much better to the heat treatment than the Al-Si-Cu alloy.

KNUST



CHAPTER 1

INTRODUCTION

1.1 Industrial Applications of Aluminium Alloys

Pure aluminium is soft and ductile and has 1 wt. % of both silicon and iron (Seifeddine, 2006). It is very versatile, therefore making it the commonly used metal after steel (Bogdanoff and Dahlström, 2009). Aluminium has a density of 2.70 g/cm^3 , which is one third that of steel, atomic weight of 26.97 amu, melting point of $660 \text{ }^\circ\text{C}$ and a boiling point of $2520 \text{ }^\circ\text{C}$. It also has a modulus of elasticity of 68.9 GPa. Aluminium has lower tensile properties compared to steel.

Aluminium is used for industrial applications because it has excellent strength-to-weight ratio. Aluminium and aluminium alloys have very good properties; the metallic industry does not go past aluminium and its alloys due to its striking industrial applications. Aluminium metal has vast collection of applications. Examples are, they are used to make soft ductile foils and they are very demanding in the heavy engineering industries. Aluminium and its alloys is used in the production of light vehicles, marine vehicles and has several applications in the construction industry due to its low density and specific strength (Elahetia, 2013). Aluminium and its alloys have gained several applications in the aerospace, automotive, building, marine, sports and exercise, rail, energy distribution, packaging and mechanical industry, as designers seek to design light weight vehicles and aircrafts with improved fuel efficiency and reduced carbon footprint (Prillhofer et al., 2014). Some examples of these aluminium alloys are Al-Cu, Al-CuMg and Al-Si-Mg.

Pure aluminium has good corrosion resistance and conducts electricity. It has applications as electrical cables and foils. Addition of other elements to pure aluminium helps to improve certain

properties as corrosion resistance, lightness, formability, impact strength, tensile strength and hardness makes it desirable in several applications.

1.2 Aluminium Castings classification

Aluminium alloys are divided into two groups. We have wrought and cast alloys. Wrought alloys, are originally cast as ingots or billets and later hot and/or cold worked mechanically into the desired form that is, rolling, extrusion, forging and forming. Wrought alloys are grouped into heat treatable wrought alloys and non-heat treatable.

Cast alloys are directly cast into their final shape by one of various methods such as green sand casting, low and high pressure die casting, lost foam casting and gravity die casting. High levels of silicon help to improve the castability of these alloys. Aluminium wheels in passenger cars are made commonly from Low pressure die casting. Big V-engine blocks are also produced from this process. Its casting's productivity is restricted by solidification time, and this leads to cycle times of typically several minutes.

High pressure die casting is a difficult process because it is not economically feasible. The automotive industry leads the use of aluminium castings. The process has grown at the cost of iron castings. Due to the requirement to reduce vehicle weight and increase fuel efficiency aluminium castings continues to be used though it is more expensive than iron castings. This requirement drives the replacement of ferrous parts by aluminium. Aluminium castings are widely used in producing several car parts. Examples include rocker covers, steering boxes, engine blocks, heads, differential casings, pistons, inlet manifolds, brackets, wheels etc.

In this research work, the casting process which will be used is the green sand casting. It is relatively inexpensive to produce, especially in low-volume runs. It is also used to produce large

parts and also has ability for casting ferrous and non-ferrous materials and low cost for aftercasting tooling. It is also the most used casting method in the country.

1.3 Aluminium Castings defect

The following casting defects can harm the quality of cast aluminium alloys;

- Shrinkage: Aluminium alloys shrink by 3.5–6.0% during solidification
- Gas porosity: this comes about due to gases expelled during solidification after pick-up in the molten metal state
- Oxide inclusions: oxides are formed in molten aluminium and entrapped in castings due to exposure to the atmosphere.

All this casting defects can be reduced considerably by ensuring:

- Efficient degassing of the molten metal
- Grain modification
- Change of structure
- Filtration of metals
- Moulds are filled slowly and steadily

These processes have helped to improve general quality of castings in recent years

1.4 Mechanical properties

Properties which are of significance in aluminium and its alloys are, tensile strength, yield strength, hardness, ductility, fatigue behavior, wear resistance and impact strengths. These properties stated

above are basically controlled by the material's physical properties as well as chemical properties; physical properties include microstructure, grain size, grain structure and orientation. Chemical properties talks about elemental chemical constitution, the concentration and effects of alloying. Alloying with copper, silicon, magnesium, zinc, tin and iron helps to improve these properties (Grosselle et al., 2009). Table 1-1 below compares the mechanical properties of sand and chill cast test bars in European Standards.



Table 1-1 Mechanical properties of Sand and Chill cast test bars EN 1706

sand and chill casting alloys	Mechanical properties for test bars	Property description
-------------------------------	-------------------------------------	----------------------

Alloy Classification according to: Numeric ISO	Condi tions	Breaking strength Rm (MPa) min	Yield strength Rp0.2 (MPa) min.	Elongation A ₅₀ % min	Brinell hardness HBS min	
EN AC-42000 ISO Al Si7Mg	SF ST6 KF KT6 KT64	140 220 170 260 240	80 180 90 220 200	2 1 2.5 1 2	50 75 55 90 80	Eutectic alloy with good casting properties. Good machinability, good weldability, and high chemical resistance
EN AC-43000 ISO Al Si10Mg(a)	SF ST6 KF KT6 KT64	150 220 180 260 240	80 180 90 220 200	2 1 2.5 1 2	50 75 55 90 80	Near-eutectic alloy with excellent casting properties and good resistance to hot tearing. Good machinability, excellent weldability, and high chemical resistance
EN AC-43100 ISO Al Si10Mg(b)	SF ST6 KF KT6 KT64	150 220 180 260 240	80 180 90 220 200	2 1 2.5 1 2	50 75 55 90 80	Near-eutectic alloy with excellent casting properties and good resistance to hot tearing. Good machinability, excellent weldability, and high chemical resistance
EN AC-47000 ISO Al Si12(Cu)	SF KF	150 170	80 90	1 2	50 55	Eutectic alloy with excellent casting properties, excellent fluidity and high resistance to hot tearing. Good machinability, excellent weldability.
EN AC-46200 ISO Al Si8Cu3	SF KF	150 170	90 100	1 1	60 75	Good castability, universal alloy.

Source: Brown, 1999

Key

- EN 1706= European standard 1706
- AC = Component cast in aluminium
- S =Sand casting
- K = Chill casting
- F = Cast conditions
- T6= Solution annealed and artificially aged.
- T64 = Solution annealed and artificially aged (under-aged).
- (The designations are equivalent to SS-EN 1706)
- 1 MPa = 1 N/mm²

1.5 Aluminium alloying elements

- Zinc is added to enhance corrosion resistance which has good application in marine vehicles.
- Copper improves strength, hardness, machinability and thermal conductivity. 4–6% Cu gives the most effective heat treatment of the alloys. Copper reduces castability, hot tear resistance and corrosion resistance.
- Magnesium when added in the range of 0.25–0.5% Mg allows Al–Si alloys to be heat treated and the precipitation of finely distributed Mg₂Si improves mechanical properties. Proof stress is doubled. 1% in high silicon piston alloys. Higher levels, 3–6% Mg, are used in low silicon alloys to enhance the anodising character and give a bright surface finish to make components attractive.

- Silicon when added to aluminum gives it good fluidity during casting. The primary Si phase in hypereutectic alloys is refined by phosphorous addition. The effects of Na and Sr eutectic modifiers are reduced by low levels of phosphorous in hypoeutectic alloys.
- Nickel when combined with copper, enhances strength and hardness at elevated temperature. Some of the most frequently used cast aluminum systems are the Al-Si-Mg based alloys, Al-Si-Cu alloys and Al-Si-Cu-Mg based alloys, Al-Fe-Mn-Si, Al-Cu-Mg, Al-Mg-Si, Al-Mg, Al-Cu, and Al-Mn. In applications requiring strength and good castability, alloys used are Al-Cu and Al-Si-Mg based alloys.

The mechanical properties of castings can be improved by work hardening and heat treatment. Different properties of the material can be changed by heat treatment. This can be used to increase or decrease the hardness or yield strength of the material (Dingmann and Hlandze, 2003).

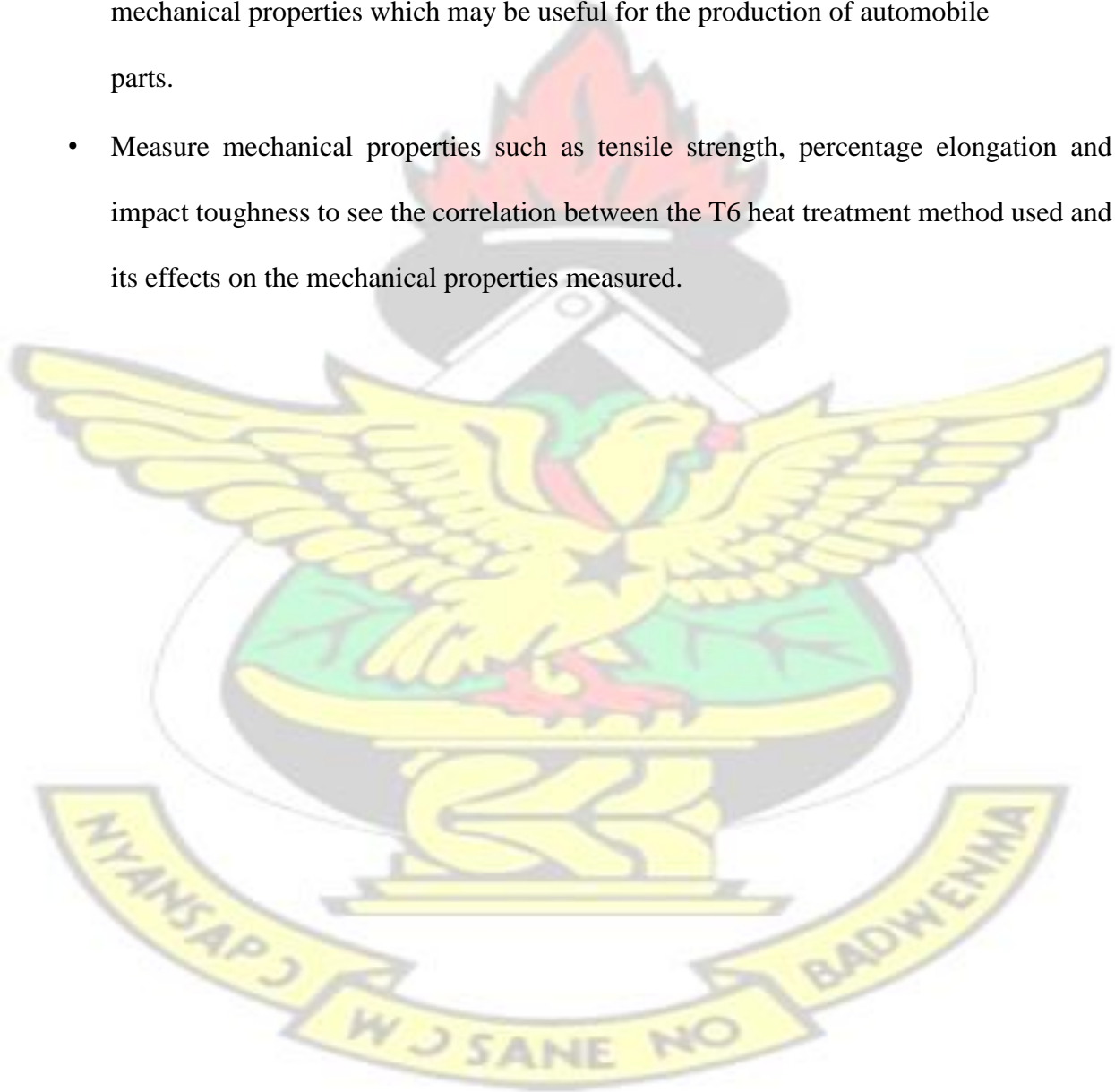
The material is exposed to high temperatures just below its melting point for some hours in a furnace to change its structure and suddenly quenching to seize the structure changes. A material with better mechanical properties is produced. Automobile parts such as aluminum alloy wheels, gear box housings, exhaust manifolds cylinder heads are being strengthened by this process (Cavaliere et al., 2004).

Foundries in Ghana use aluminum alloys to produce items such as motor vehicle parts and household items. These applications do not involve heat treatment. Bigger foundries produce parts which are of commercial value in the automotive industry. These applications require heat treatment to achieve the needed mechanical properties for good service applications.

Aluminium alloys which will be used in this work are Al-Si-Mg and Al-Si-Cu.

1.6 Research Objectives

- The objective of the research is to produce Al-Si-Mg and Al-Si-Cu aluminum casting alloys and carry out chemical analysis on them.
- Subject the Al-Si-Mg and Al-Si-Cu alloys to the T6 heat treatment (which comprises of solution heat treatment, quenching and artificial aging) processes to get the optimum mechanical properties which may be useful for the production of automobile parts.
- Measure mechanical properties such as tensile strength, percentage elongation and impact toughness to see the correlation between the T6 heat treatment method used and its effects on the mechanical properties measured.



1.7 Justification of the Study

Recently, small and medium scale companies in the country are moving into small scale car assembly. Currently, some of these companies have started assembling cars on a small scale level. Parts used by these companies are all imported CKD (Completely Knocked Down) automobile. The long term goals of these companies are to build the various components and parts used in the car assembly from scratch and stop the importation of the CKD. Technicians working in these small and medium scale companies lack the pre-requisites and knowledge of the various heat treatment processes which are used to impart good mechanical properties to castings for good service applications. This research will serve as the basis for capacity building for these companies to be able to produce mechanically sound castings by improving the practices and providing proper portfolio of the various heat treatment processes needed for the production of good quality castings. A spin-off of this project is that, these companies may be able to produce spare parts like, pistons, cylinder heads, gear housing, engine blocks, which can save them a lot of foreign exchange.

CHAPTER 2

LITERATURE REVIEW

2.1 Aluminium and its Alloys

Aluminium alloys are grouped into two categories namely wrought and cast aluminium alloys. Wrought aluminium alloys are cast into ingots or billets first before they are hot or cold worked mechanically to the preferred shape by processes such as rolling, forging and extrusion (Kaufman, 2000). Cast aluminium alloys are cast directly into near net shape parts or form by processes such as sand casting, pressure casting, die casting etc (Kaufman and Rooy, 2004).

In the wrought alloy aluminium designation classification, the initial digit (**Xxxx**) shows the principal alloying element, which has been added to the aluminium alloy. It is often used to describe the aluminium alloy series that is 1000 series, 2000 series, and 3000 series up to 8000 series. The following digit (**xXxx**) shows an alteration of the specific alloy and the third and fourth alloy (**xxXX**) are arbitrary numbers given to identify a specific alloy in the series. An example is aluminium alloy 5183; the first digit, five (5) indicates the major alloying class of the series, the digit one (1) for the first variation and the 83 identify it in the 5xxx series. An exception to this alloy numbering system is the 1xxx series aluminium alloys (pure aluminium), where the last two digits provides the minimum aluminium percentage above 99%. That is alloy 13(50) (99.50% minimum aluminium) (European Aluminium Association, 2002).

The cast alloy designation system is based on a 3 digit-plus decimal designation xxx.x (356.0). The first digit (**Xxx.x**) indicates the principal alloying elements added to the aluminium alloy. The second and third digits (**xXX.x**) are arbitrary numbers given to identify a specific alloy in the series. The number which follows the decimal point indicates whether the alloy is casting or an ingot. When a zero follows after the decimal point it indicates a casting .0. When one 1 or two

(2) follows after the decimal point, it indicates an ingot .1 or .2. A capital letter indicates a modification to a specific alloy (European Aluminium Association, 2002).

The tables below show the American National Standards Institutes (ANSI) designation system for both wrought and cast aluminium alloys.

Table 2-1 Main alloying elements in the wrought alloy designation system

Alloy	Main alloying elements
1xxx	Mostly, pure aluminium; no alloying elements
2xxx	Copper
3xxx	Manganese
4xxx	Silicon
5xxx	Magnesium
6xxx	Magnesium and Silicon
7xxx	Zinc
8xxx	Other elements (eg, iron and tin)
9xxx	Unassigned

Source Kaufman, 2000

Table 2-2 Main alloying elements in the cast alloy designation systems

Alloy	Main alloying elements
1xx.x,	Pure aluminium (99% or greater)
2xx.x,	Copper
3xx.x,	Aluminium-Silicon + Copper and/or Magnesium
4xx.x,	Aluminium-Silicon
5xx.x,	Aluminium-Magnesium
7xx.x,	Aluminium-Zinc
8xx.x,	Aluminium-Tin
9xx.x,	Aluminium + other elements
6xx.x,	Unused series

Source: Kaufman and Rooy, 2004.

In the wrought and cast aluminium alloy systems, there are heat treatable and non-heat treatable groups. The heat treatable groups in the wrought alloys are 2xxx, 6xxx and 7xxx, whilst the heat treatable cast alloys are 2xx.0, 3xx.0 and 7xx.0 (Kaufman and Rooy, 2004; Kaufman, 2000).

In this work sand cast Al-Si-Cu and Al-Si-Mg aluminium alloys, which belong to the 3xx.0 series of the cast aluminium designation system were sand cast. Table 2-3 shows the temper designation for heat treatment of aluminium alloys.

Table 2-3 Temper Designation for Heat Treatment of Aluminium Alloys

O	Annealed
F	As fabricate
W	Solution heat treatment: spontaneous natural aging after solution treatment
T1	Cooled after high-temperature processing and naturally aged to substantially stable condition
T2	Cooled after high-temperature processing, cold worked and naturally aged to substantially stable condition
T3	Solution heat- treated, cold worked and naturally aged to substantially stable condition
T4	Solution heat-treated and naturally aged to substantially stable condition
T5	Cooled after high temperature processing and artificially aged
T6	Solution heat-treated and artificially aged, usually to maximum strength
T7	Solution heat-treated and stabilized or overage
T8	Solution heat-treated, cold worked and artificially aged
T9	Solution heat-treated, artificially and cold worked
T10	Cooled after high temperature processing, cold worked and artificially aged

Source: Handbook of Aluminium, volume 2

2.2 Aluminium Casting Methods

There are a lot of casting methods for aluminium alloys and metals in general. Casting helps in producing near net shape products. The casting mould can be grouped into permanent and expandable mould (Groover, 2010). Some casting methods used to produce aluminium products are Green sand casting, Die casting or Permanent mould casting, Investment casting or Lost foam casting, Pressure die casting (high and low pressure die casting), Squeeze casting, Thixocastings (European Aluminium Association, 2002).

2.2.1 Green sand moulding process

Green sand moulding is by far one of the moulding processes used for metal casting or used for aluminium castings (Groover, 2010). The advantages of using this method are as follows,

- Most ferrous and nonferrous metals can be used
- Low materials and pattern cost
- Almost no limit on size or shape of part to be produced.
- Tooling cost for this method is low
- Used for large and small number of castings

In this research work, green sand casting method was chosen to produce the alloy samples. This is because it is the commonest method used in most foundries across the country. The mould used in this work was able to cast a maximum of fifty (50) cylindrical bars.

2.3 Methods of Strengthening Metals

Metals deform due to the movement of dislocations. The process of impeding the movement of dislocation renders the material harder and stronger. Metals can be strengthened in many ways to enhance upon their mechanical properties. The targeted mechanical properties are yield strength, tensile strength, ductility, hardness and impact toughness (Callister and Rethwisch, 2009). Some of the methods for strengthening metals and alloys are as follows:

- Solid-Solution Strengthening (alloying)
- Strengthening by grain size reduction and Dispersion strengthening
- Cold working
- Precipitation Strengthening (natural and artificial ageing)

2.3.1 Strengthening by alloying

Metals deform due to the movement of dislocation through the metal (Callister and Rethwisch, 2009) Solid solution strengthening employs the phenomenon of introducing atoms of another element into parent lattice to improve strength of the parent material. Impurity atoms go to

substitute atoms of the parent material (substitutional solid solution). Stressful are fields are generated around solute atoms which interact with stress fields of a dislocation movement, thereby increasing the stress required for plastic deformation. Impurity atoms anchor dislocations thus restricting its motion produced (Askeland and Wright, 2009). Increasing the concentrations of impurity atoms means more anchoring of dislocations and this tend to increase the yield and tensile strength of such materials as in the figure (a) below.

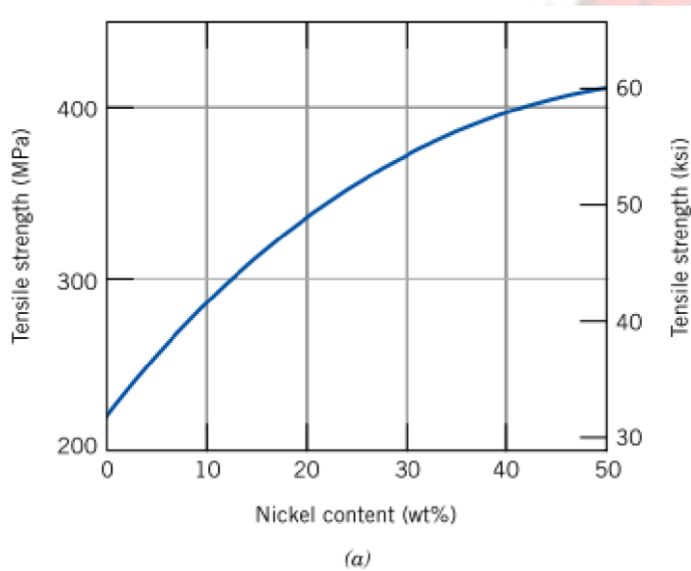


Figure 2-1 Variation of nickel content on tensile strength for copper-nickel alloy, showing strengthening (Callister and Rethwisch, 2009).

2.3.2 Dispersion strengthening

In dispersion strengthening, small second-phase particles distributed in a ductile matrix can hinder dislocation motion thus increasing the strength of the material. Second phase particles can be introduced by mixing or consolidation and it has little solubility in the matrix even at elevated temperatures (Callister and Rethwisch, 2009). Second phase particles resist growth and overaging. Dislocations moving through the matrix either cut the precipitates particles and also bends around and goes around them. When there is an interphase or sudden change in particle orientation, cutting

of particles by dislocation becomes difficult so dislocations bend around and bypass. Good strengthening is attained by bending process when particles are submicroscopic in size. Degree of strengthening from second phase particles depends on the particle distribution in the matrix. The spacing between second phase particles should be a few hundred angstroms to be able to achieve optimum strengthening (Askeland and Wright, 2009).

2.3.3 Cold working

Cold working (strain hardening) is used to impart strength to a ductile material by plastically deforming the material. Strengthening that, results from cold working is by dislocation to dislocation strain field interactions. Dislocation density is increased with cold working due to formation of new dislocations or dislocation multiplication. Dislocation-dislocation interactions are repulsive. The final result is that the motion of a dislocation is impeded by the presence of other dislocations. With increase in dislocation density, the resistance to dislocation movement by other dislocations becomes more. Therefore the stress needed to deform a metal increases with cold working (Callister and Rethwisch, 2009). For effective cold working, the presence of grain boundaries acts as effective obstacles to dislocation movement.

2.3.4 Precipitation strengthening

Precipitation hardening, or age hardening, is one of the most widely used mechanisms for the strengthening of metal alloys. It is produced by solution treating and quenching an alloy in which a dissolved solute is in solid solution at an elevated temperature but precipitates upon quenching and aging at a lower temperature. The second phase must be soluble at the elevated temperature but must exhibit decreasing solubility with decreasing temperature. The diagram below shows the three steps in the age-hardening process for Al-Cu.

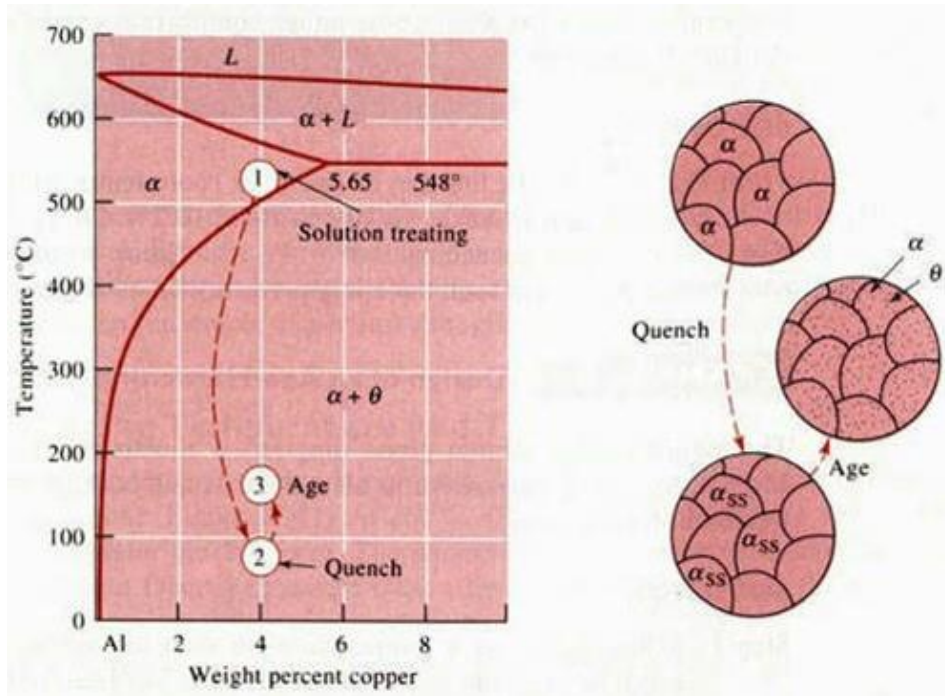


Figure 2-2 The aluminum rich end of the Al-Cu phase diagram showing the three steps in the age-hardening heat treatment and the microstructures that are produced (Askeland and Wright, 2009).

The hardening mechanisms that are at work during the ageing process are solid solution hardening; this is where all strengthening is provided by the dissolved copper trapped in the supersaturated solution. Guinier-Preston zones (GP zones) form and all the copper is removed from solution and solid solution strengthening disappears. The next step is coherency stress hardening; this is where coherency strains around GP zones and θ'' precipitates generate stresses which prevent dislocation movement. The GP zones give the greater hardening effects. Lastly is precipitation hardening; the precipitates obstruct dislocation directly but their effectiveness is limited by the fact that, dislocations can cut through them or bow around them. See Figure 2-3 and Figure 2-4 below. The cutting stress increases with ageing and the bowing stress decreases with ageing when precipitates spacing increases from 10 nm to 1 μm (Ashby and Jones, 2005).

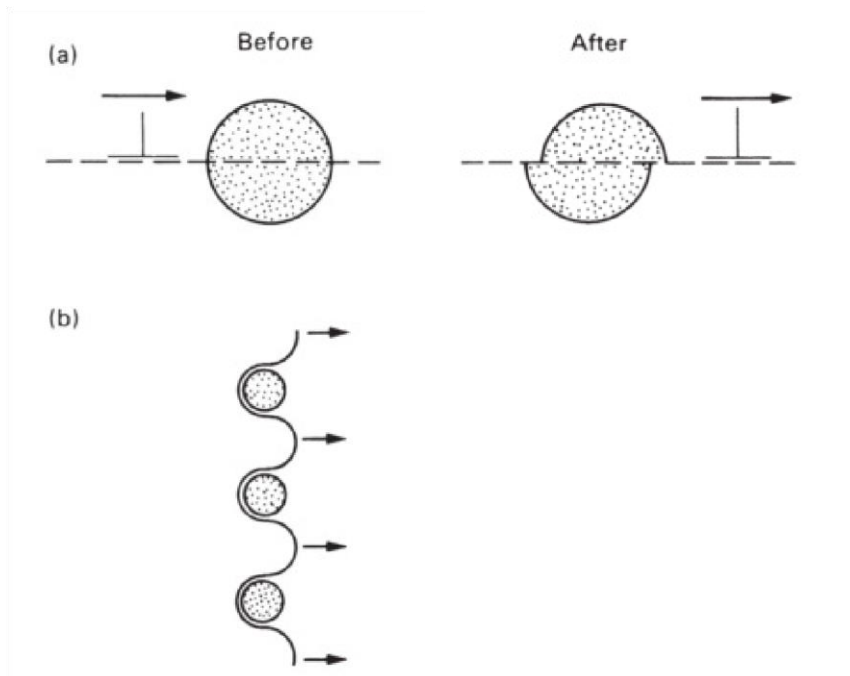


Figure 2-3 dislocations can get pass precipitates by (a) cutting (b) bowing (Ashby and Jones, 2005)

A major advantage of precipitation hardening is that it can be used to increase the yield strength of many metallic materials via relatively simple heat treatments and without creating significant changes in density. Thus, the strength-to-density ratio of an alloy can be improved substantially using age hardening. For example, the yield strength of an aluminum alloy can be increased from about 137.89 MPa to 413.69 MPa a result of age hardening (Askeland and Wright, 2009).

2.3.4.1 Ageing of Al-Si-Cu alloys

In this alloys, the typical heat treatment that is adapted is the T6 solution heat treatment (Sjölander and Seifeddine, 2010). Solution heat treatment is applied for a sufficiently long period of time to get a homogenous supersaturated structure. This structure is then quenched to maintain the supersaturated structure at ambient temperature. The purpose of this treatment is as follows

(Mohamed and Samuel, 2012):

- To homogenize the as cast

- Dissolution of the Al_2Cu phase and
- Refine the eutectic silicon particles.

Age hardening follows after solutionizing and quenching. It entails strengthening by coherent precipitates which are capable of being sheared by dislocation. Controlling the ageing time can produce varying mechanical properties and sometimes stabilize microstructure. The general precipitation hardening sequence in Al-Cu alloys is as follows; Supersaturated $\alpha \rightarrow$ GP1 zones \rightarrow GP2 zones (θ'' phase) \rightarrow θ' phase \rightarrow θ phase (CuAl_2) (Kaufman and Rooy, 2004). This can be best explained using Figure 2-4 below.

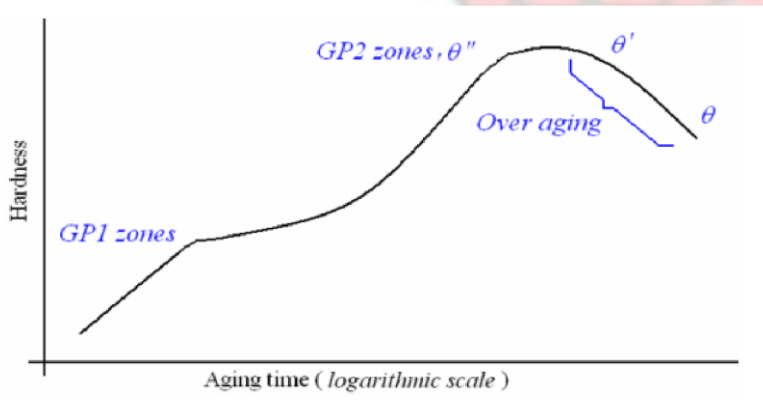


Figure 2-4 Correlation of structures and hardness for Al-4% Cu alloy (Callister and Rethwisch, 2009).

With further ageing, θ phase which has a BCT (base centered tetragonal) structure and incoherent with the matrix is produced. At this stage the hardness decreases because of the incoherency. Growth of these particles leads to over aging. Figure 2-4 above, describes variation of hardness and aging time.

From Figure 2-5 below, at around $550\text{ }^\circ\text{C}$, a single phase α - solid solution exist with 4% Cu, and at room temperature as a mixture as α with less than 0.5% Cu, and an intermetallic compound,

CuAl₂ (θ) with 52% Cu. On slow cooling α rejects excess Cu as precipitate particles of θ . These particles are relatively coarse in size and can cause only moderate strengthening effect. Rapid cooling of the alloy creates a supersaturated solution that can be obtained at room temperature. As a function of time at room temperature, and at higher temperatures up to 200 °C, the diffusion of Cu atoms may take place and the precipitate particles can form.

GP1 zone which is coherent and produced by Cu atoms segregating in α , with segregation regions disk shape in nature and thickness ranging from 0.4-0.6 nm and 8-10 nm produced on {100} planes of the matrix are produced at lower temperatures. GP2 zones, which have tetragonal structure, produced on {100} planes are coherent with the matrix and produce further hardening. As ageing progresses their sizes range from 1-4 nm and 10-100 nm. They are produced at lower temperatures. θ' phase which has a tetragonal structure and forms platelets with thickness 10-150 nm, which nucleates heterogeneously on dislocation and partially coherent with the matrix. This is produced at higher temperatures (Bacon and Hull, 2001).

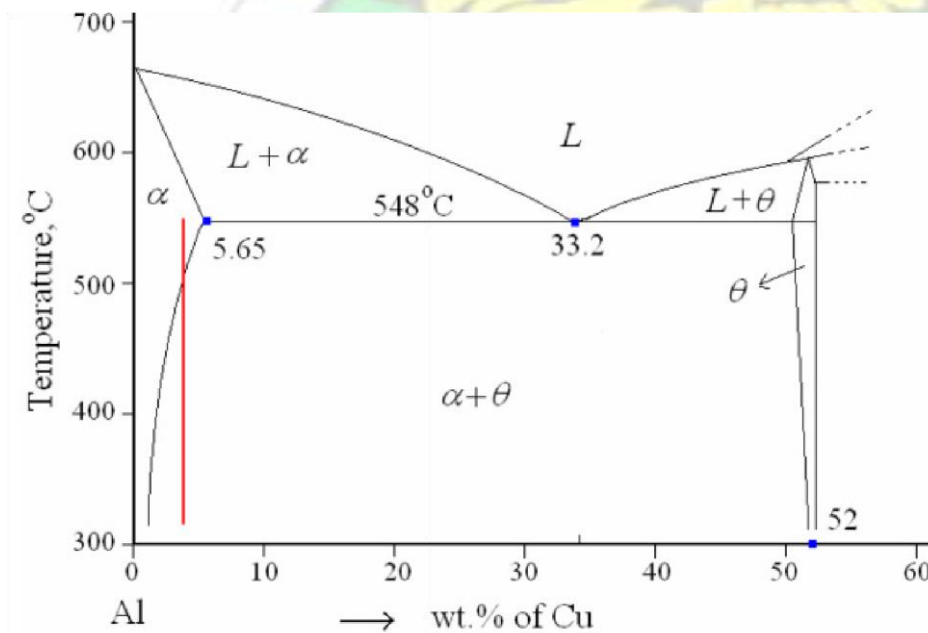


Figure 2-5 Aluminium rich end of Al-Cu phase diagram (Bacon and Hull, 2001).

Al-Si-Cu alloys generally do not respond to heat treatment compared to Al-Si-Mg alloys (Mohamed and Samuel, 2012). The general microstructure, for Al-Si-Cu alloys are Al_2Cu , $\text{AlAl}_2\text{Cu-Si}$, $\text{Al}_5\text{Mg}_8\text{Cu}_2\text{Si}_6$ and Cu_2FeAl_7 . These intermetallic phases are responsible for the strengthening of the alloy. The Al-Al₂Cu-Si dissolves into Al_2Cu phases to provide more strengthening during ageing of the alloy (Hurtalová et al., 2012).

2.3.4.2 Ageing of Al-Si-Mg alloys

The successive precipitation sequence in Al-Si alloys which contain magnesium is represented by $\beta_{\text{SSS}} \rightarrow \text{GP zones } (\beta'') \rightarrow \beta' \rightarrow \beta \text{ Mg}_2\text{Si}$. The sequence for these alloys begins with the formation of spherical GP zones consisting of an enrichment of Mg and Si atoms. The GP zones elongate and develop into a needle shaped coherent β'' phase. The needles grow to become semicoherent rods (β' phase) and finally non-coherent platelets (stable β phase) (Sjölander and Seifeddine, 2010). Al-Si-Mg alloys respond very well to heat treatment (Mohamed and Samuel, 2012). According to (Fatai Olufemi, 2012) the magnesium silicide (Mg_2Si) that is formed is the principal hardening phase in Al-Si-Mg alloys. According to the European standard for aluminium alloys, the breaking strength for sand and chill cast ISO Al Si7Mg, ISO Al Si10Mg and ISO AlSi12Cu in the T6 conditions are 260, 260 and 170 MPa respectively (Brown, 1999).

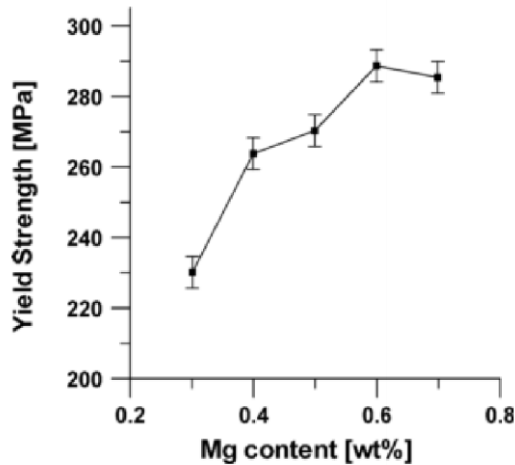


Figure 2-6 Graph of Yield strength against small Mg content for a peak-aged Al-7Si-Mg alloy (Taylor, St John, Barresi, and Couper, 2000).

Evidence from XRD pattern shows that the general microstructures of Al-Si-Mg alloys comprises of excellent distribution of precipitates such as $\text{Al}_{18}\text{Cr}_2\text{Mg}$, Mg_2Si (cubic), $\text{Al}_{12}\text{Si}[\text{Fe}, \text{Cr}]$ (cubic), CrFe_4 (cubic), AlMg (cubic), Al_3Cr (cubic), $\text{Al}_8\text{Cr}_5, \text{Al}_5\text{Cr}$, Al_9Si (cubic), $\text{Al}_8\text{Mg}_3\text{FeSi}_{16}$ (hexagonal), $\text{Al}_{12}\text{Mg}_{17}$ (cubic), TiZn_{16} (orthogonal), AlCuMg (cubic), MnCr , AlFeSi , $\text{AlSi}[\text{Fe}, \text{Al}_{12}\text{Mg}_2\text{Si}, \text{CrFe}_{19}]$ (cubic), These are the strengthening phases in Al-Si-Mg alloys (Abdulwahab et al., 2011). The AlFeSi phase is the most dangerous phase as it is brittle and occurs in plate-like particles (Rodríguez et al., 2012).

2.4 Grain Size Reduction Strengthening

Metals can be strengthened by reducing their grain sizes. The size and average diameter of grains influence the mechanical properties of materials because decrease in grain size means a decrease in the average distance a dislocation can pass through. Dislocations start to stack at grain boundaries which lead to an increase in yield strength of the material. The Hall-Petch equation ($\sigma_y = \sigma_0 + k_y/\sqrt{d}$) where d is the average grain diameter, σ_0 and k_y being material constants expresses this fact. Methods of grain size reduction are plastic deformation, rate of solidification

and cold working. Fine grained materials are stronger than coarse grained materials because the fine grain material has a better total grain boundary area to obstruct dislocation movement (Callister and Rethwisch, 2009).

2.5 Impact Properties of Materials

Impact toughness is recently one of the critical properties that are being investigated. Data obtained from impact toughness is used to improve design; this gives us the energy that is taken before failure. It also practically assesses the ductility of the material under rapid loading (Paray, Kulunk, and Gruzleski, 2000). The Charpy impact test is the common method of impact testing and its used as a means of quality control and selection of materials. The impact toughness of AlSi-Mg alloys are dependent on the characteristics of eutectic silicon particles, α -Al dendrites, size and morphology of intermetallic phases that are formed in Al-Si alloys (Fatai Olufemi, 2012). The impact toughness of Al-Si-Cu alloys are dependent on the characteristics of the silicon particles, and the α -Al dendrites. The size and shapes of the intermetallic phases that are formed in Al-Si containing Cu_2Al alloys influences the impact energy of these alloy (Basavakumar, Mukunda, and Chakraborty, 2008a, 2008b).

CHAPTER 3

RESEARCH METHODOLOGY

3.1 Sand Casting Aluminium Alloys

3.1.1 Mould design and Preparation

A moulding box of dimensions 60 cm x 60 cm x 90 cm was prepared and moulding sand, which was made up of bentonite and silica was used to make the mould for the samples. The moulding sand was put in the moulding box and rammed to produce a very good compact of the sand in the mould. A cylindrical rod pattern of length 37 cm and diameter 20 mm equal to the dimensions of the cylindrical bars to be used for the research was used to create the mould in the moulding sand. The mould was left to dry for 1 week to remove enough moisture from the moulding sand, to produce casting with good surface finish, before the casting operation was carried out.

3.1.2 Casting Operation for Al-Si-Mg alloy

High purity aluminium 99.80%, high purity magnesium 99.80%, and Silicon were used for this alloy. The Al-Si-Mg alloy was prepared by first charging 1400 g of the silicon with melting point (1,414 °C) in a diesel fired crucible furnace for about 30 minutes. This was done because the silicon has a very high melting temperature. Firing it early enables it to fuse for some time before the low melting point aluminium with melting point (660 °C) metal is introduced into the melt. 8000 g of the pure aluminium was introduced into the melt 30 minutes later. The aluminium metal fused with the silicon to help it melt very early. The aluminium was introduced into the melt after 30 minutes to prevent it from boiling, because of its low melting point compared to the silicon. When the aluminium metal boils it can lead to reduced strength of the metal. After two hours of continuous firing, the aluminium and silicon metals, 0.3 g of the magnesium was introduced into the alloy for

a few minutes and stirred for about 10 minutes before pouring the melt into the mould, to prevent evaporation of the magnesium from the melt. After about two and half-hours of continuous firing, the alloy melt was ready for casting. The melt was poured into the mould at a steady rate, to prevent turbulence in the mould. The mould was allowed to cool for about an hour before the samples were removed from the mould. 35 samples were produced per Mould for each alloy type

3.1.3 Casting Operation for Al-Si-Cu alloy

High purity aluminium 99.80%, copper coil and silicon were used for this alloy. The alloy was prepared by first charging 1400 g of silicon and 300 g of copper into the crucible. This charge (silicon and copper) was fired constantly for an hour due to the high melting temperatures of both the silicon (1414 °C) and copper (1,085 °C). After an hour of continuous firing, the low melting point aluminium metal was introduced into the melt. The aluminum helped the copper and silicon to fuse and melt very early to prevent too much fuel usage. After about three hours of continuous firing, the alloy melt was ready to cast. The molten metal was poured into the mould at a steady rate, to prevent turbulence in the mould. The mould was allowed to cool for about an hour before the samples were removed from the mould. Thirty five (35) samples were produced per mould for each alloy type.



Figure 3-1 Fuel fired lift out crucible furnace used for the melting operation



Figure 3-2 Shows (A) Pure aluminium and (B) shows pure magnesium which 0.3 g was used

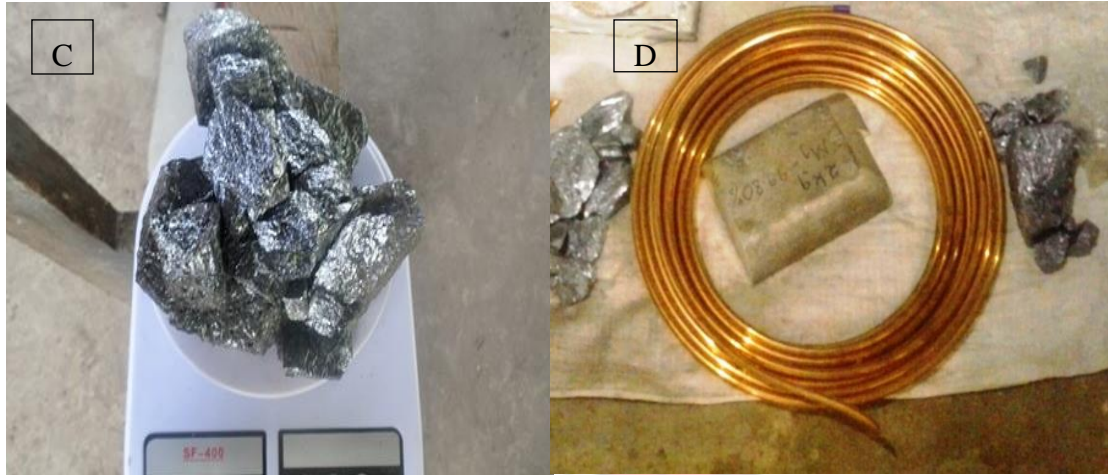


Figure 3-3 Shows (C) Pure silicon used and (D) shows copper coil, 300 g was used

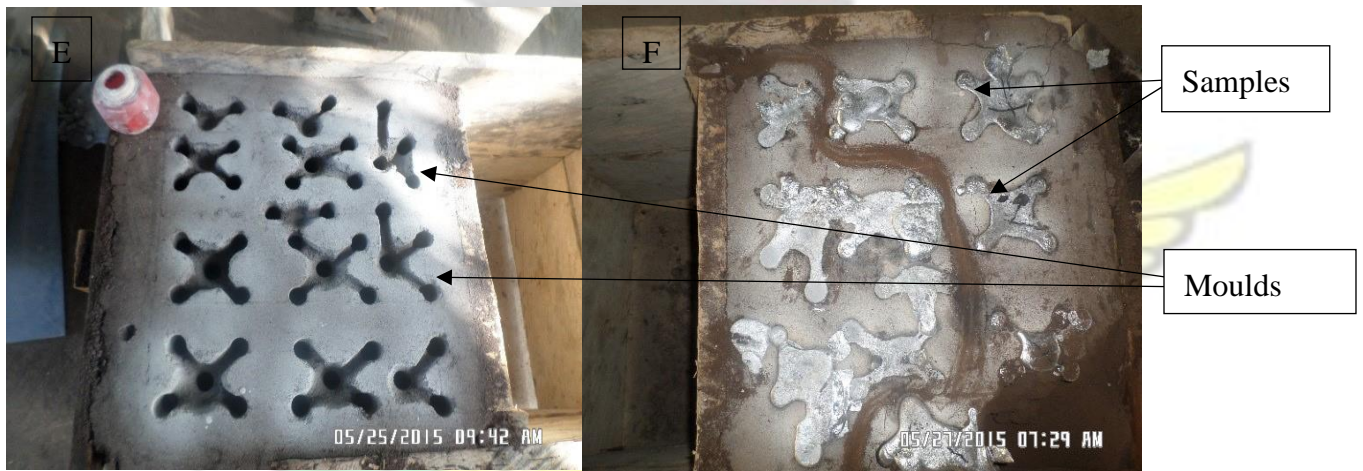


Figure 3-4 Picture of (E) Moulds and (F) samples cooling in moulds after casting operation



Figure 3-5 Picture of (G) samples fresh out of mould and (H) machined samples with good finish

3.2 Chemical Analysis of Samples

Chemical analysis of alloy samples was verified by using an optical emission spectrometer (Quantometer) at Valco Ghana limited, Tema. Discs of both alloys were prepared at the foundry to be used for the chemical analysis. The surfaces of the specially prepared discs were cut smooth by a Computer Numerical Control Lathe machine to remove all contaminants from them. After that, control samples were run in both alloys mode. The control samples put the equipment in good shape for repeatability, consistency and accuracy in the analysis. The sample was sparked to vaporize the atoms and emit radiations which passed through the optical fiber in the equipment for separation into spectral components. The radiation intensity being proportional to the concentrations of elements in the samples could be shown directly in percent concentrations.

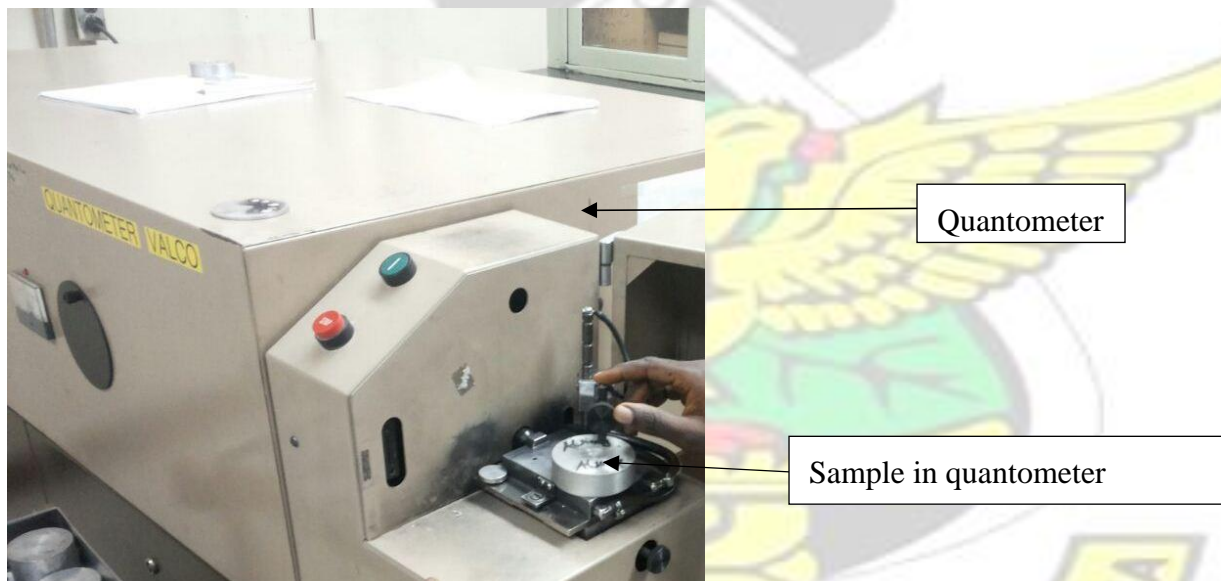


Figure 3-6 Picture of sample in quantometer to be tested

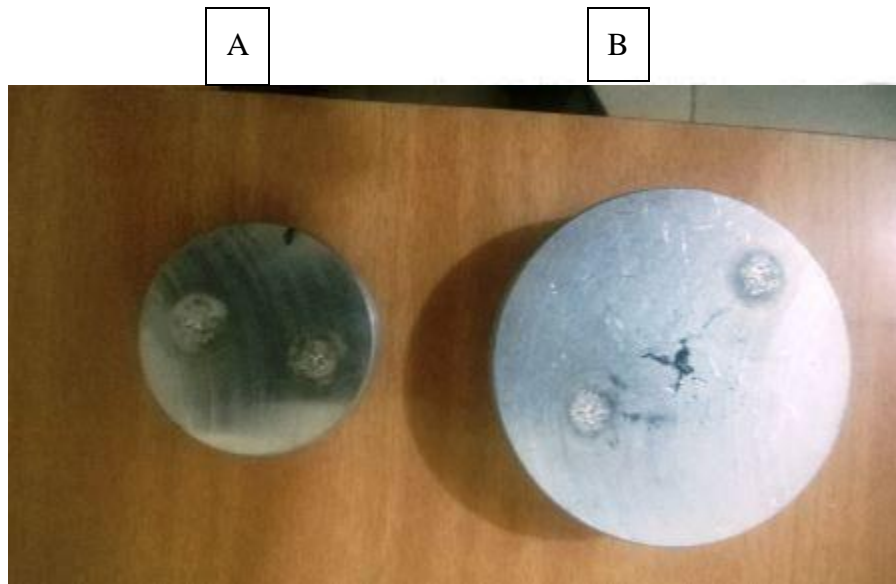


Figure 3-7 Picture of (A) Al-Si-Cu and (B) Al-Si-Mg discs used for the chemical analysis

3.3 Solution Heat Treatment

All aluminum alloy samples which were to be used for this work were solution heat treated. AlSi-Cu samples were placed in a Lenton electric furnace and solution treated at 480 °C for time 6 hours. The time for the solution heat treatment was based on literature study. The temperature of 480 °C was to prevent the melting of Al_2Cu , which melts at 520 °C. After solution heat treatment all samples were quenched in water of temperature 28 °C

Al-Si-Mg samples were solutionized at 530 °C to prevent melting of the Mg_2Si , which melts at 550 °C. The solution treatment time was 6 hours. After all the samples have been solutionized, they were quenched in water of temperature 28 °C.

3.3.1 Artificial ageing of Al-Si-Cu and Al-Si-Mg alloys

Artificial ageing was carried out on the samples in the Lenon electric furnace with an automatic temperature regulating device called Eurotherm and Crabolyte electric furnace after solution heat treatment at 480 °C. Al-Si-Cu samples were aged at temperatures of 155 °C and 165 °C. Al-SiMg samples were artificially aged at temperatures of 160 °C and 170 °C after solution heat treatment of 530 °C. The times for the artificial aging were 1, 2, 3, 4, 5, 6, and 7 up to a maximum of 8 hours. After each artificial aging, samples were air cooled.

3.4 Tensile Testing

Test specimen was prepared for the cast samples of both alloys. Samples were also prepared for the solution heat treatment of Al-Si-Mg and Al-Si-Cu alloys. Artificially aged tensile test samples were also prepared for the copper containing samples at two different artificially aged temperatures of 155 °C and 165 °C. Artificially aged tensile test samples were also prepared for the magnesium containing alloys for ageing at 160 °C and 170 °C.

3.4.1 Sample preparation

The samples were prepared to the right standard for tensile testing by a Centre lathe machine. Figure 3-8 below shows the schematic of a sample after machining operation with the Centre lath.

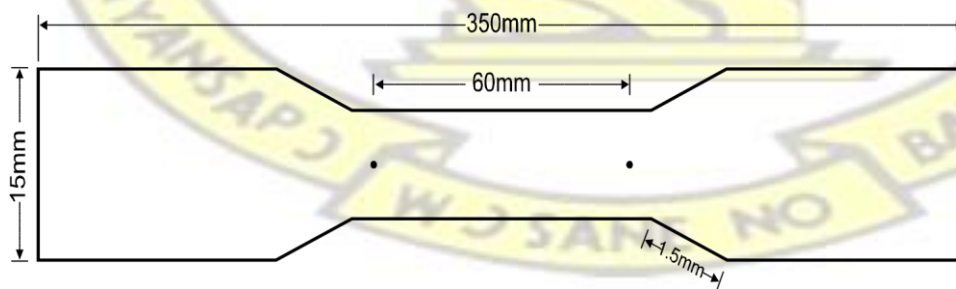


Figure 3-8 Schematic diagram of tensile test sample

3.4.2 Tensile test

All specimens were machined according to the schematic in Figure 3-8 above and tested in a computer controlled tensile testing machine (CONTROLS) at the Ghana Standards Authority, Accra. The specimen was placed in the hydraulic controlled jaws of the tensile machine and pulled to fracture. An internal extensometer was used to measure the extension to get the percentage elongation. The gauge length was set to 60 mm.

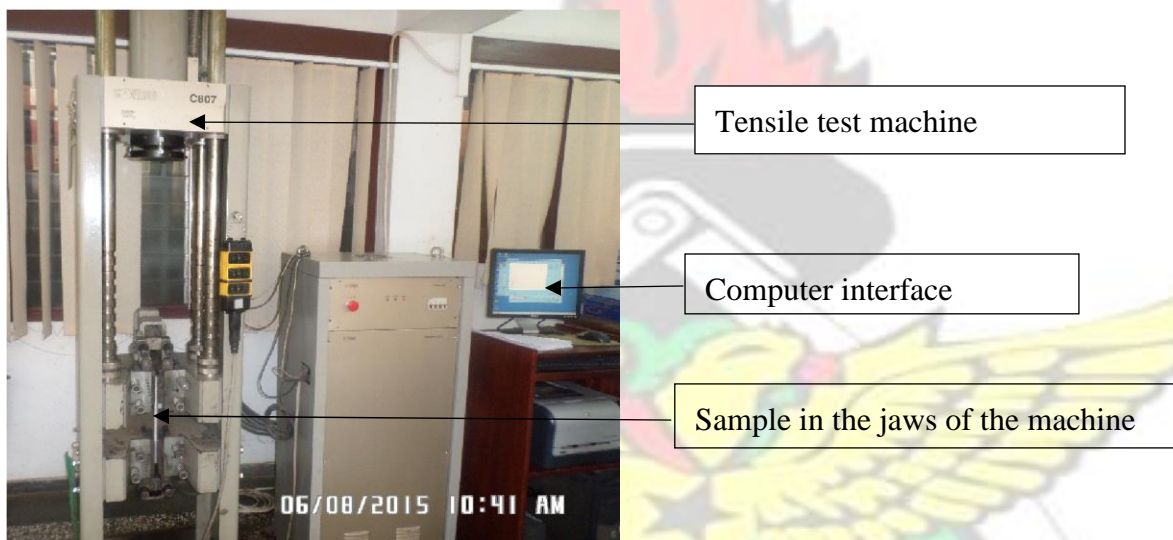


Figure 3-9 Picture of sample in the tensile testing machine

3.5 Charpy Impact Test

The impact testing samples were made up of the solution heat treat samples of both Al-Si-Cu and Al-Si-Mg and artificially aged samples of Al-Si-Cu for temperatures 155 °C and 165 °C and AlSi-Mg samples of artificial ageing temperatures of 160 °C and 170 °C. The two batches of samples were produced into square prisms using the shaping machine for accuracy and repeatability of contour. The dimensions of the square prism as given by the American Society for Testing and

Materials (ASTM): B 108 Standards are 10 mm x 10 mm x 55 mm. A V-notch of depth 2 mm and base radius 0.25 mm and angle opening of 45 °C were cut in the mid-section of the length of the samples. Impact testing of the samples was performed using the Tinius Olsen machine.

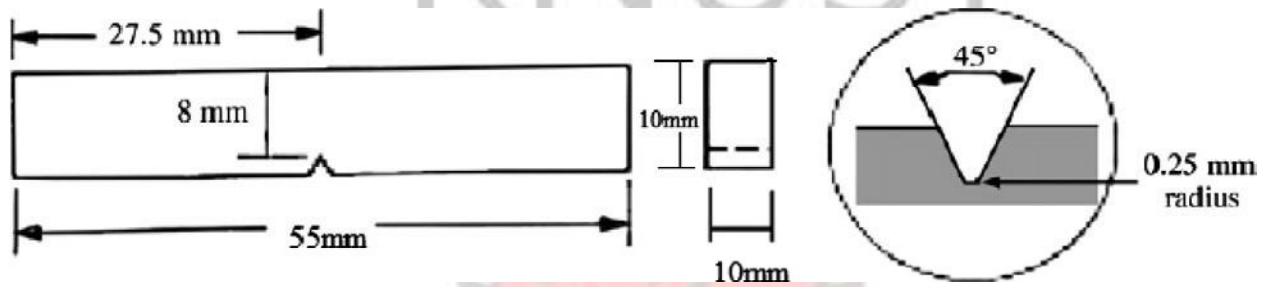


Figure 3-10 Schematic of impact test sample

3.6 Impact Test

The sample in the form of square prism was clamped in the impact testing machine. The hammer was then released from a preset height to come and strike the sample on the opposite side to the notch. After the sample was broken the pendulum hammer swung on and the energy used in fracturing the specimen was read off a scale on the machine in joules.



(a)

(b)

Figure 3-11 Picture of (a) The Impact testing machine and (b) loading of sample

3.7 Microstructural Analysis

3.7.1 Specimen preparation

Both samples of the alloys were prepared for microstructural analysis. Microstructural analysis was conducted on the cast alloys, the solutionized samples and artificially age samples. Short cylindrical specimens which could stand flat on the table of the microscope were used for microstructural analysis by using the LEICA computer-interfaced microscope shown in Figure 3-12.

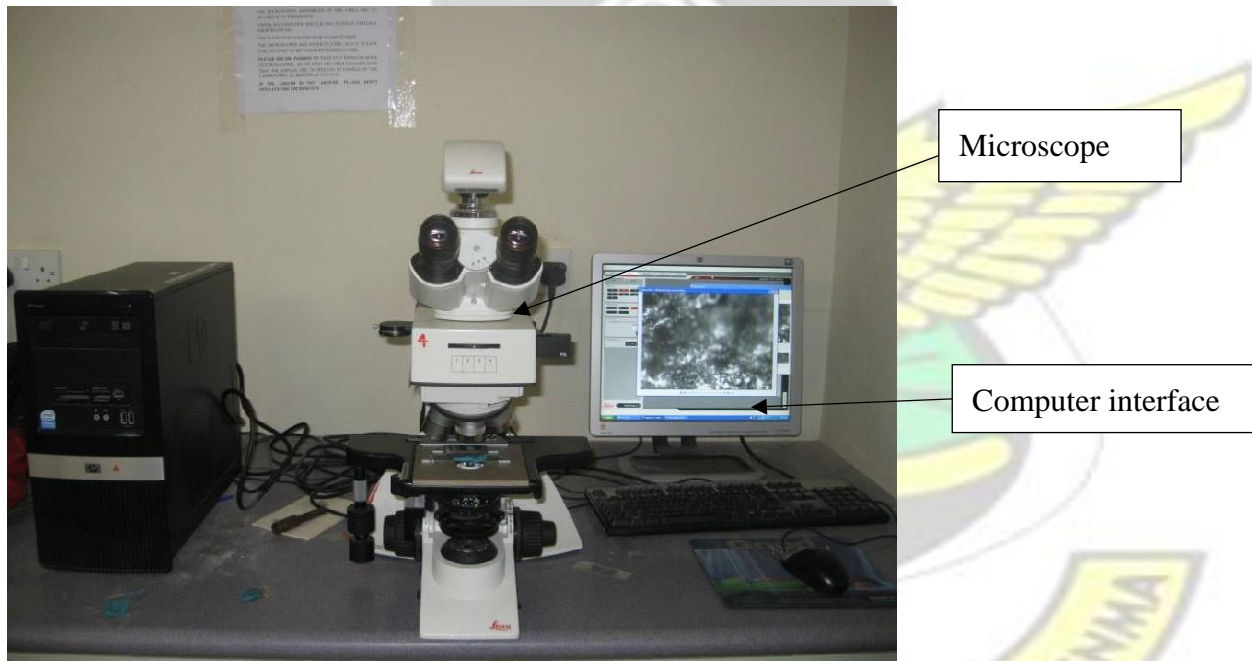


Figure 3-12 LEICA Microscope with computer interface

The microstructural analysis required a meticulous step by step process for preparation of the specimen. The samples were sectioned by using a hacksaw slowly and gently to reduce the roughness of the surface. Before the samples were to be mounted on the microscope, grinding

process was done by using SiC water proof abrasive papers of grits, 240, 400, 600 and 1000 in succession on electrically powered grinding wheels. Moving up the grits produces a very fine surface for the specimen. After grinding, each sample was washed thoroughly in water to remove any debris from the previous stage before proceeding to the next stage. After using the 1000 grits paper, the samples were washed very well. The first stage of sample polishing was later carried out on an electric- powered disc covered with nylon. 25 micron aluminum oxide particles suspended in water was periodically poured on the sample and nylon covering while the sample was gently pressed down on it against the direction of rotation of the disk. This stage removed the final grinding layer completely. Final polishing was done using a 5 micron aluminum oxide particles suspended in water. This process produced a very fine surface free of scratches, and ready to be etched. A new nylon cloth was used for each stage of polishing. After the polishing, the specimen was etched with KELLER'S reagent made up of (190 ml Distilled water+ 5 ml Nitric acid + 3 ml HCL+ 2 ml HF). The samples were agitated in the KELLER'S reagent for 60 seconds, rinsed in ethanol then later in distilled water. After, the samples were dried in air.

3.7.2 Microscopic examination

The samples were each mounted on the stage of the microscope (Leica DM 2500 M optical microscope) which is capable of producing magnification of (100X to 1000X). The specimen surface was perpendicular to the optical axis.

CHAPTER 4

RESULTS AND DISCUSSION

4.1 Chemical Analysis of Al-Si-Mg and Al-Si-Cu Alloys

Table 4-1 Elemental Compositions of Sand Cast Al-Si-Mg alloy (wt. %)

Al	Si	Fe	Cu	Mn	Mg	Zn	Ni	Ti	Li	Sr	V	
80.889	14.400	0.102	0.010	0.003		0.288	0.007	0.5233	0.002	0.000	0.008	0.014
B	Ca	Pb	Cr	GA	Sn	Zr	Be	Bi	Na	Cd	P	
0.000	0.001	0.000	0.000	0.008	0.000	0.001	0.000	0.000	0.000	0.000	3.749	

Table 4-2 Elemental Compositions of Sand Cast Al-Si-Cu alloy (wt. %)

Al	Si	Fe	Cu	Mn	Mg	Zn	Ni	Ti	Li	Sr	V	
78.806	14.445	0.214	2.688	0.004		0.002	0.0251	0.534	0.004	0.000	0.000	0.014
B	Ca	Pb	Cr	GA	Sn	Zr	Be	Bi	Na	Cd	P	
0.000	0.001	0.000	0.000	0.008	0.000	0.001		0.000	0.000	0.000	0.000	3.495

The data in Tables 4-1 and 4-2 were obtained from the chemical analysis carried out at Valco Ghana Limited. The main solid solution strengthener was found to be magnesium in Al-Si-Mg alloy which lead to an increase in the response to precipitation hardening (Abdulwahab et al., 2011). It combines with silicon to form magnesium silicide (Mg_2Si) which is the principal hardening phase (Fatai Olufemi, 2012). Binary Al-Si alloys are non-heat treatable, changes in Si solubility in the aluminium with temperature does not change this non-heatreability. Additional

alloying of binary Al-Si alloys with magnesium and copper makes these alloys susceptible to quenching and ageing (Zolotarevsky, Belov, and Glazoff, 2007). The silicon, magnesium and copper compositions were within expected values.

4.2 Microstructural Evaluation

4.2.1 Microstructure evaluation of Al-Si-Mg alloys

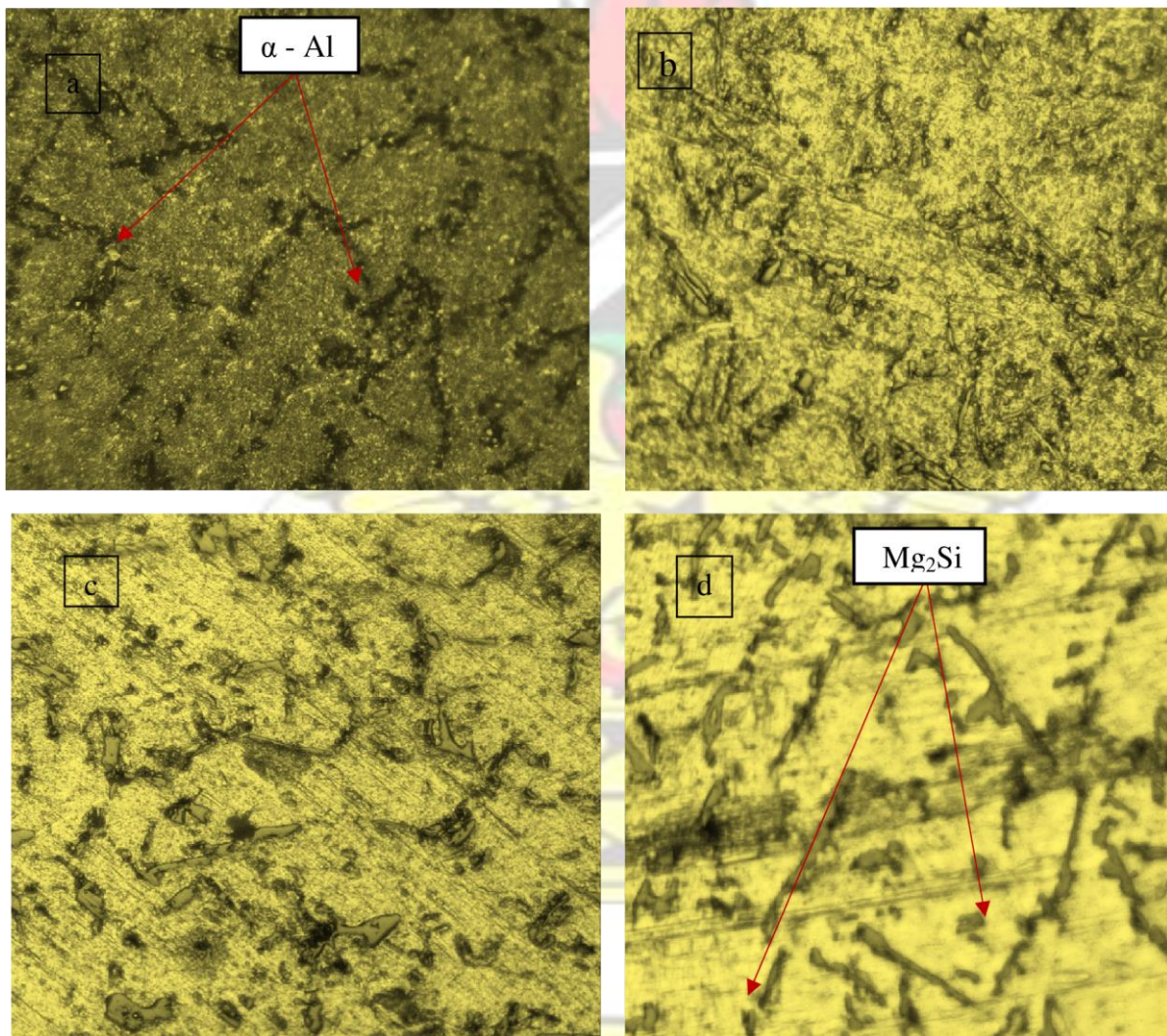


Figure 4-1 Optical microstructures of Al-Si-Mg (a) as cast (b) SHT for 6 hours (c) aged 2 hours and (d) aged 3 hours at 170 °C (x200).

The microstructures in Figure (4-1) show how heat treatment changes the microstructure of AlSi-Mg alloys used in this research work. Figure 4-1 (a) shows the as-cast microstructure which is made up of α -Al dendrites. Figure 4-1 (b) shows a supersaturated alloy microstructure with trapped solid solutes after solution heat treatment. Figure 4-1 (c) shows precipitates forming after age hardening for 2 hours. Figure 4-1 (d) shows more precipitates forming after 3 hours of ageing. The Mg_2Si is the principal hardening phase and precipitates of this structure in the microstructure results in increase in tensile and yield strength of the alloy as well as hardness (Fatai Olufemi, 2012). This precipitates impede dislocation movements (Abdulwahab et al., 2011).

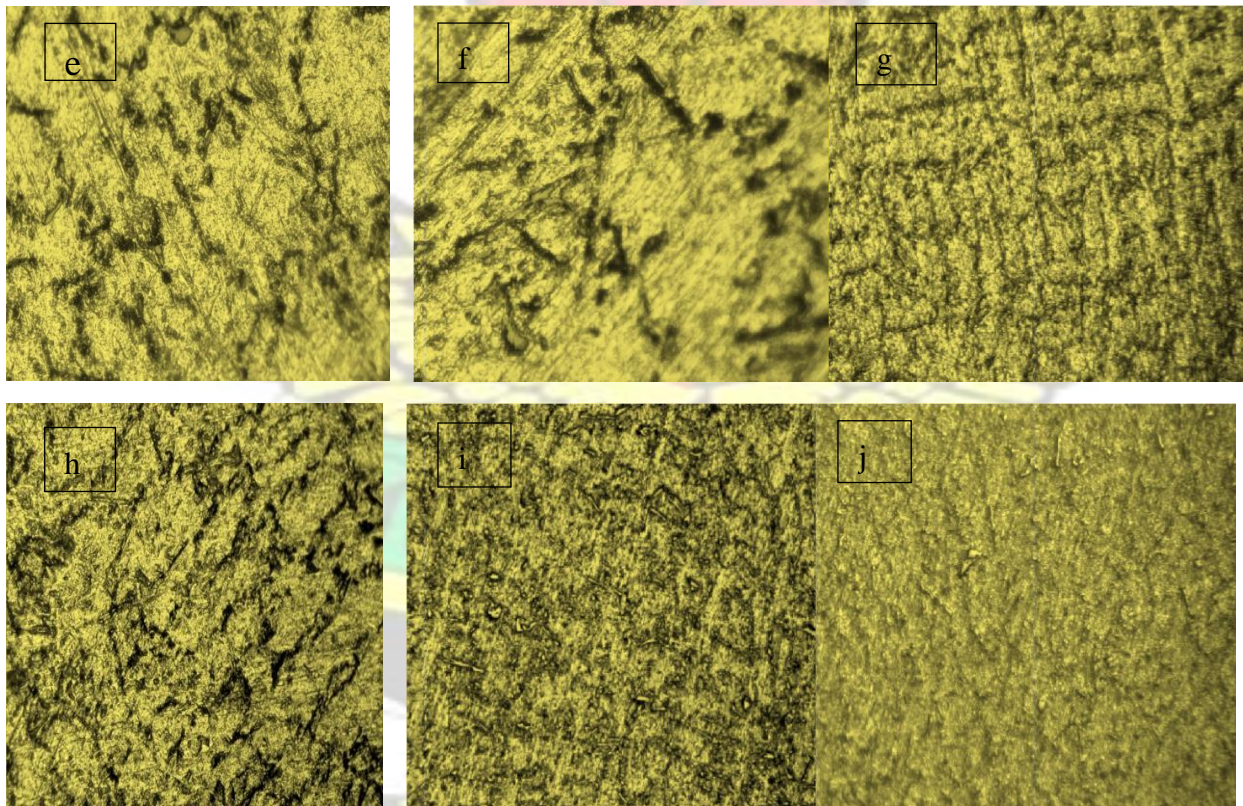


Figure 4-2 Optical microstructures of Al-Si-Mg alloy (e)1 hour (f) 4 hours (g) 5 hours (h) 6 hours (i) 7 hours and (j) 8 hours at 160 °C (x100)

4.2.2 Microstructural evaluation of Al-Si-Cu alloy

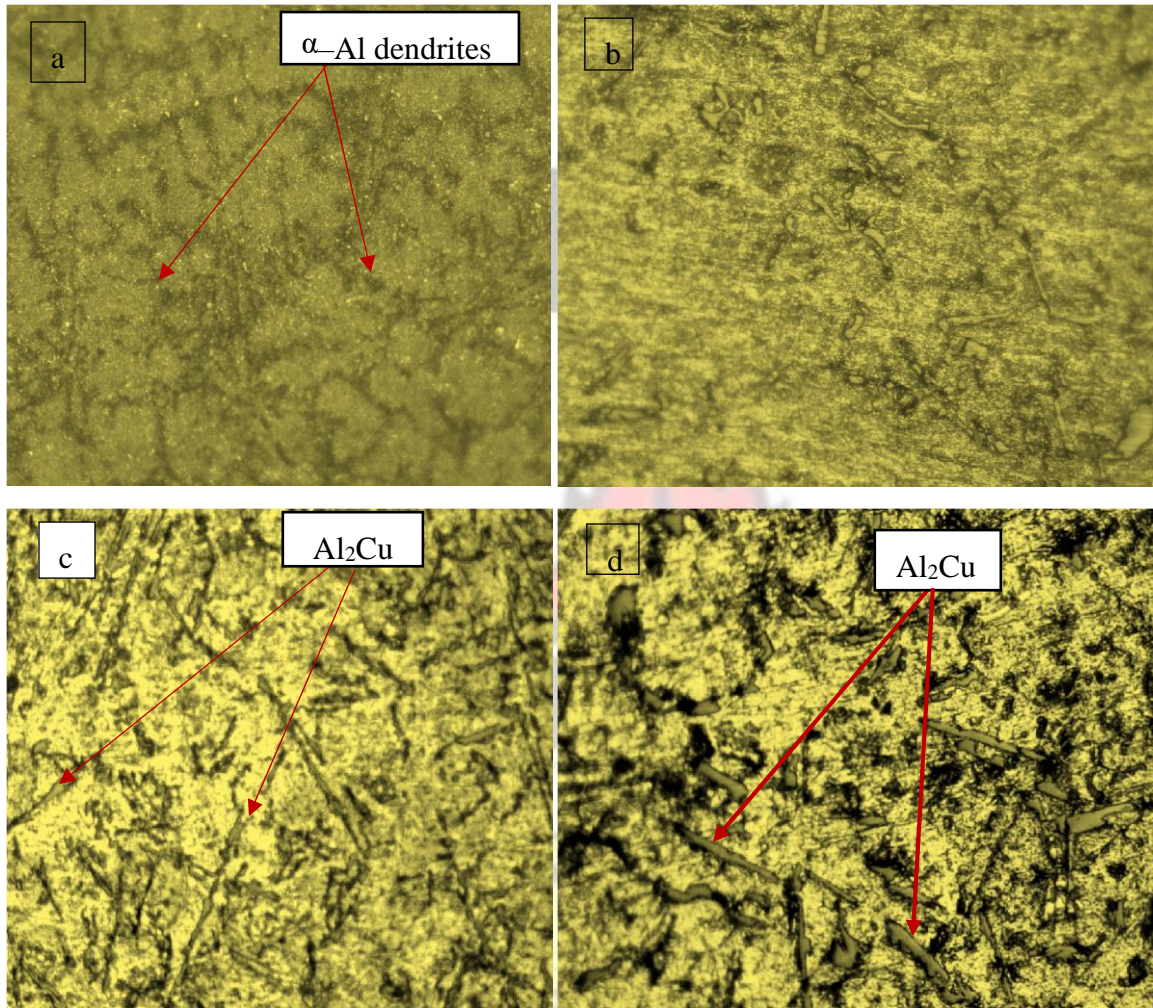


Figure 4-3 Optical microstructures of Al-Si-Cu (a) as cast (b) SHT for 6 hours (c) aged for 4 hours (d) aged for 6 hours at 165 °C (x200)

Figure 4-3 (a), depicts a microstructure of α -Al dendrites. This structure was changed significantly when the Al-Si-Cu alloy was subjected to a solution heat treatment at 480 °C for 6 hours. Figure 4-3 (b) shows supersaturated alloy microstructure with trapped solid solutes after solution heat treatment. Figure 4-3 (c) shows precipitate forming. Figure 4-3 (d) shows precipitates formed after 6 hours of ageing. These dispersed precipitates of Cu_2Al in the microstructure impede dislocation movement, therefore giving strength to the alloy (Sjölander and Seifeddine, 2010).

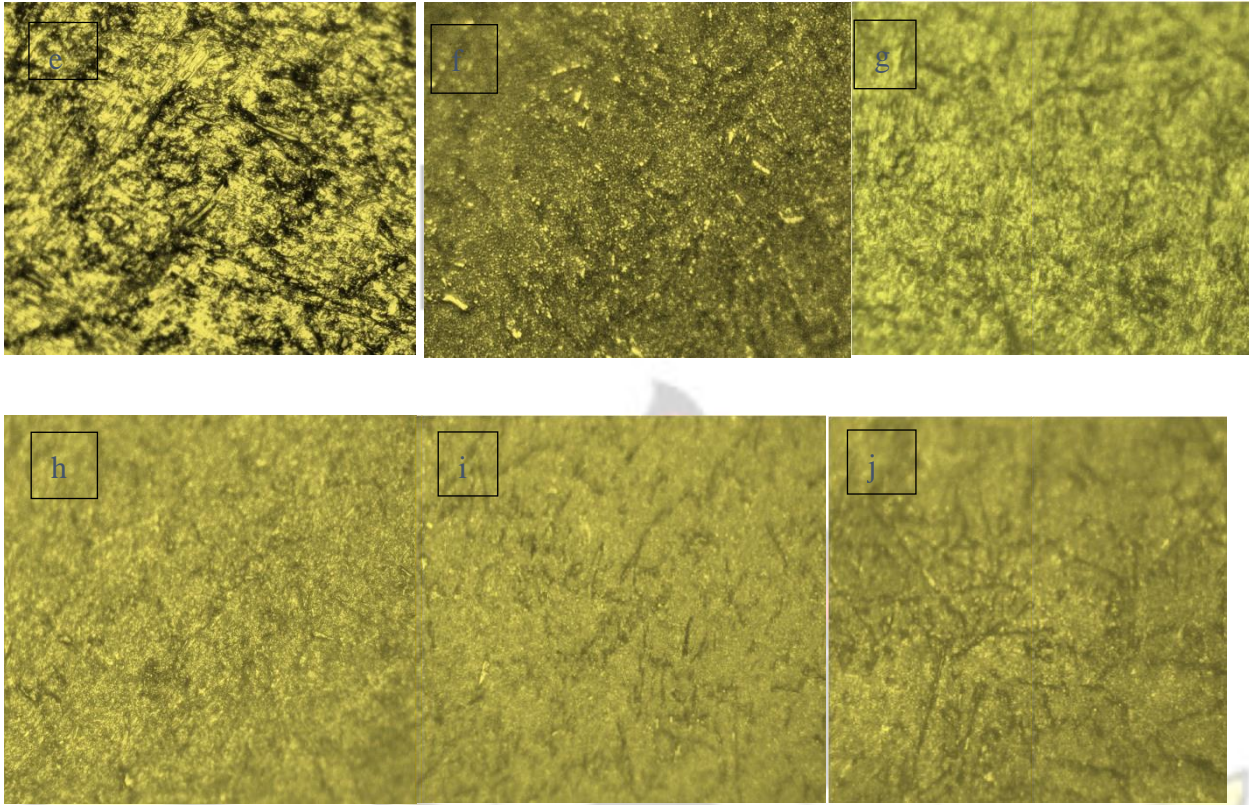


Figure 4-4 Optical microstructures of Al-Si-Cu (e) 1 hour (f) 2 hours, (g) 3 hours, (h) 5 hours, (i) 7 hours and (j) 8 hours at 155 °C (x100)

4.3 Mechanical Properties

4.3.1 Tensile properties of Al-14%Si-0.288Mg

Tensile test is a common method used in quantifying the mechanical property of aluminium alloys.

Tensile properties of Al-Si-Mg alloys are dependent on their microstructures and porosity.

TENSILE TEST - ASTM A370 / EN 10002 - STRESS/STRAIN GRAPH

Client: EBENEZER DONKOH KNUST

Label: AL-SI-MG AS IT IS

Test date: 2015 06-03

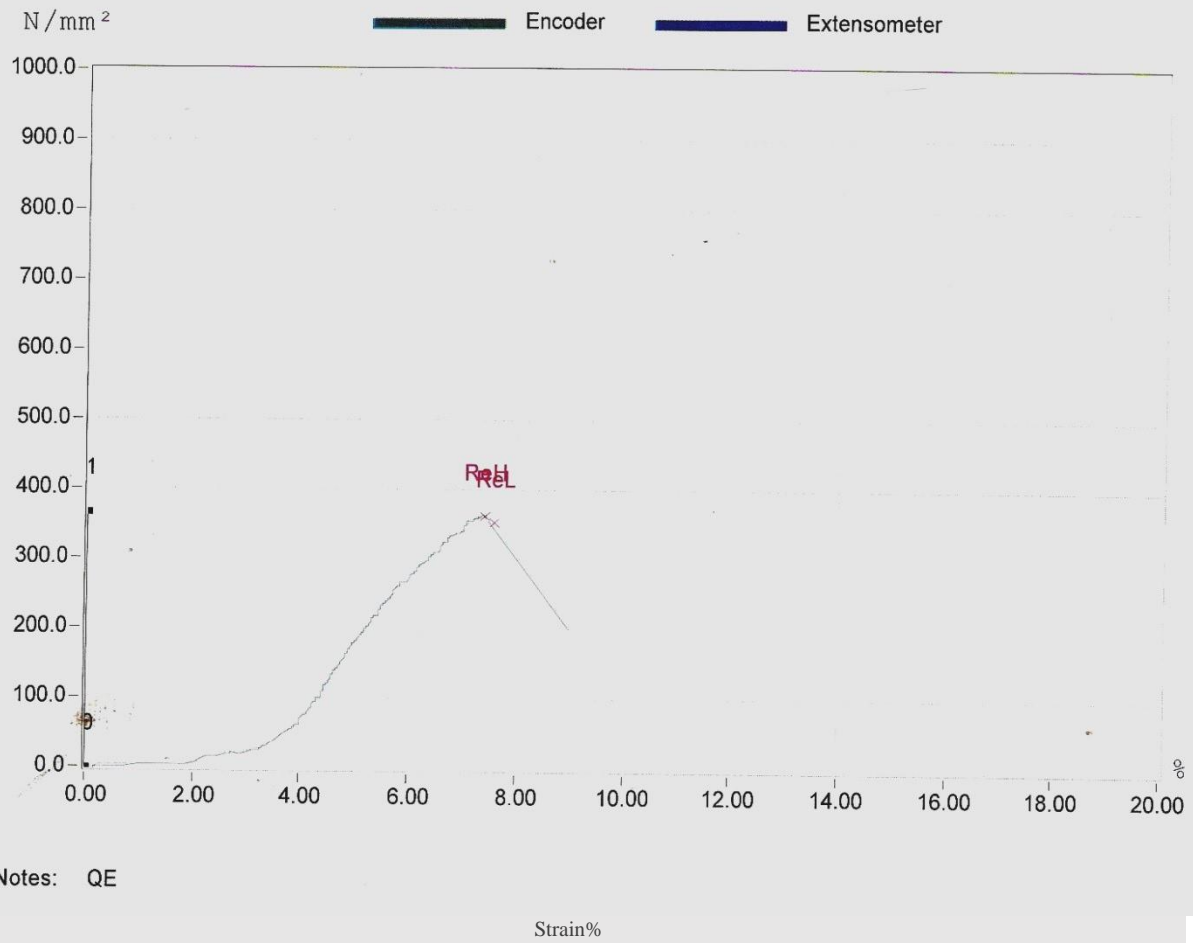
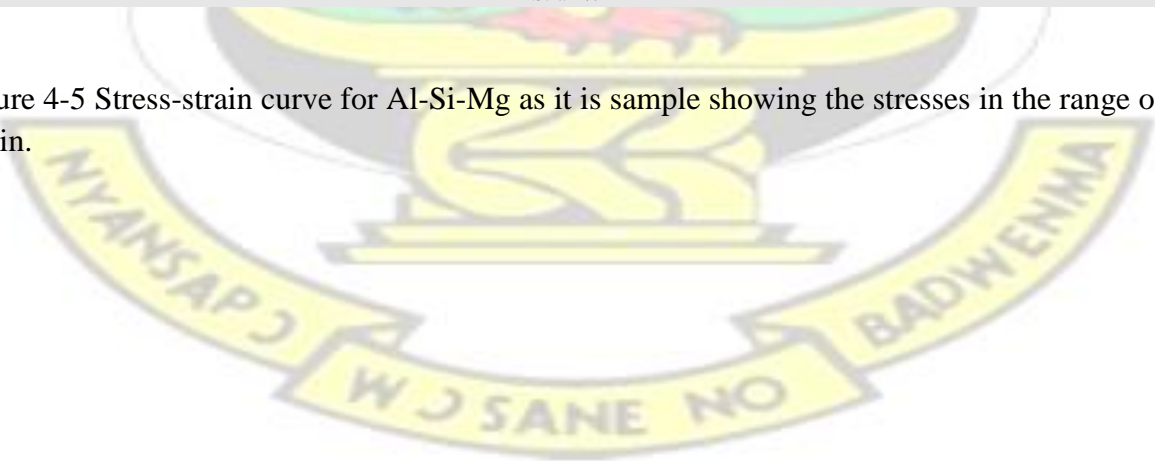


Figure 4-5 Stress-strain curve for Al-Si-Mg as it is sample showing the stresses in the range of the strain.



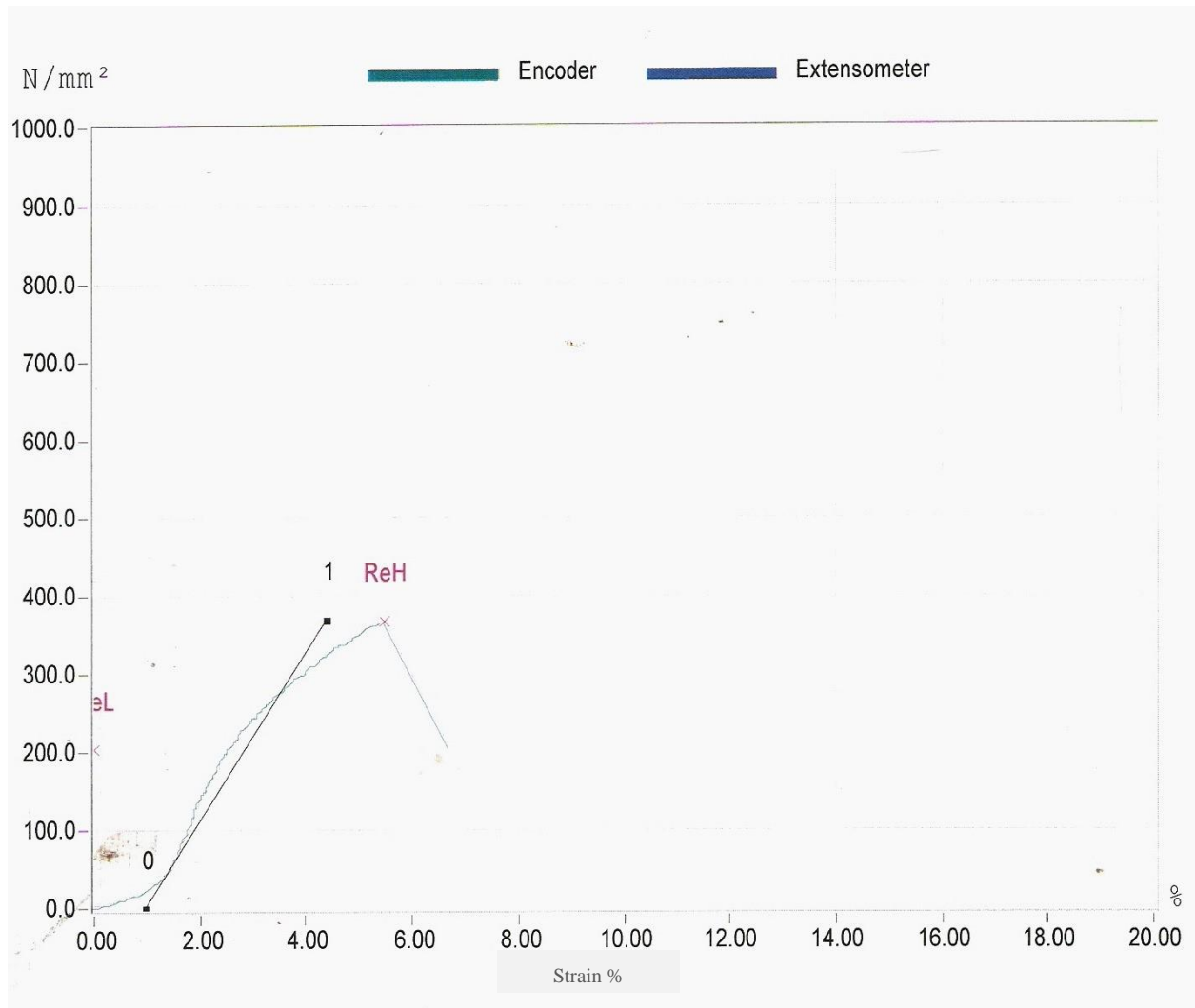


Figure 4-6 Stress-strain curve of Al-Si-Mg alloy Solution Heat treated at 530 °C for 6 hours sample, showing the stresses in the range of the strain.

Some key mechanical properties such as ultimate tensile strength and ductility (measured in terms of percentage elongation) were determined from the curves of Figure 4-5 and Figure 4-6. The yield and elastic modulus could not be determined directly due to the tensile machine being coded to steel. From the plots, the as it is Al-Si-Mg alloys showed high ultimate tensile strength and low percentage elongation than the solution heat treated sample. The decrease in ultimate tensile strength is attributed to slow cooling rate during quenching of the sample which causes

particles to precipitates heterogeneously at grain boundaries or at the dislocations; resulting in a decrease in the super saturation of solute atoms and resulting in reduction in ultimate tensile strength (Ishak, Amir, and Hadi, 2013).

The following stress-strain plots show the effects of heat treatment time on the ultimate tensile strength and the ductility (measured in percentage elongation) at temperature 170 °C.

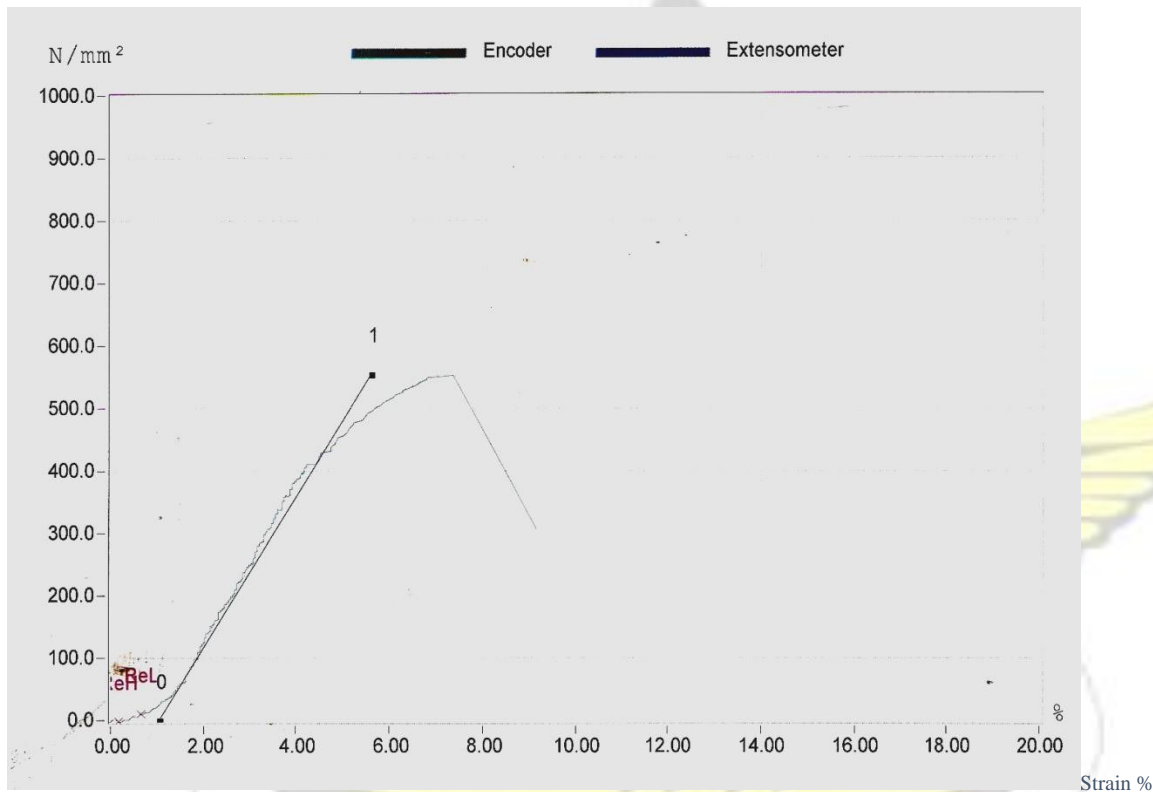


Figure 4-7 (a) Stress-strain graph for Al-Si-Mg alloy at 170 °C artificially aged for 1 hour

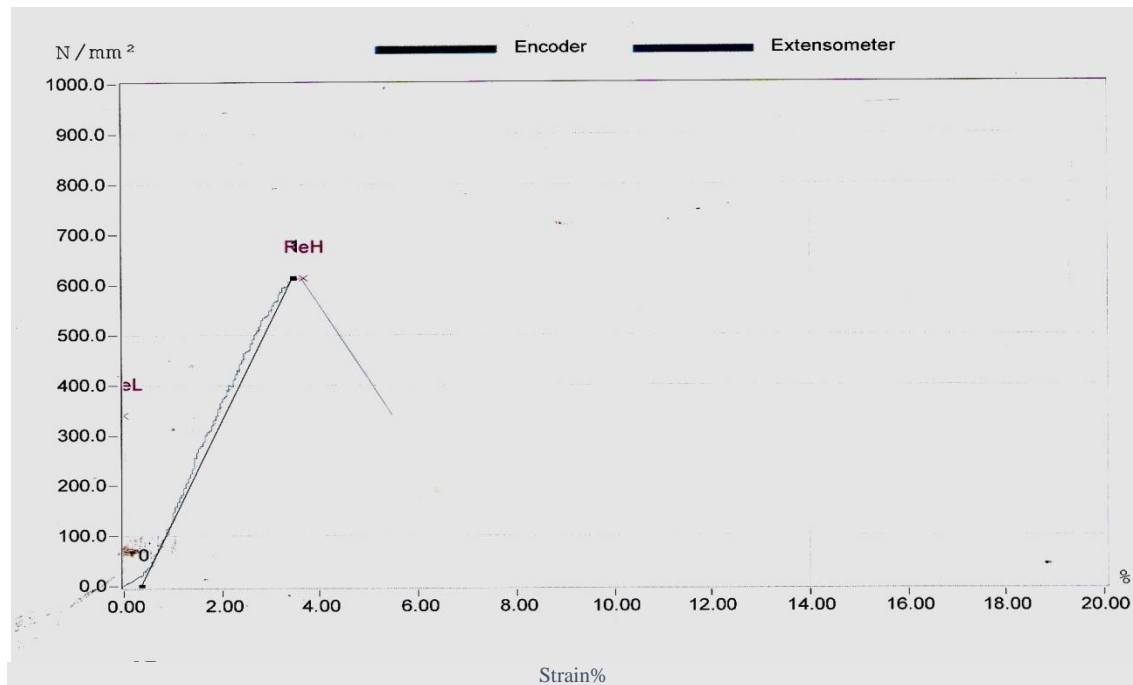


Figure 4-8 Stress-Strain plot of Al-Si-Mg alloy at 170 °C artificially aged for 2 hours

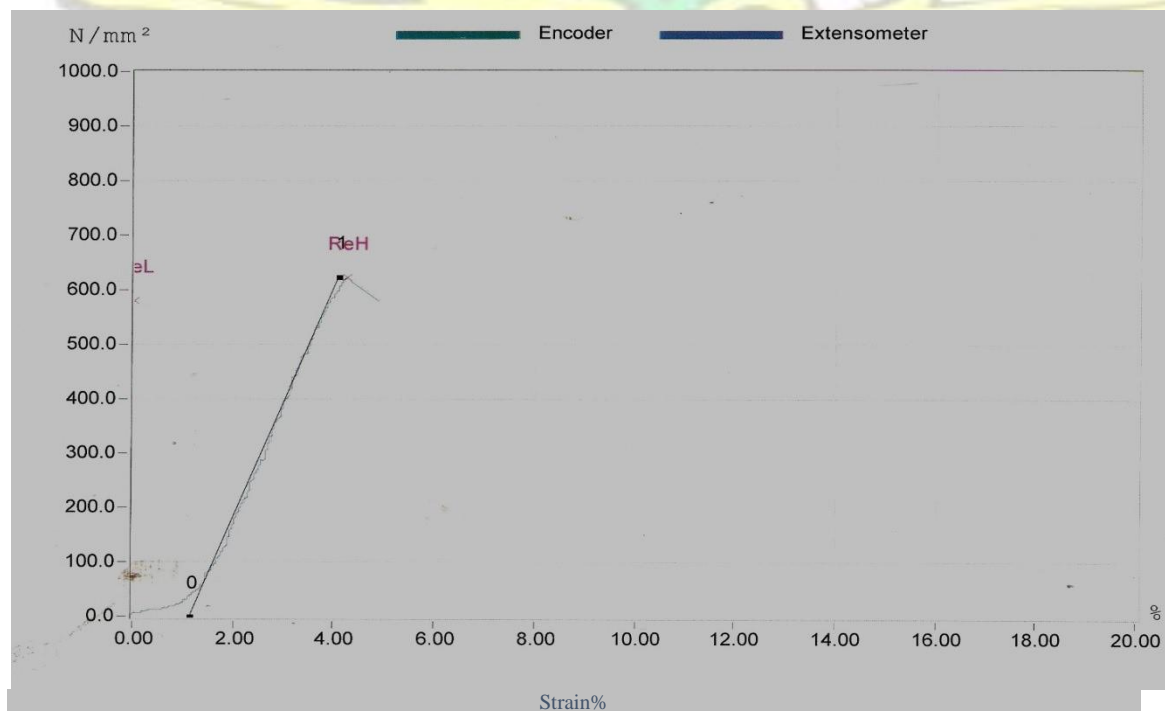


Figure 4-9 Stress-strain plot of Al-Si-Mg alloy at 170 °C artificially aged for 3 hours

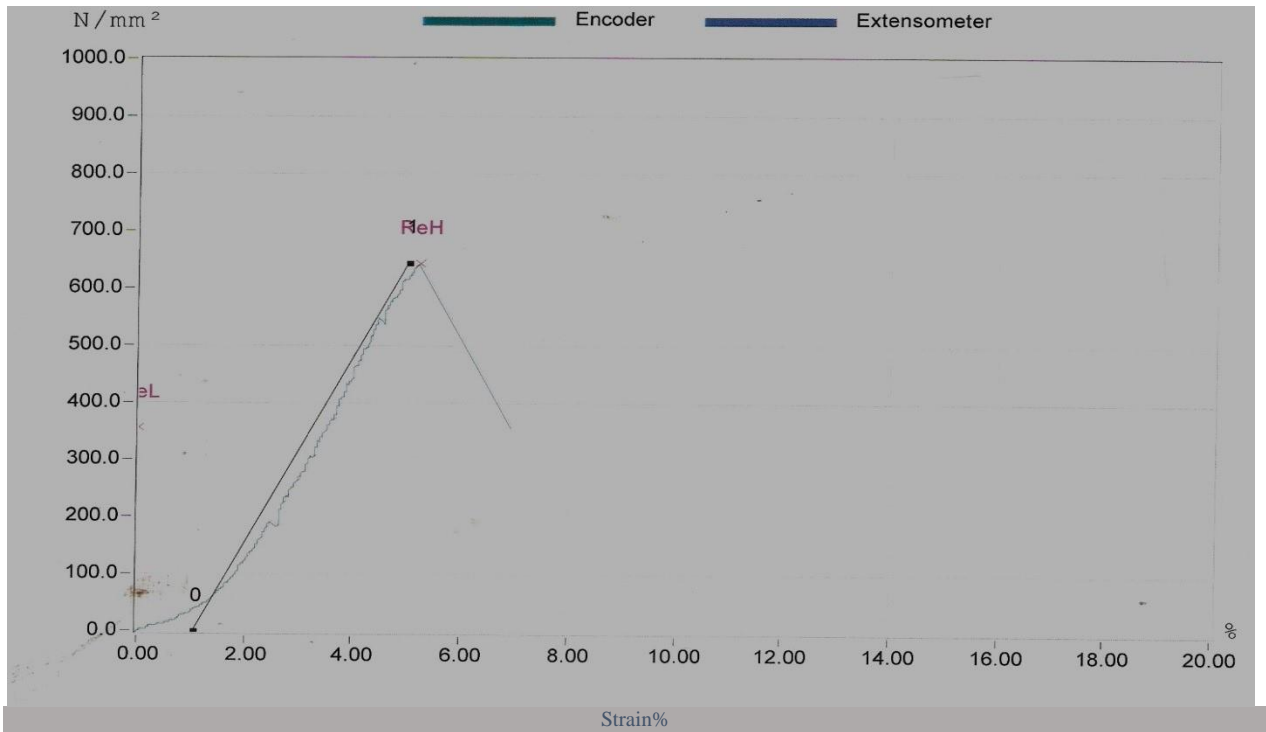


Figure 4-10 Stress-strain plot of Al-Si-Mg alloy at 170 °C artificially aged for 4 hours

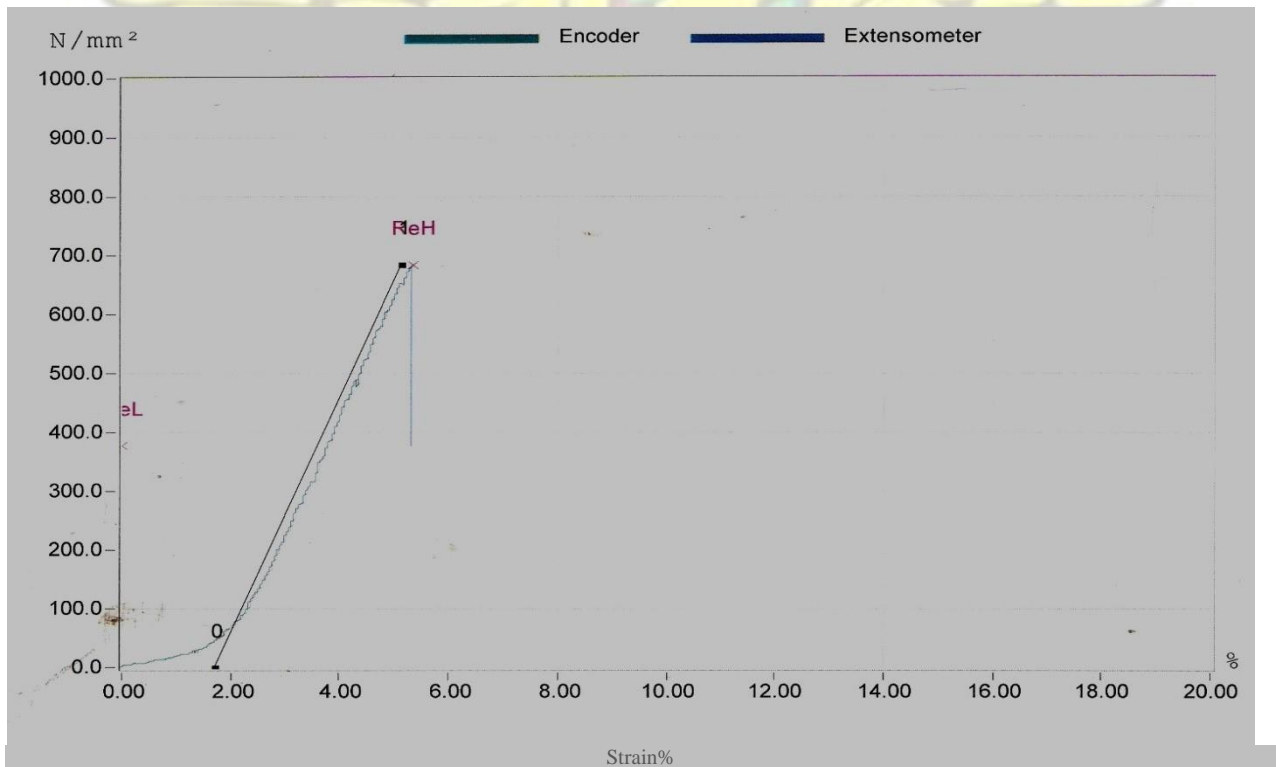
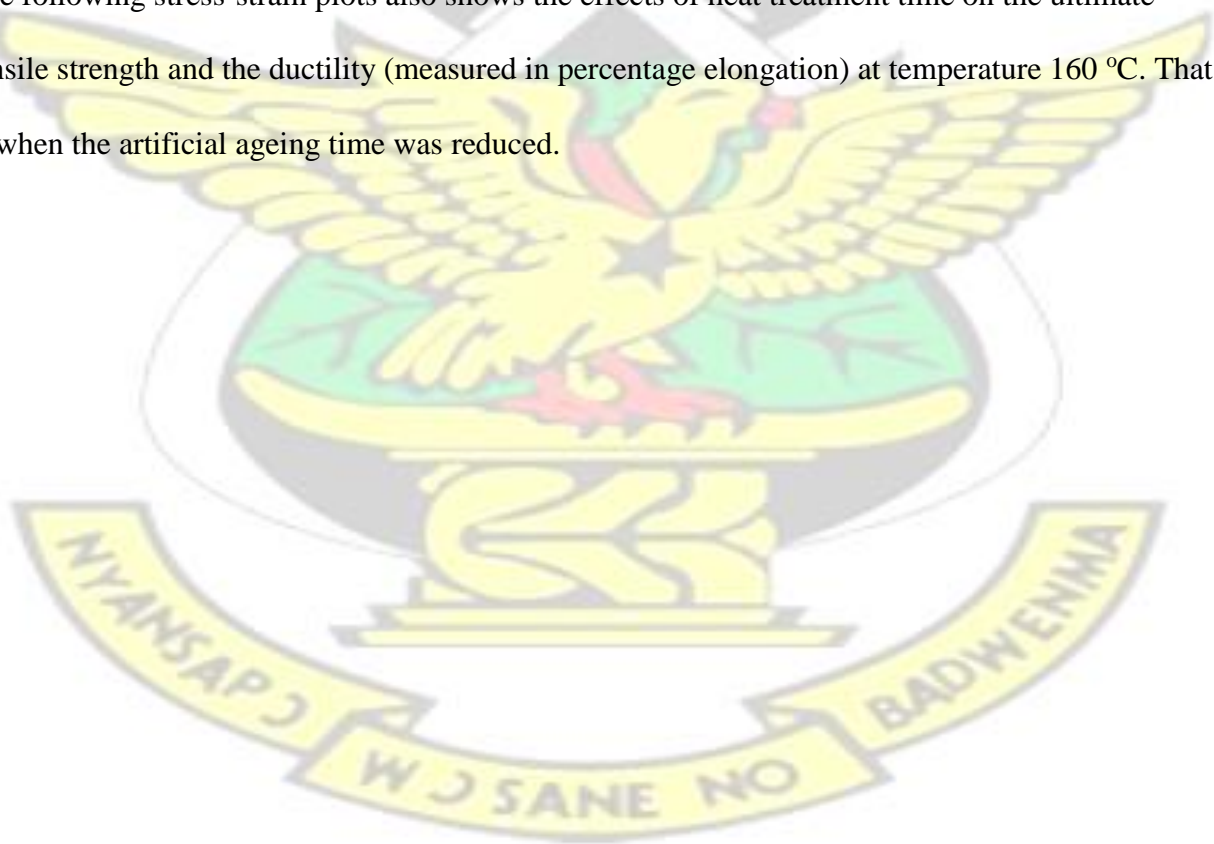


Figure 4-11 Stress-strain plot of Al-Si-Mg alloy at 170 °C artificially aged for 5 hours.

From Figure 4-7 to Figure 4-11, it was observed that as the artificial ageing time was increased from the first hour through to the fifth hour, the stress increased with a corresponding decrease in elongation. The alloy at this time and temperature produces UTS which is due to the accelerated production of Mg_2Si and other strengthening phases. Clusters are formed which impede the movement of dislocations therefore high UTS is recorded (Abdulwahab et al., 2011). As the strength increases the elongation is also reduced. The highest stress was recorded at the fifth hour for the Al-Si-Mg alloy artificially aged for 1 hour to the 8 hour. The remaining graphs for the AlSi-Mg alloys artificially aged at 170 °C can be found in the appendix.

The following stress-strain plots also shows the effects of heat treatment time on the ultimate tensile strength and the ductility (measured in percentage elongation) at temperature 160 °C. That is when the artificial ageing time was reduced.



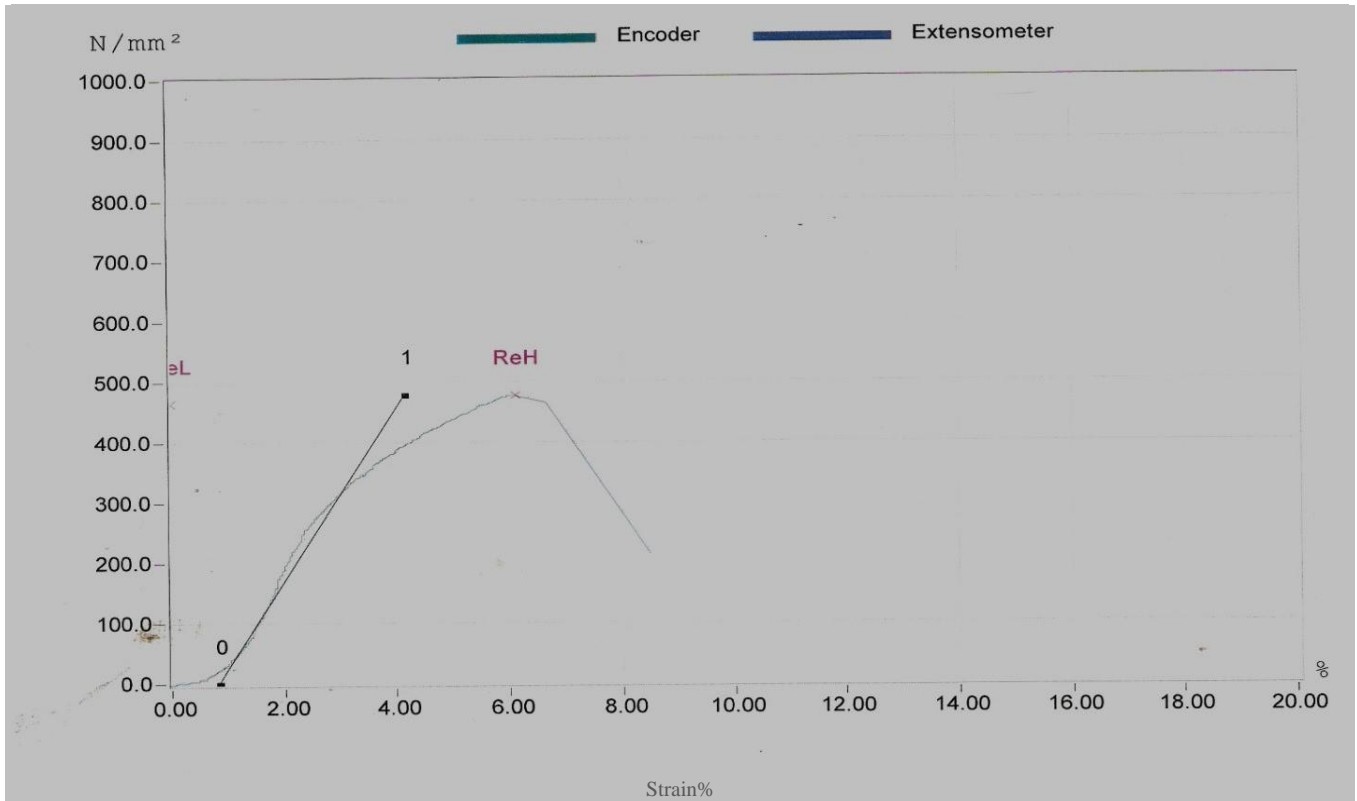


Figure 4-12 Stress-strain plot of Al-Si-Mg alloy at 160 °C artificially aged for 1 hour

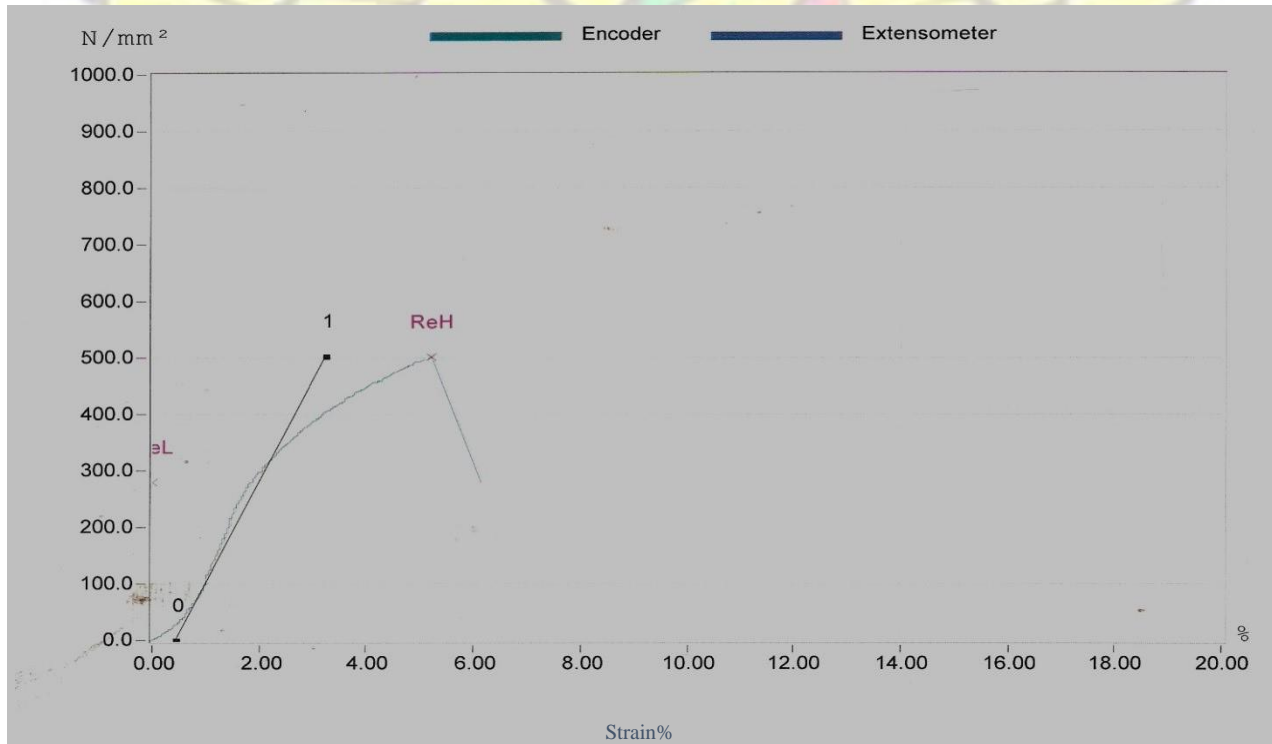


Figure 4-13 Stress-strain plot of Al-Si-Mg alloy at 160 °C artificially aged for 2 hours

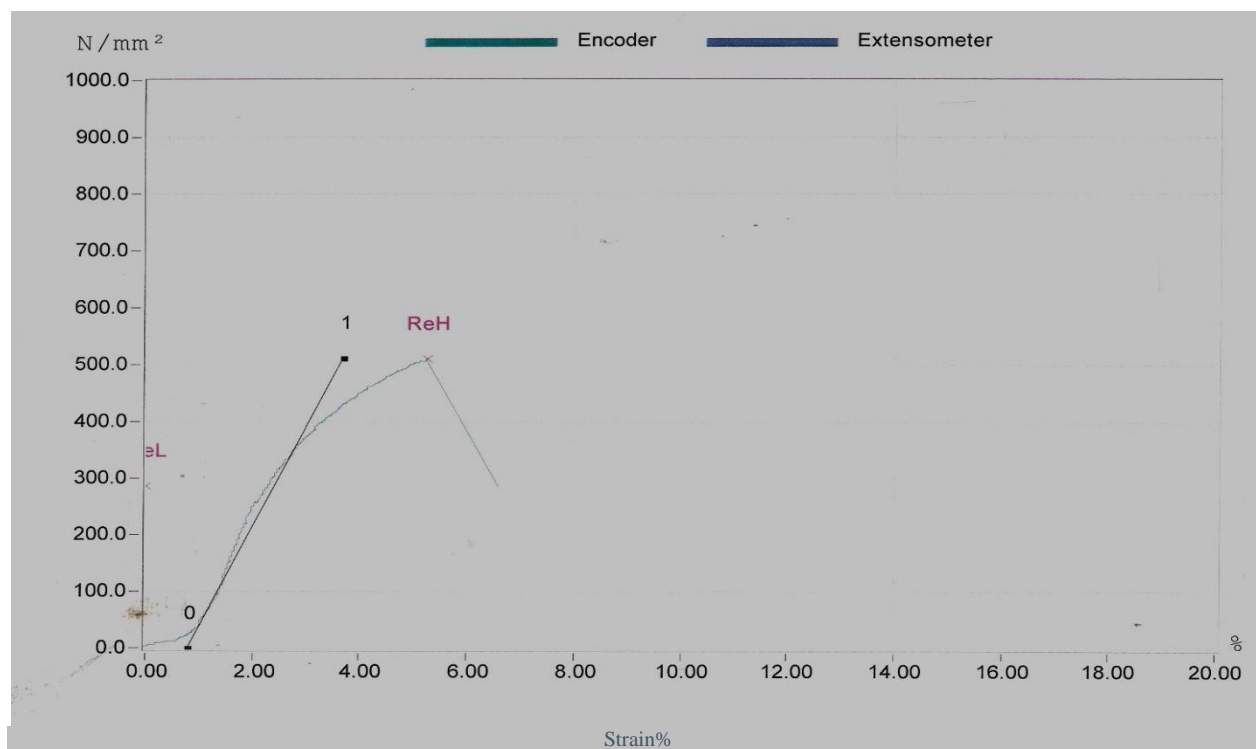
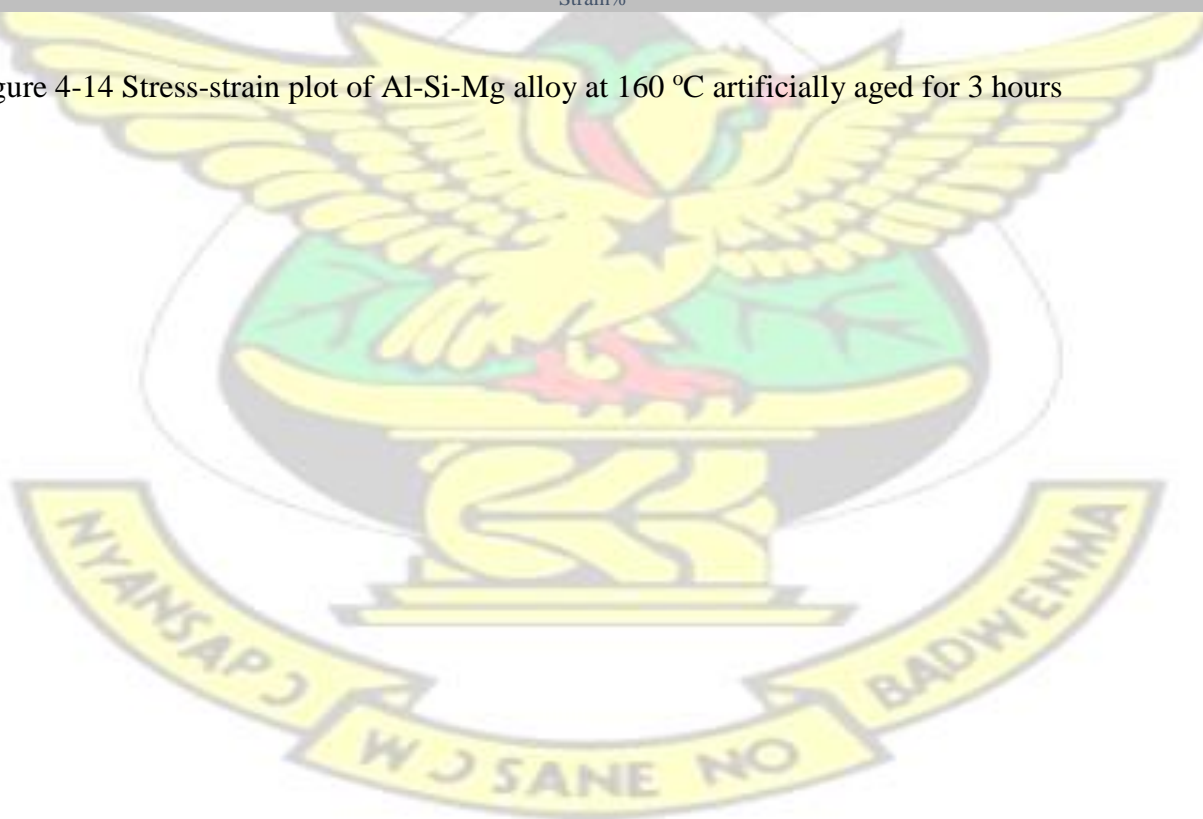


Figure 4-14 Stress-strain plot of Al-Si-Mg alloy at 160 °C artificially aged for 3 hours



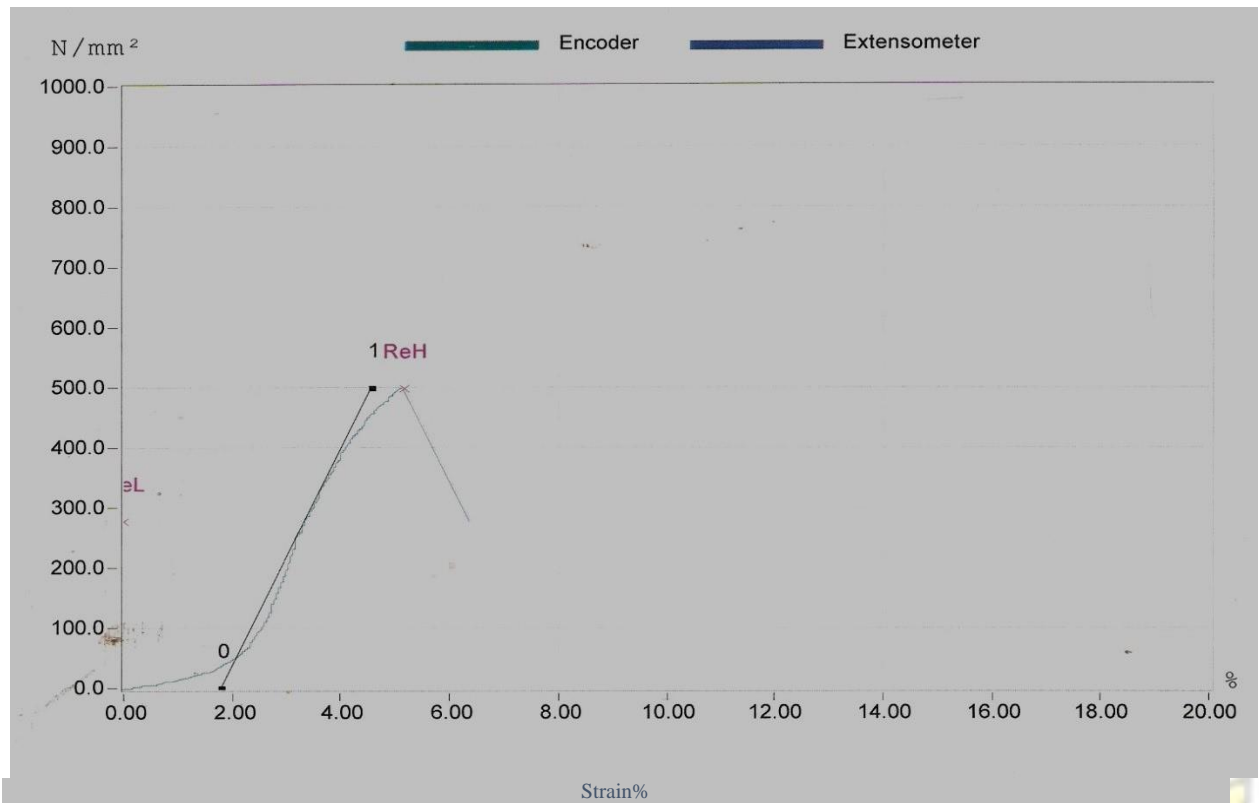
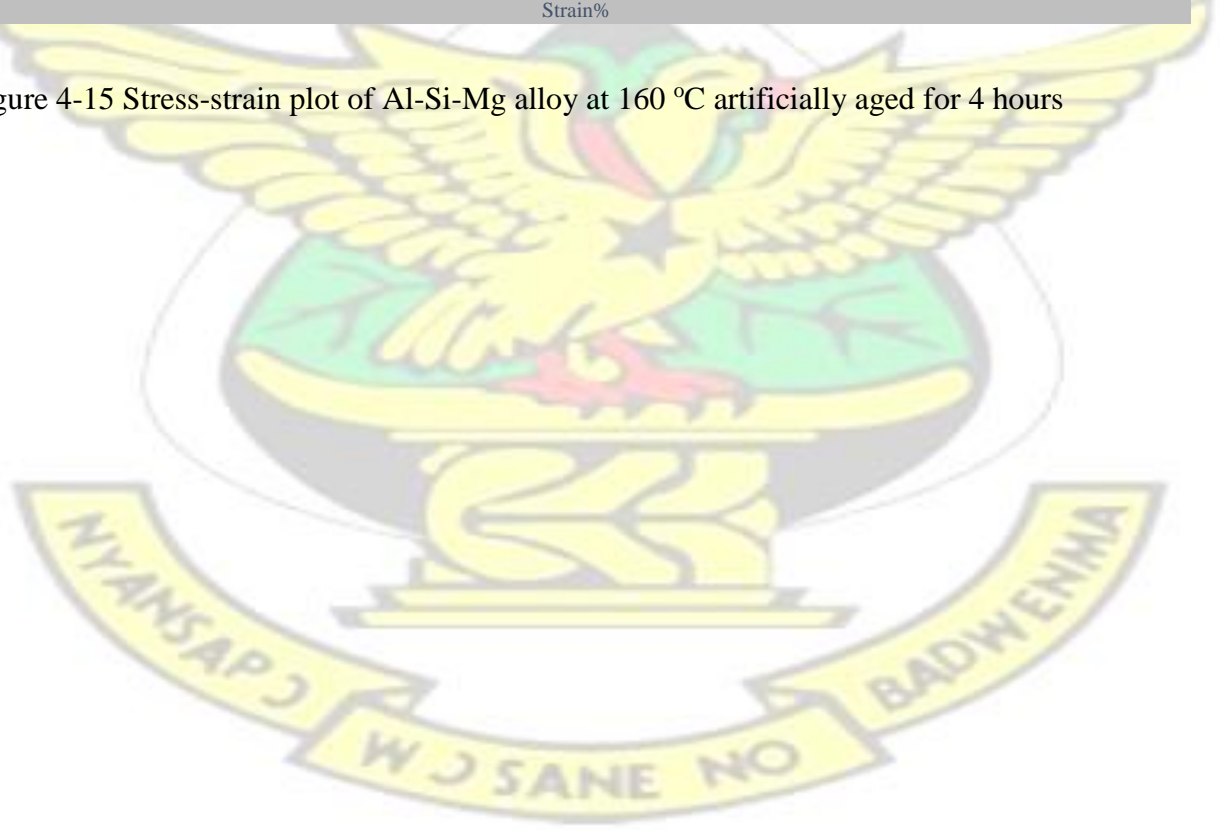


Figure 4-15 Stress-strain plot of Al-Si-Mg alloy at 160 °C artificially aged for 4 hours



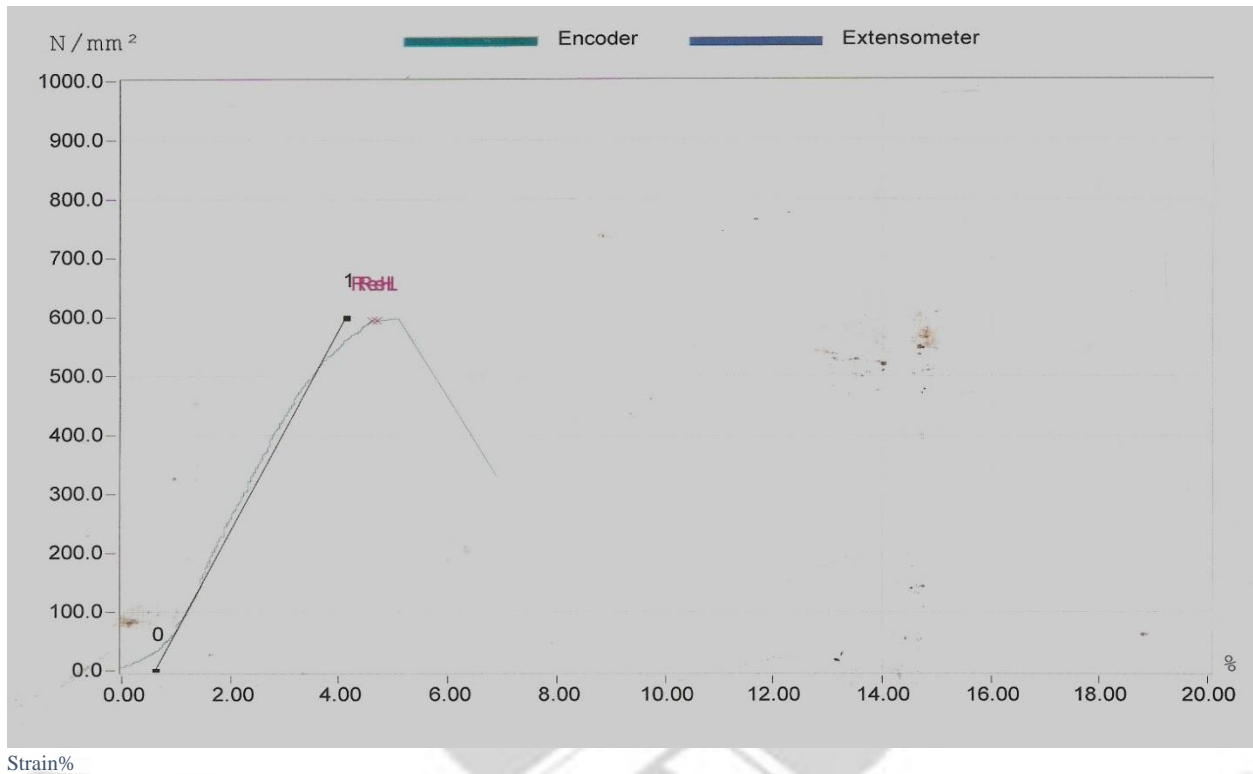
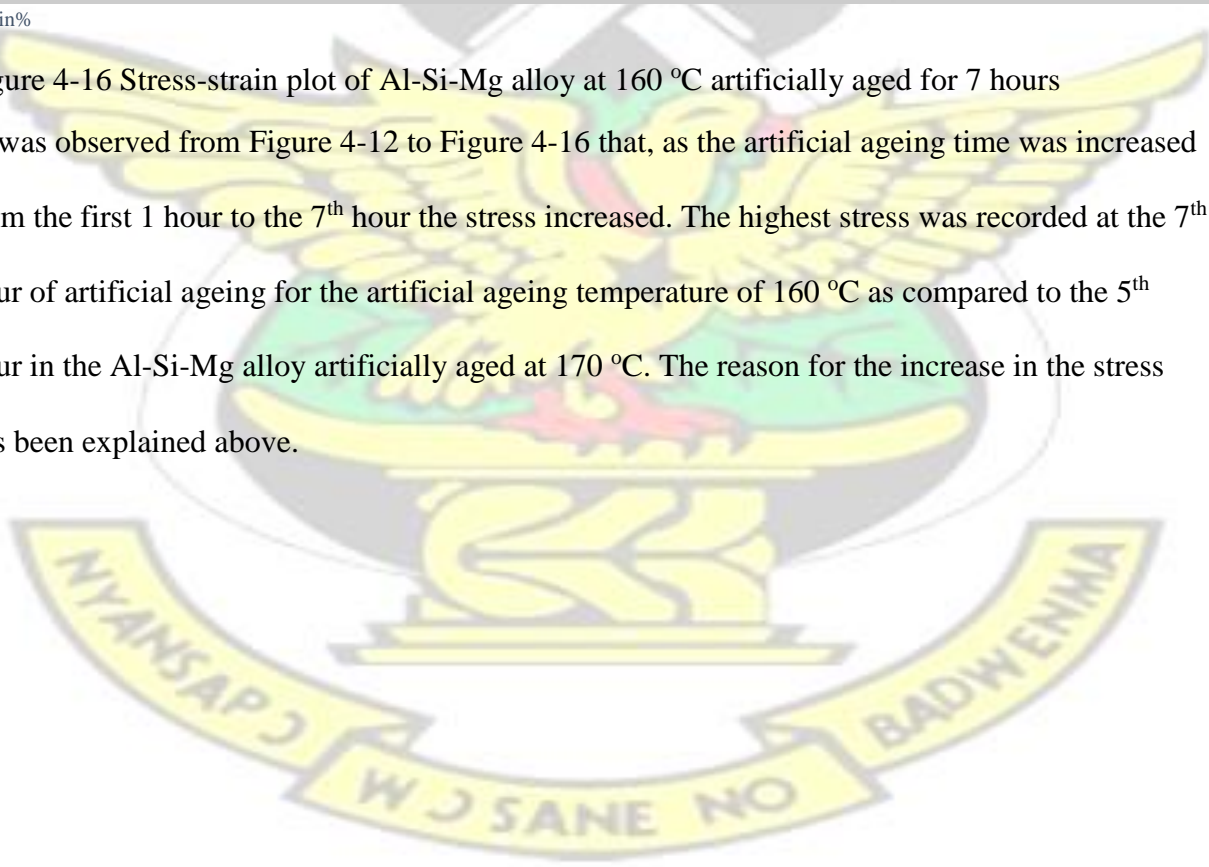


Figure 4-16 Stress-strain plot of Al-Si-Mg alloy at 160 °C artificially aged for 7 hours

It was observed from Figure 4-12 to Figure 4-16 that, as the artificial ageing time was increased from the first 1 hour to the 7th hour the stress increased. The highest stress was recorded at the 7th hour of artificial ageing for the artificial ageing temperature of 160 °C as compared to the 5th hour in the Al-Si-Mg alloy artificially aged at 170 °C. The reason for the increase in the stress has been explained above.



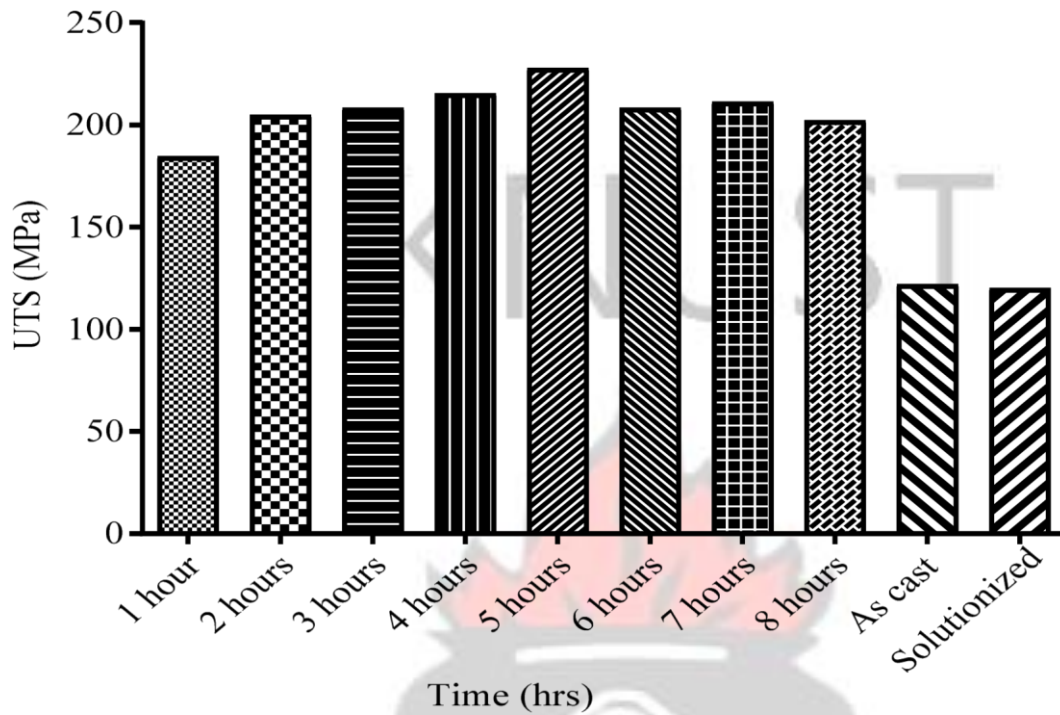


Figure 4-17 Composite bar charts of UTS of as cast, solutionized and ageing time between 1 and 8 hours for Al-Si-Mg alloy at 170 °C.

Figure 4-17 depicts a composite ultimate tensile strengths for the as cast, solution heat treated sample and all artificial ageing time used in the work. This bar chart helps to understand how the T6 heat treatment has improved the ultimate tensile strength of the material (Al-Si-Mg) alloy at 170 °C.

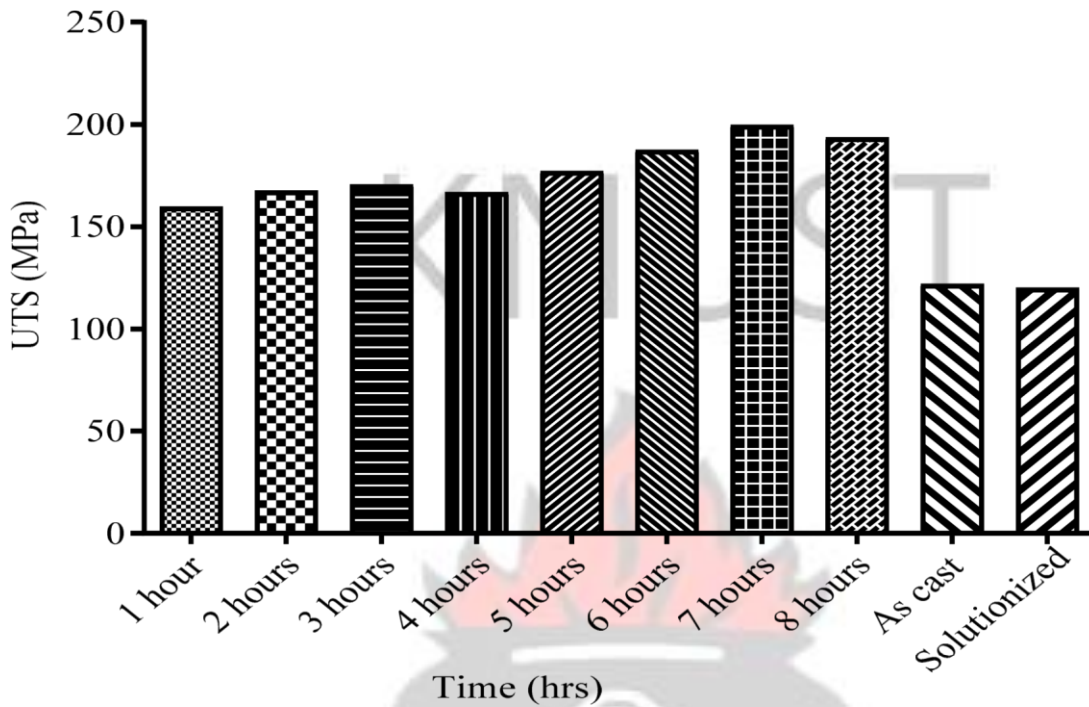


Figure 4-18 Composite bar charts of UTS of as cast, solutionized and ageing time between 1 and 8 hours for Al-Si-Mg alloy at 160 °C.

Figure 4-18 depicts a composite graph of ultimate tensile strengths for the as cast, solution heat treated sample and all artificial ageing time used in the work. This bar chart helps to understand how the T6 heat treatment has improved the ultimate tensile strength of the material (Al-Si-Mg) alloy at 160 °C. It was observed that as the ageing temperature is increased the UTS value also increases. Looking at the two graphs and comparing them the bars for the 170 °C in Figure 4-17 were a little bit higher than that of the 160 °C samples.

Table 4-3 Tensile properties of Al-14%Si-0.288Mg as cast, SHT, Peaked aged at 160 °C and 170 °C respectively

<u>Alloy</u>	<u>Condition</u>	<u>Time(hrs)</u>	<u>UTS(MPa)</u>
Al-14Si-0.288Mg	As cast		122.00
	SHT(530 °C)	6	120.00
	Peak aged 160 °C	7	200.40
	Peak aged 170 °C	5	228.32

Table 4-3, above presents the as cast, solution heat treated, peak aged at 160 °C and 170 °C ultimate tensile values.

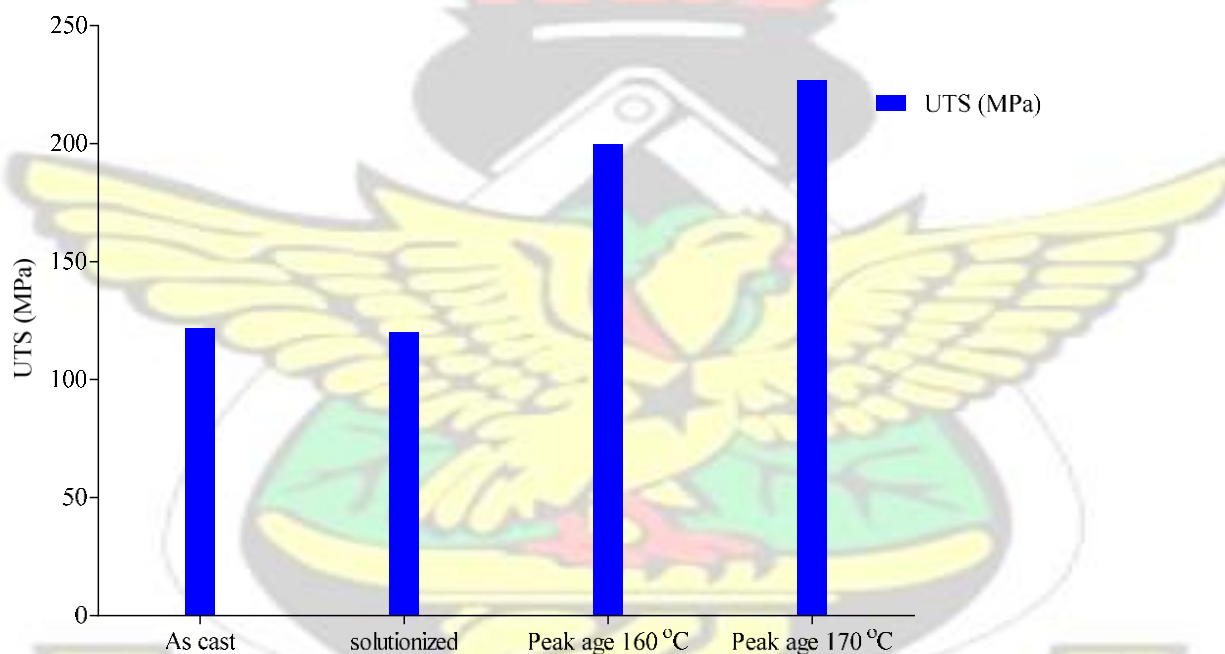
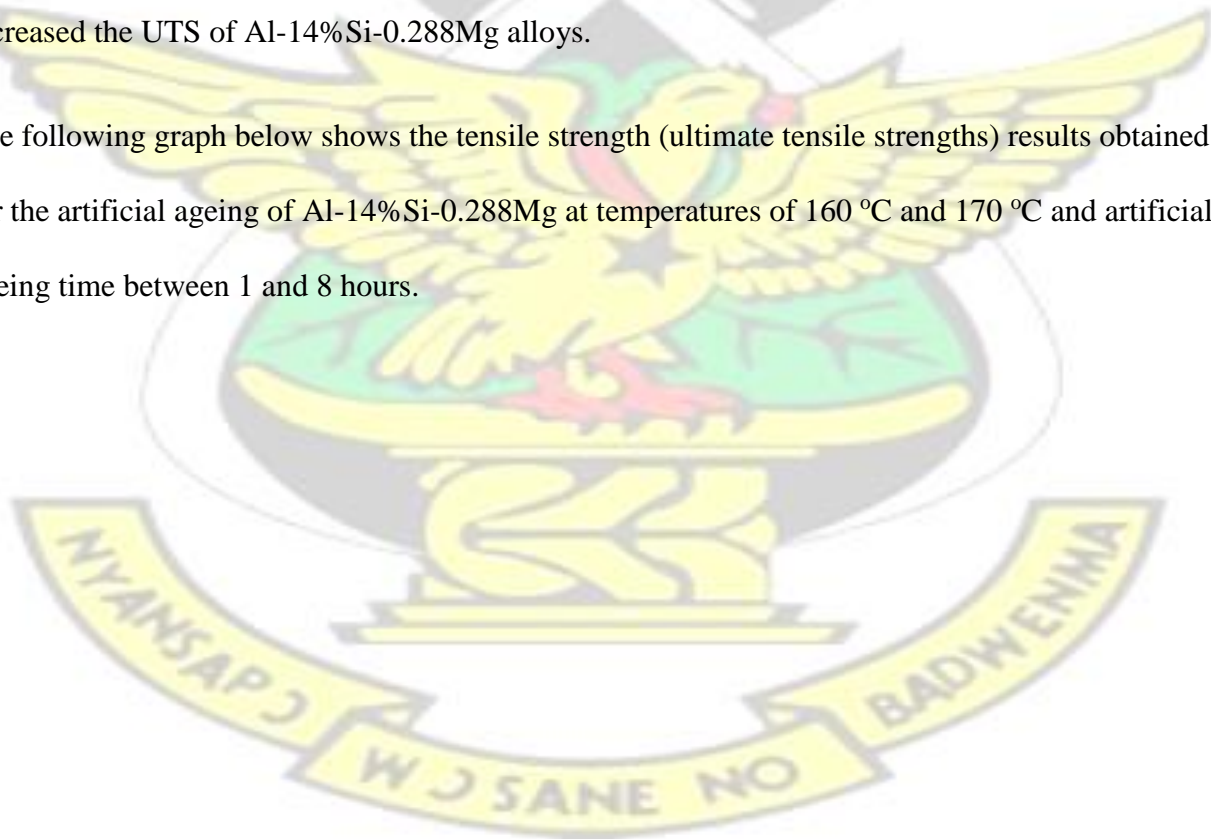


Figure 4-19 Tensile strengths of Al-14%Si-0.288Mg as cast, SHT, Peak-aged at 160 °C and Peak-aged at 170 °C.

Figure 4-19, above depicts the variations in the UTS of Al-14%Si-0.288Mg under various conditions such as, as-cast, SHT, and Peak-aged at 160 °C and 170 °C respectively. The UTS of the as-cast alloy was (122±0.70 MPa) and (120±0.70 MPa) when the alloy was solutionized at 530

°C for 6 hours in the furnace, the percentage reduction in strength was 1.67%. Decrease in ultimate tensile strength was attributed to slow cooling rate during quenching of the sample which caused particles to precipitates heterogeneously at grain boundaries resulting in a reduction in the super saturation of solute atoms and resulting in reduction in ultimate tensile strength (Ishak et al., 2013) As expected, there was 63.6% and 66.31% increase in strength from the cast and the solutionized samples when aged at 160 °C, that is (122±0.70) to (200.40±0.98 MPa) and (120±0.70 MPa) to (200.40±0.98 MPa). There was also an increase in strength of 86.4% from the as cast structure when the samples were peak aged at 170 °C, that is from (122±0.70 MPa) to (228.32±0.93 MPa). It is also seen that the peak ageing time was 5 hours for the 170 °C temperature and 7 hours for 160 °C temperatures. This shows that increase in temperature, increased the UTS of Al-14%Si-0.288Mg alloys.

The following graph below shows the tensile strength (ultimate tensile strengths) results obtained for the artificial ageing of Al-14%Si-0.288Mg at temperatures of 160 °C and 170 °C and artificial ageing time between 1 and 8 hours.



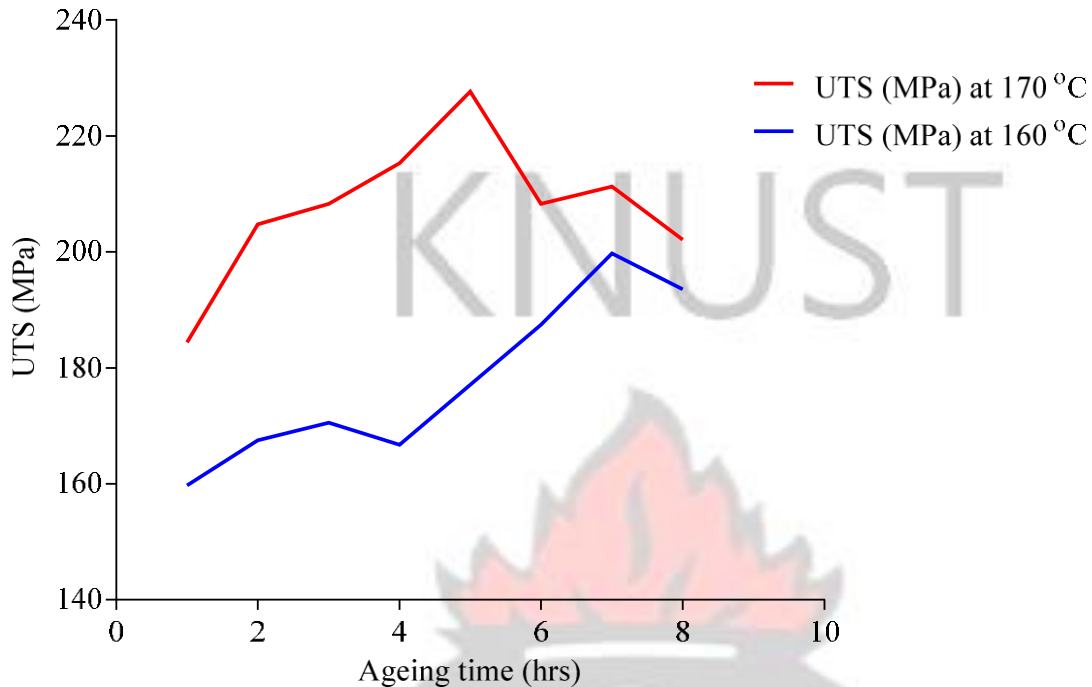


Figure 4-20 Composite curves for Al-14%Si-0.288Mg at 160 °C and 170 °C for 8 hours

Figure (4-20) show that as the ageing time is increased, the UTS value also increased up to $(171 \pm 0.70 \text{ MPa})$ at 3 hours and drops slowly at time 4 hours. After this time, the UTS value increased up to $(200.40 \pm 0.98 \text{ MPa})$ at 7 hours which is the peak and drops, as indicated in Figure (4-20) for the alloy studied at 160 °C. This drop may be the fact that a reduction in ultimate tensile strength is linked to a rise in inter-particle gaps between precipitates which makes dislocation bowing very easier (Ashby and Jones, 2005).

The increase in ultimate tensile strength at 170 °C was quick at 3 hours with a value of $(208.60 \pm 0.42 \text{ MPa})$. This value further increased to $(228.32 \pm 0.93 \text{ MPa})$ which is the peak UTS.

The microstructure has been developed by the aging into finely dispersed Mg_2Si , AlFeSi , $\text{Al}_{12}\text{Mg}_2\text{Si}$ and $\text{Al}_8\text{Mg}_3\text{FeSi}_6$ particles or precipitates. With strengthening phase β'' which is consistent together with the semi-consistent $\beta\text{-Mg}_2\text{Si}$ (Fatai Olufemi, 2012). The alloy at this time and temperature produces UTS which is due to the accelerated production of Mg_2Si and

other strengthening phases. Clusters are formed which impede the movement of dislocations therefore high UTS is recorded (Abdulwahab et al., 2011). This UTS was within the European standards for the ultimate tensile strength of sand and chill cast aluminium alloys (ISO Al Si7Mg, ISO Al Si10Mg and ISO Al Si12Cu in the T6 conditions are 260, 260 and 170 Mp) respectively (Brown, 1999).

Figure (4-20) compares the two temperatures 160 °C and 170 °C and the various UTS values recorded for their peaks. It could be seen that the UTS values for the temperature 170 °C were higher than that of 160 °C. This confirmed the fact that increasing ageing temperature increases the tensile strength of Al-Si with added magnesium alloys (Mohamed and Samuel, 2012).

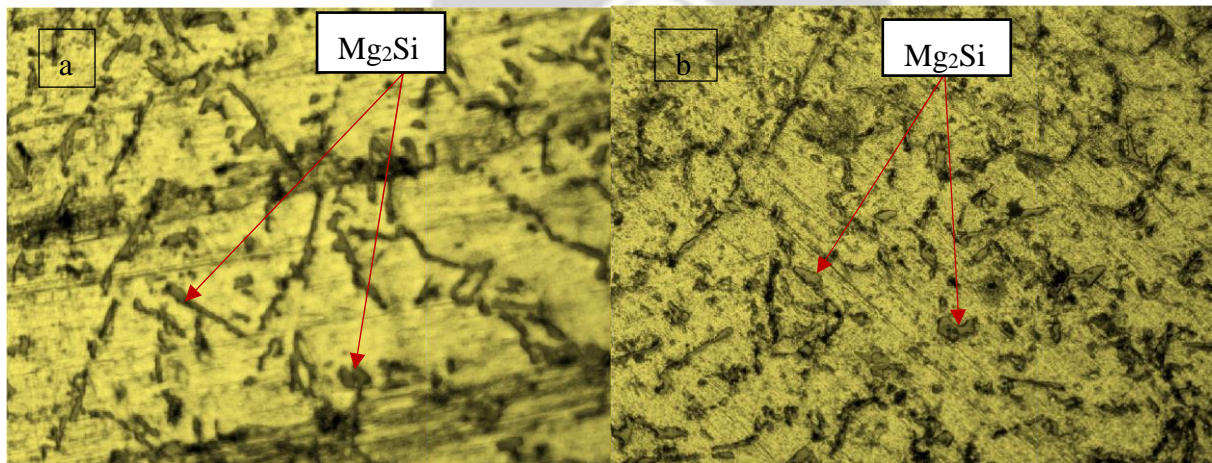


Figure 4-21 Microstructures of Al-14%Si-0.288Mg peak-aged (a) at 170 °C for 5 hours and (b) at 160 °C for 7 hours (x200).

The graphs below are bar charts of ductility measured in terms of percentage elongation against the artificial ageing time.

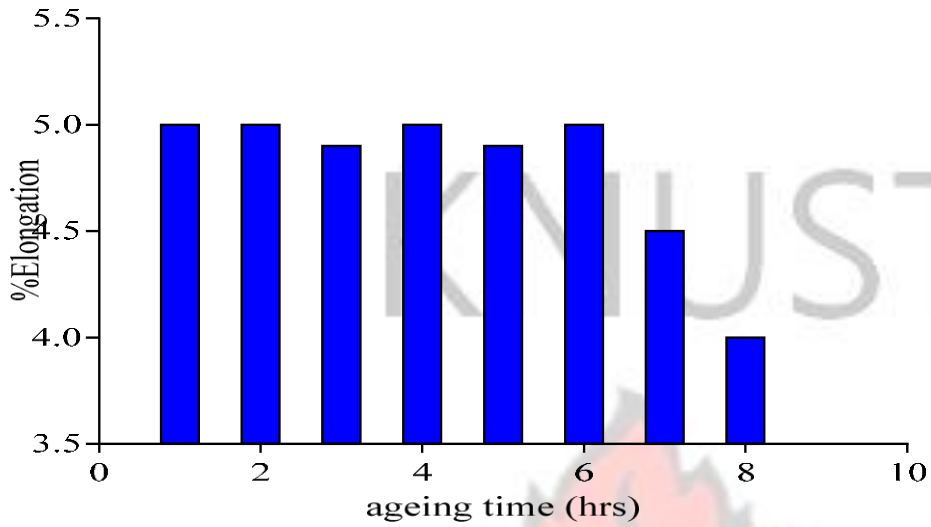


Figure 4-22 Bar charts of percentage elongation against ageing time at temperature at 160 °C

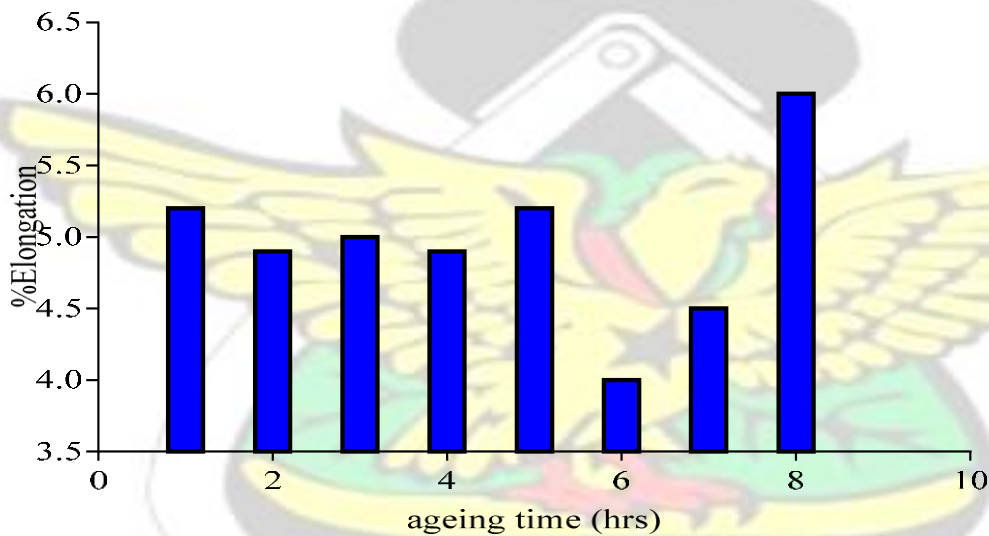


Figure 4-23 Bar charts of percentage elongation against ageing time at temperature 170 °C

Figure 4-22 and Figure 4-23 depicts that the alloy has uniform and good percent elongation from 1 hour to their peak ageing periods, which showed good mechanical properties and these mechanical properties decreased after their peak ageing times that was 7 hours and 5 hours for the alloy at ageing temperatures 160 °C and 170 °C.

The table below shows the summary of strength values for Al-14Si-0.288Mg alloys artificially aged at 160 °C and 170 °C for 1 to 8 hours.

Table 4-4 Summary of ultimate tensile strength values for Al-Si-Mg alloys

Ageing time (hrs)	Ageing temp 160 °C	
	Ageing temp 170 °C UTS (MPa)	UTS (MPa)
1	184.37	159.69
2	204.74	167.50
3	208.60	171.00
4	215.26	166.71
5	228.32	141.13
6	208.30	187.42
7	211.24	200.40
8	202.08	193.53

4.3.2 Impact Properties of Al-14%Si-0.288Mg alloys

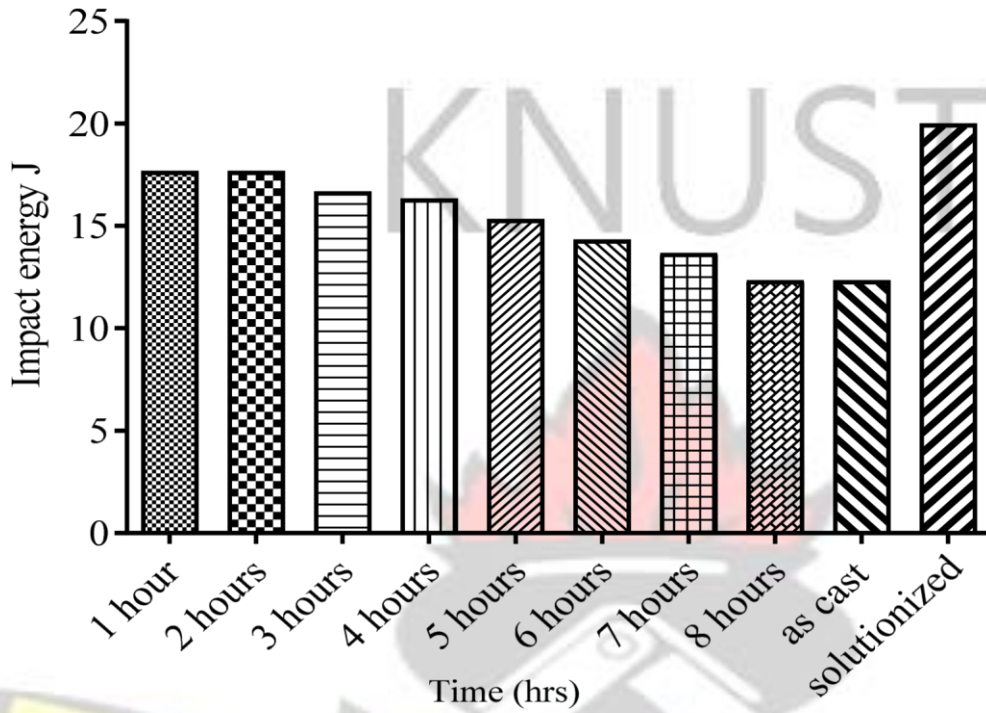


Figure 4-24 Bar charts of Impact energies at various times and conditions at 160 °C

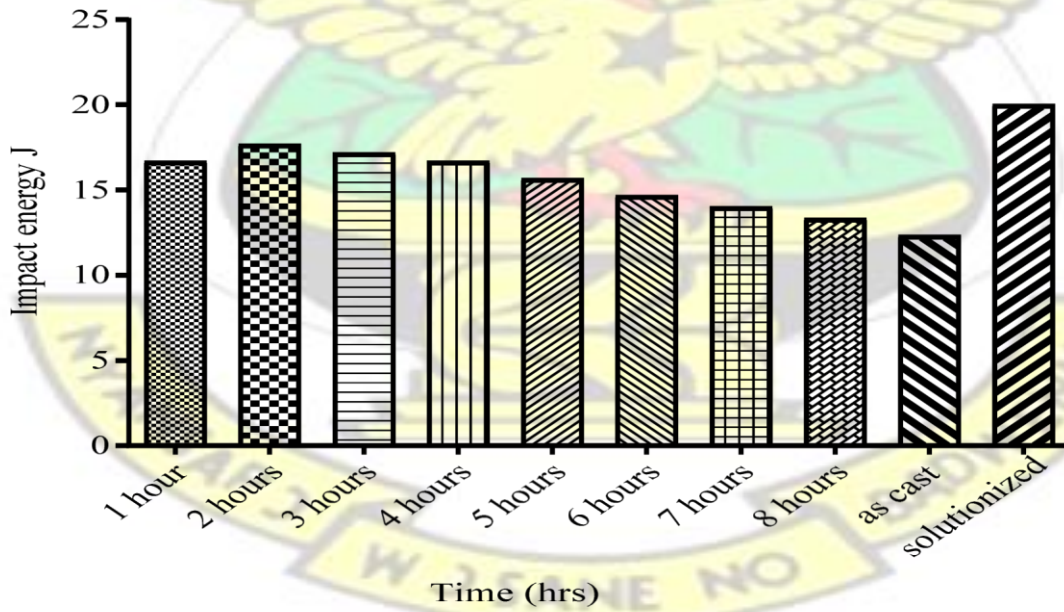


Figure 4-25 Bar charts of Impact energies at various times and conditions at 170 °C Figure 4-24 and Figure 4-25 shows the impact energies for the alloys artificially aged at 160 °C and 170 °C at the various artificial ageing times. Figure 4-26 below has been extracted from this graph to show the differences between the impact energies for the cast and solutionized sample at 530 °C.

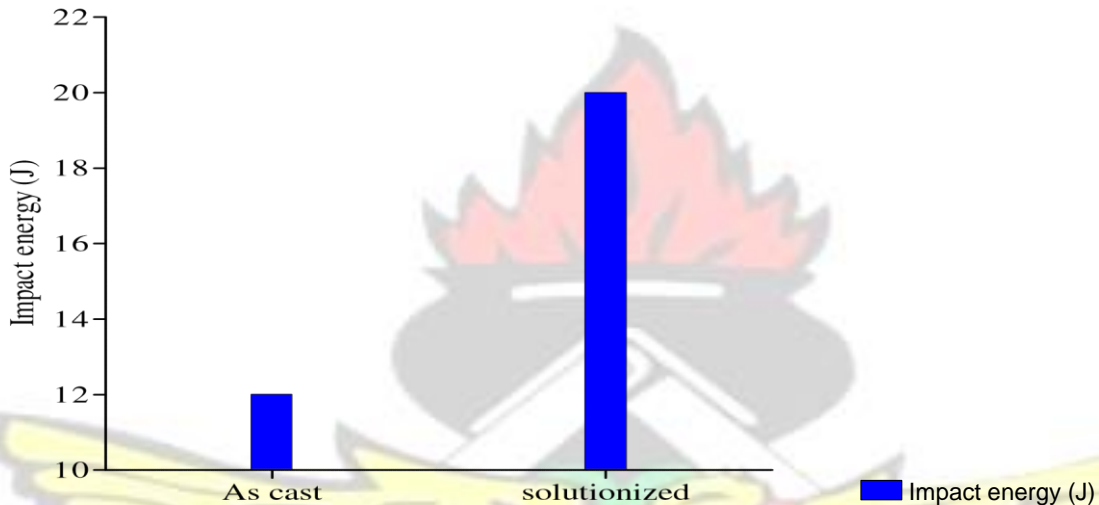


Figure 4-26 Impact energy of As-cast and Solutionized sample

The observation made from Figure 4-26 was that the impact energy of the solutionized sample was more than the cast sample. The impact energy increased from (12.33±0.58 joules) to (20±2.65 joules) respectively. This means the aging had a good result on the impact toughness of the sample. This increase in impact toughness was due to the coarsening and increases in size and shapes of the silicon particles and spacing between intermetallic particles that were formed which made dislocation movement much easier. This confirmed the observations made by (Zhang, 2002).

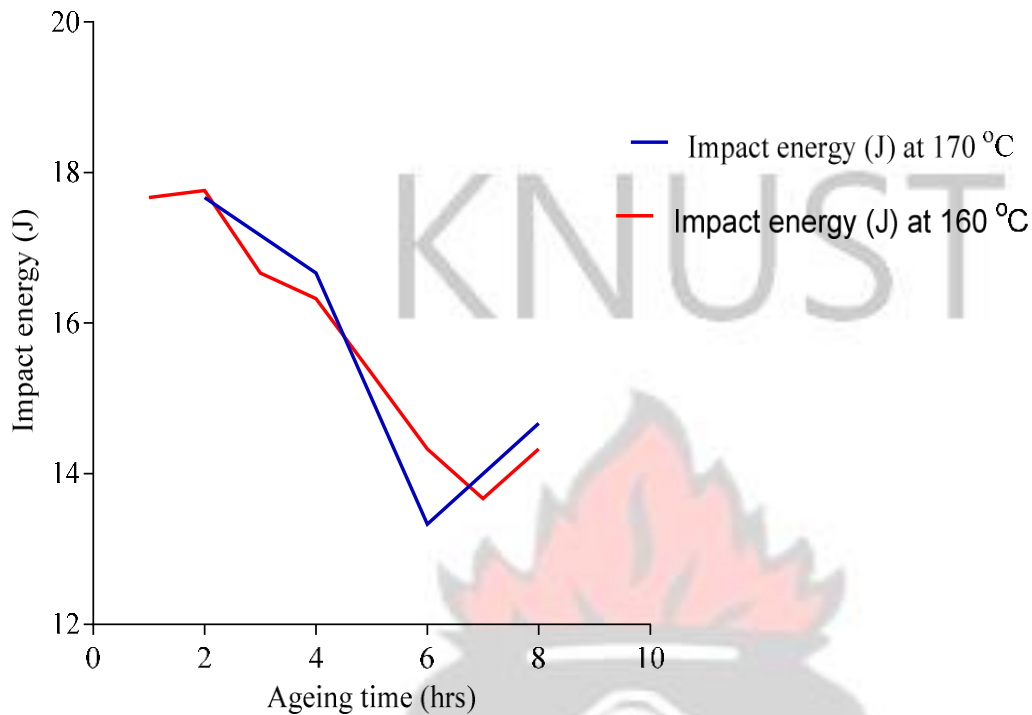


Figure 4-27 Composite curves of impact energies at 160 °C and 170 °C for Al-Si-Mg alloy

Figure (4-27), shows composite curves of impact energy at 160 °C and 170 °C for Al-Si-Mg alloy. At temperature 170 °C, there was a reduction in impact from 2 hours up to 6 hours. After 6 hours the impact energy started to increase again. The reduction in impact energy was due to the microstructure being refined by the heat treatment into finely dispersed Mg_2Si , $AlFeSi$, $Al_{12}Mg_2Si$ and $Al_8Mg_3FeSi_6$ particles or precipitates. With strengthening phase β'' which is coherent together with the semi-coherent β - Mg_2Si (Fatai Olufemi, 2012). Clusters are formed which impede the movement of dislocations (Abdulwahab et al., 2011). The increase in impact toughness after 6 hours was due to the coarsening and increases in size and shapes of the silicon particles and spacing between intermetallic particles that were formed which made dislocation movement much easier.

Temperature 160 °C showed same decrease in impact energy up to 7 hours and increase in the impact energy after 7 hours, Figure (4-27) also showed the result of aging temperature on the impact energy of the alloy samples. The aging time had a pessimistic effect on the impact toughness because of the reduction in the impact toughness as time progressed.

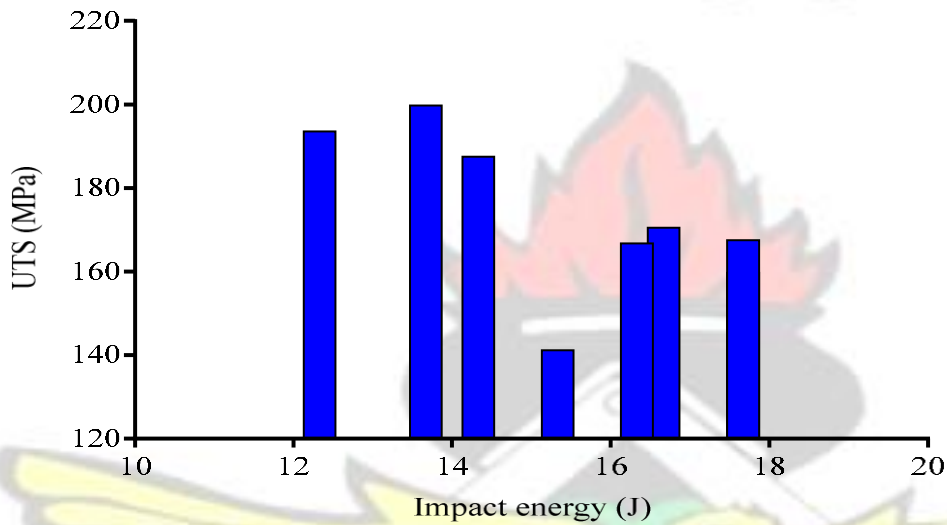


Figure 4-28 Bar charts of UTS against impact energies at ageing at 160 °C (Al-Si-Mg alloys)

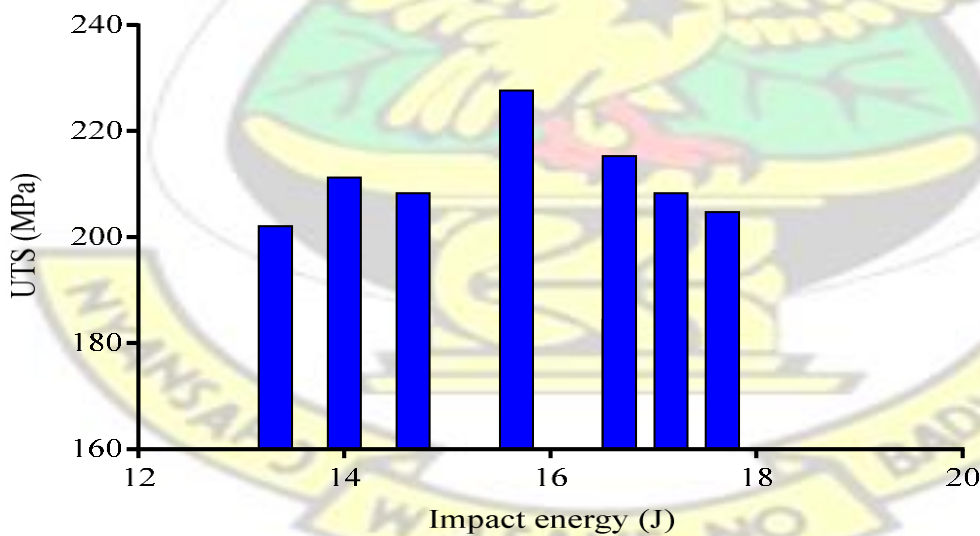


Figure 4-29 Bar charts of UTS against impact energies at ageing temperature of 170 °C (Al-SiMg alloys)

Figure 4-28 and Figure 4-29 shows the link between the impact energies and the ultimate tensile strength of Al-Si-Mg alloys at 160 °C and 170 °C. It was observed that a reduction in impact energy resulted in an increase in ultimate tensile strengths of the alloys. This balance in properties is good for engineering applications.

The table below summarizes the UTS and impact energies of the alloys samples at various heat treatment conditions.

Table 4-5 Ultimate tensile strength values versus impact energy values of Al-Si-Mg alloys at ageing temperatures of 160 °C and 170 °C

Ageing time (hrs)	Ageing Temperature 170 °C UTS (MPa)	Ageing Temperature 160 °C UTS (MPa)	Ageing Temperature 170 °C Impact Energy J	Ageing Temperature 160 °C Impact Energy J
1	184.37	159.69	16.67	17.67
2	204.74	167.50	17.67	17.67
3	208.60	171.00	17.17	16.67
4	215.26	166.71	16.67	16.33
5	228.32	141.13	15.67	15.33
6	208.30	187.42	14.67	14.33
7	211.24	200.40	14.00	13.67
8	202.08	193.53	13.33	12.33

4.3.3 Tensile Properties of Al-14%Si-2.688Cu

Tensile properties of Al-Si-Cu alloys are largely reliant on their microstructures which depend on the morphology of the Si particles, intermetallic phases that are formed and casting defects such as inclusions and porosity (Han et al., 2014). These factors affect the mechanical properties of these alloys but alloying elements and proper heat treatment processes enhances the mechanical properties.

The stress-strain graphs for the Al-14Si-2.667Cu alloys cast, solutionized and artificially age at 155 °C and 165 °C are as follows.

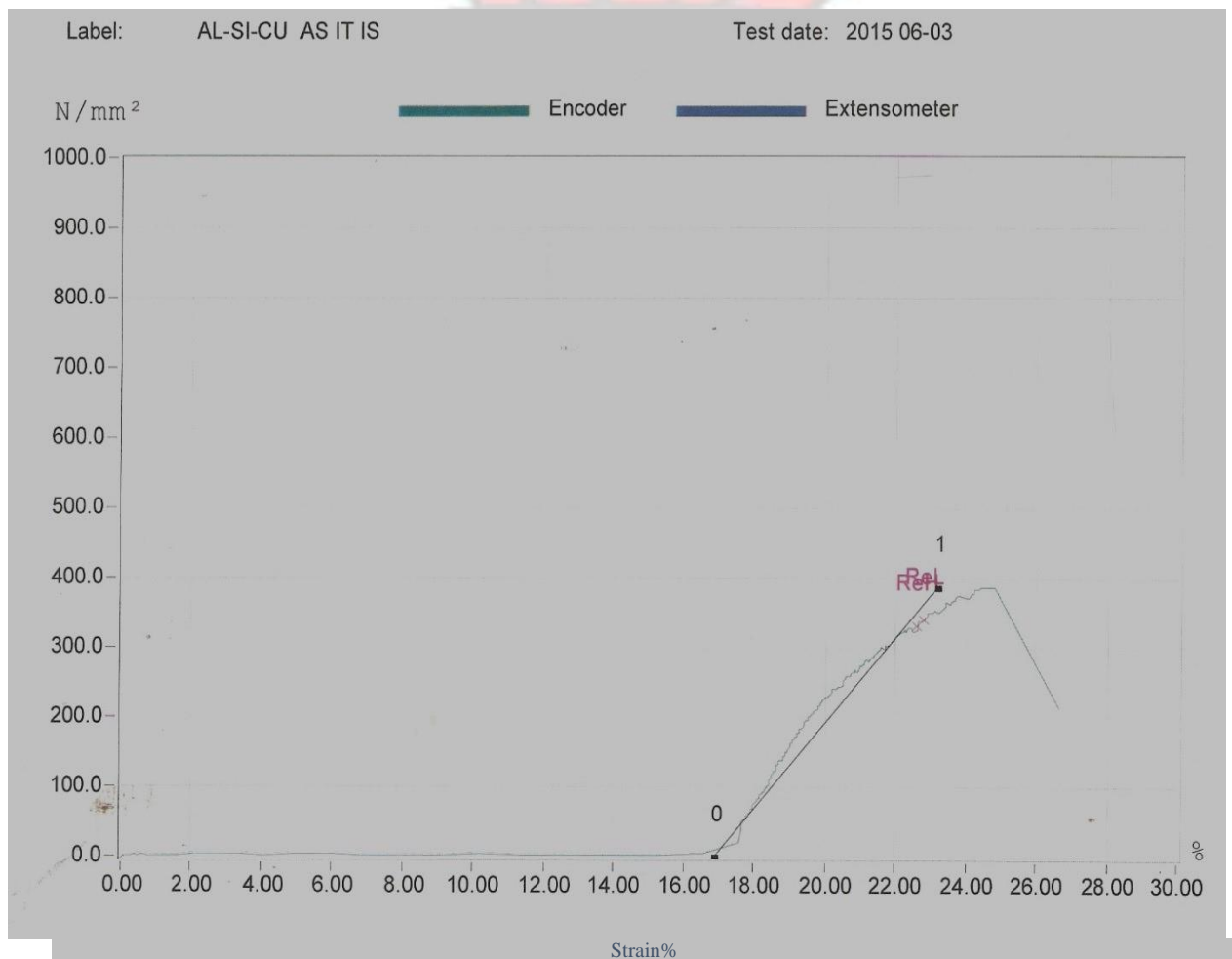


Figure 4-30 Stress-strain curve for Al-Si-Cu as it is, sample showing the stresses in the range of the strain.

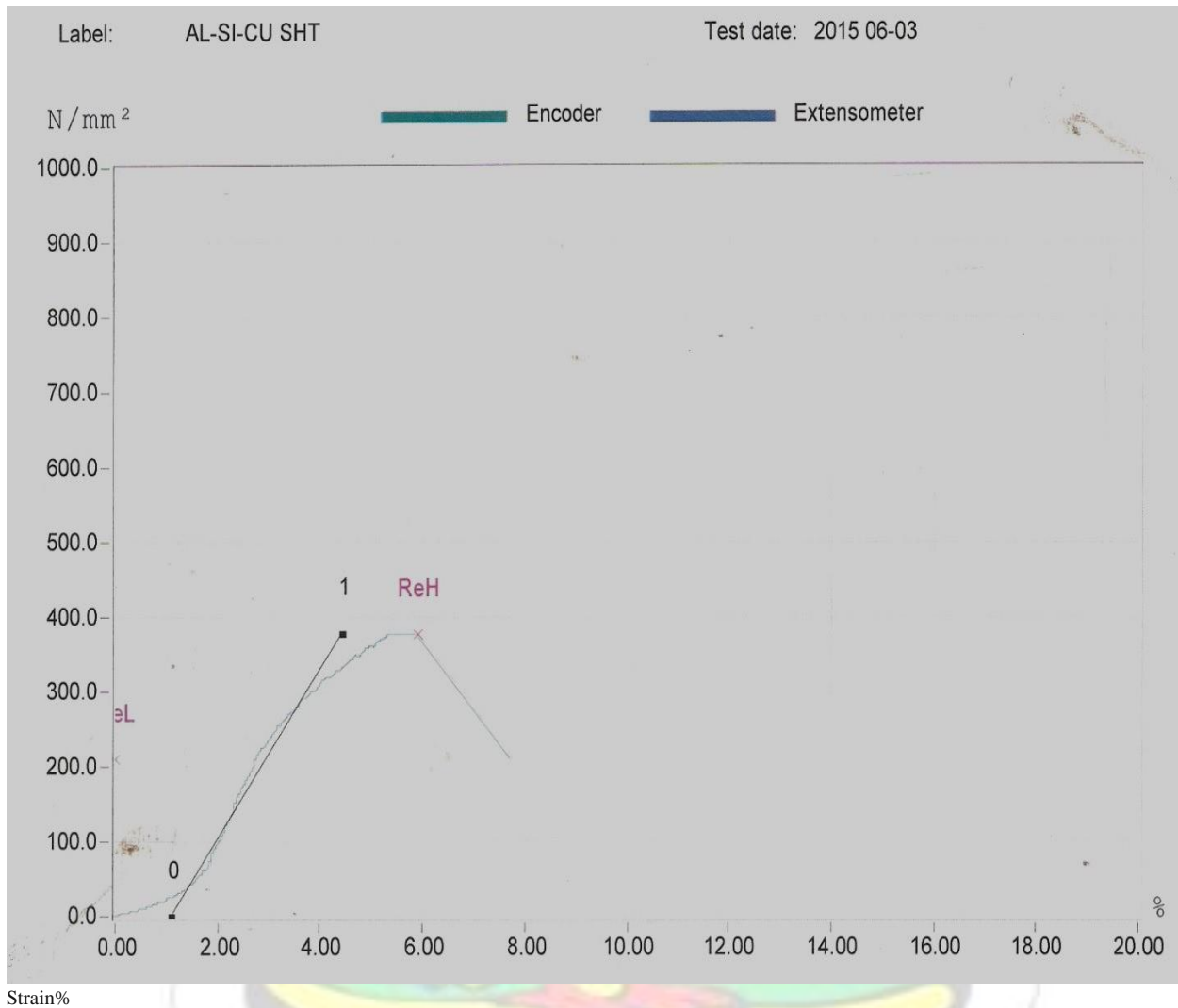


Figure 4-31 Stress-strain curves for Al-Si-Cu solution heat treated at 480 °C for 6 hours ageing time, sample showing the stresses in the range of the strain

Figure 4-30 and Figure 4-31, depicts the plots for the alloy, as-cast and solutionized after 6 hours at 480 °C. The as cast showed stress more than the solution heat treated sample. This is due to slow cooling rate during quenching of the solutionized sample, which caused particles copper to precipitate heterogeneously at grain boundaries, this caused a decrease in the super saturation of solute atoms and resulting in reduction in ultimate tensile strength (Ishak et al., 2013).

The following stress-strain plots below show the results of aging time on the UTS and the ductility (measured in percentage elongation) at temperature 165 °C.

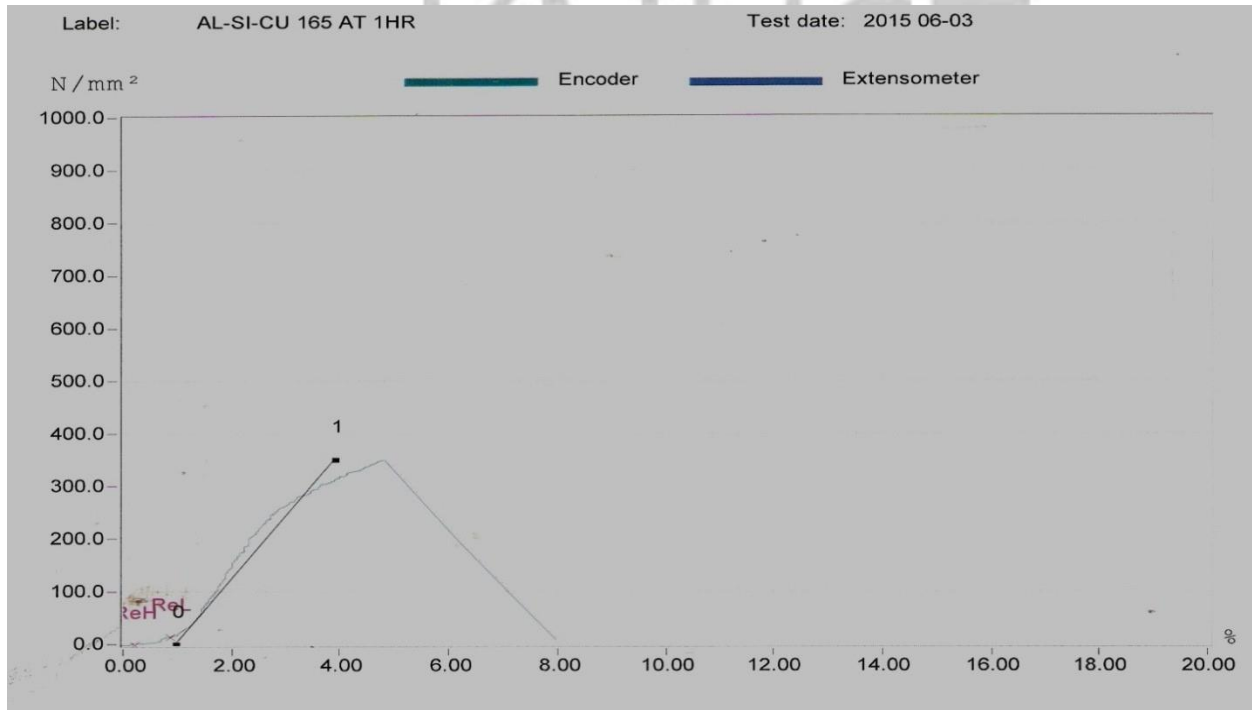
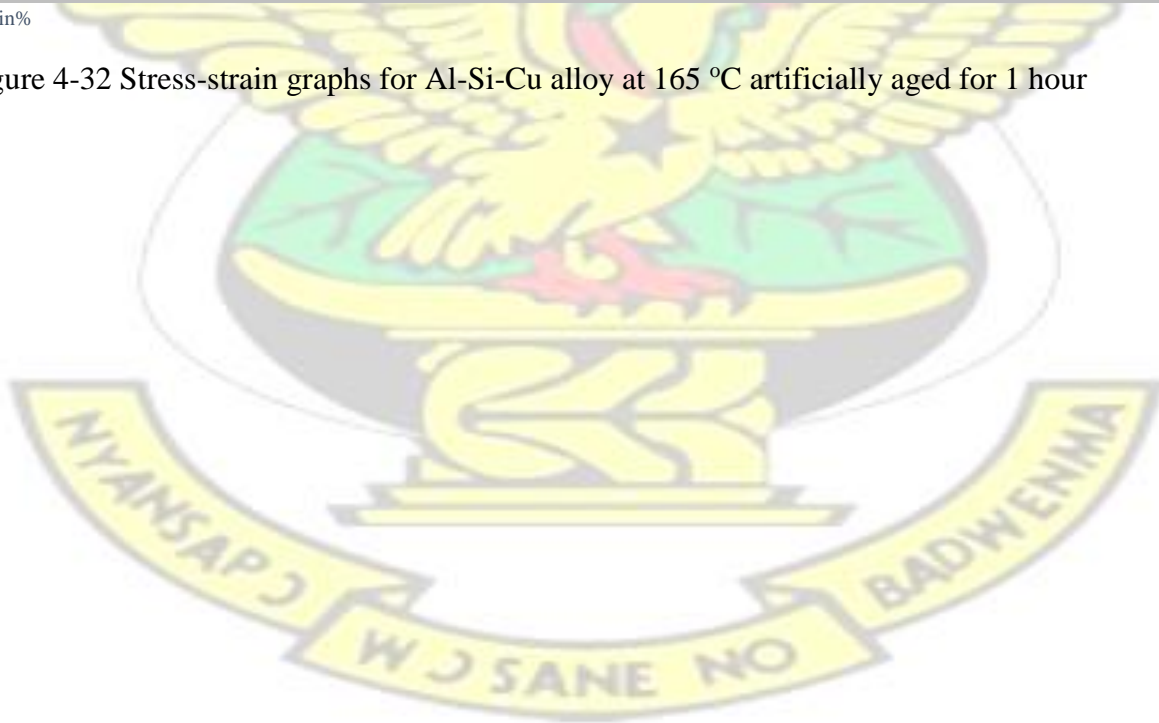


Figure 4-32 Stress-strain graphs for Al-Si-Cu alloy at 165 °C artificially aged for 1 hour



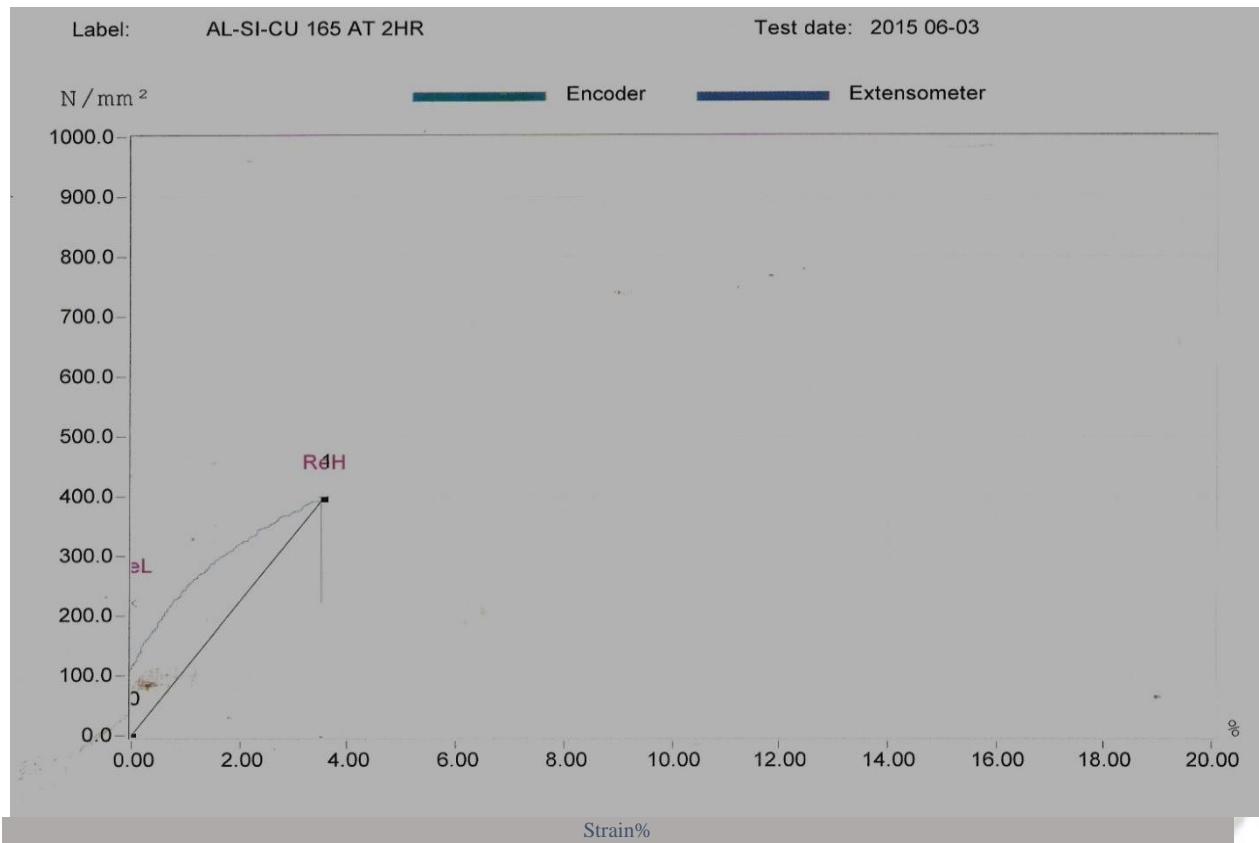


Figure 4-33 Stress-strain graphs for Al-Si-Cu alloy at 165 °C artificially aged for 2 hours

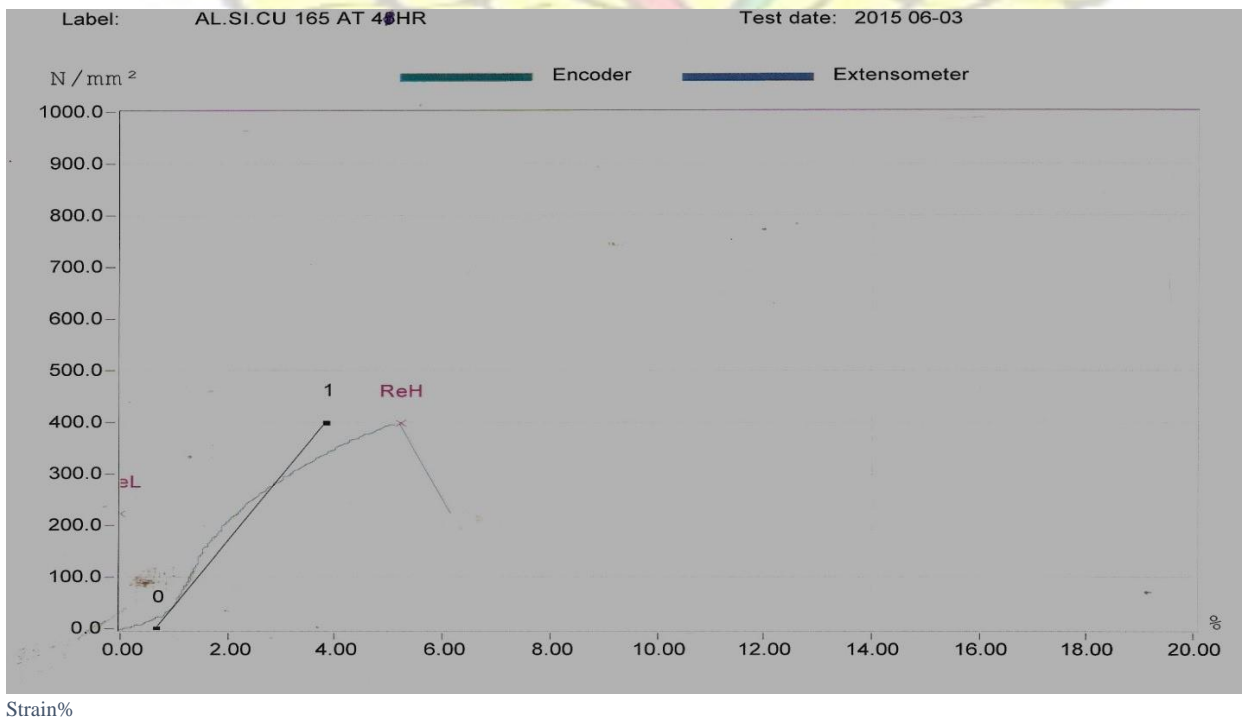


Figure 4-34 Stress-strain graphs for Al-Si-Cu alloy at 165 °C artificially aged for 4 hours

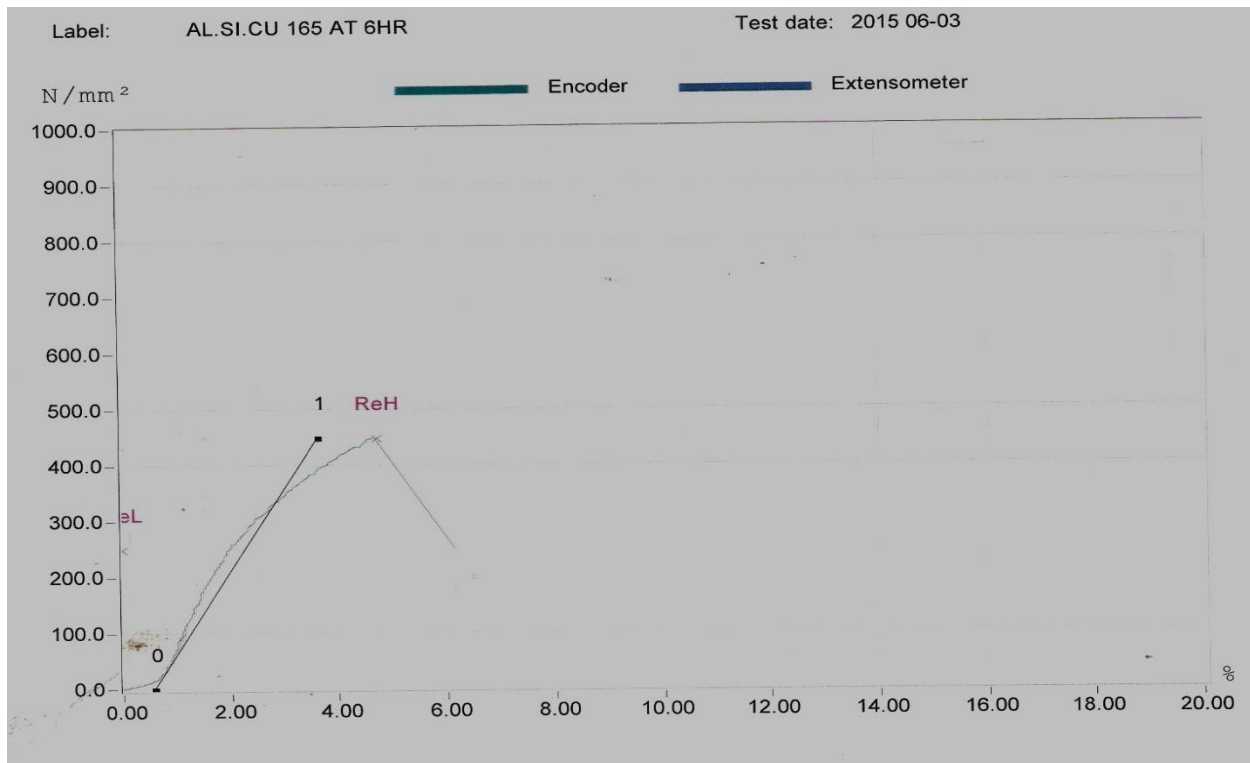
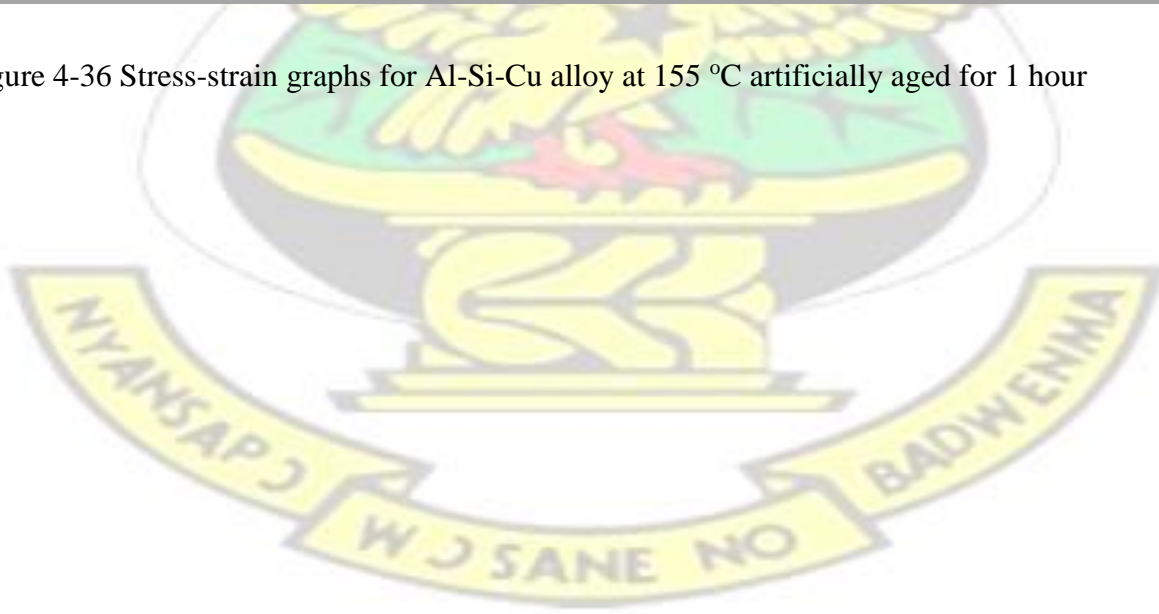


Figure 4-35 Stress-strain graphs for Al-Si-Cu alloy at 165 °C artificially aged for 6 hours From Figure 4-32 to Figure 4-35, it was observed that as the artificial aging time was increased from the first hour through to the sixth hour, the stress increased with a corresponding decrease in elongation. The alloy at that time and temperature produced ultimate tensile strength UTS which was due to the accelerated production of Cu_2Al and other strengthening phases. Clusters form which impedes the movement of dislocations therefore high stresses were recorded with a resultant boost in the UTS. As strength increased, the elongation also reduced. The highest stress was recorded at the sixth hour for the alloy artificially aged for 1 hour to the 8th hour. The remaining graphs for the alloy artificially aged at the highest temperature can be found in the appendix.

The following stress-strain plots also shows the results of aging time on the ultimate tensile strength and the ductility (measured in percentage elongation) at temperature 155 °C. That was when the artificial aging time was reduced.



Figure 4-36 Stress-strain graphs for Al-Si-Cu alloy at 155 °C artificially aged for 1 hour



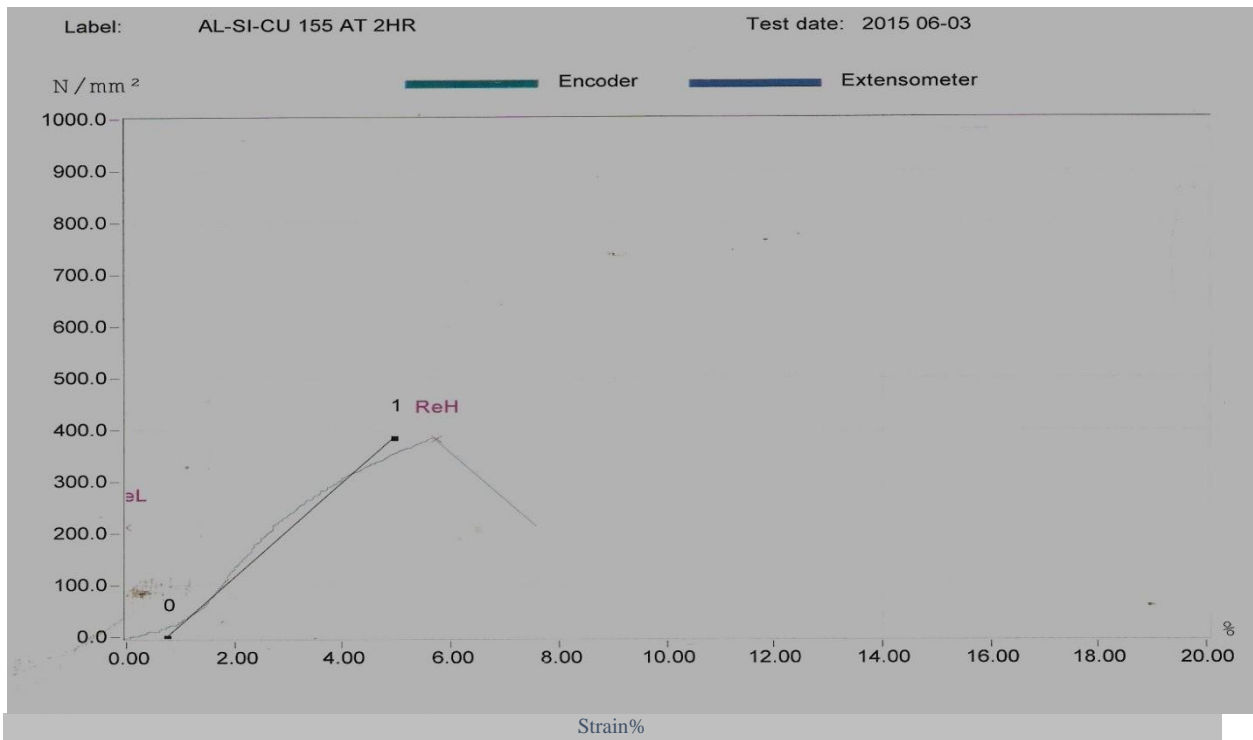


Figure 4-37 Stress-strain graphs for Al-Si-Cu alloy at 155 °C artificially aged for 2 hours

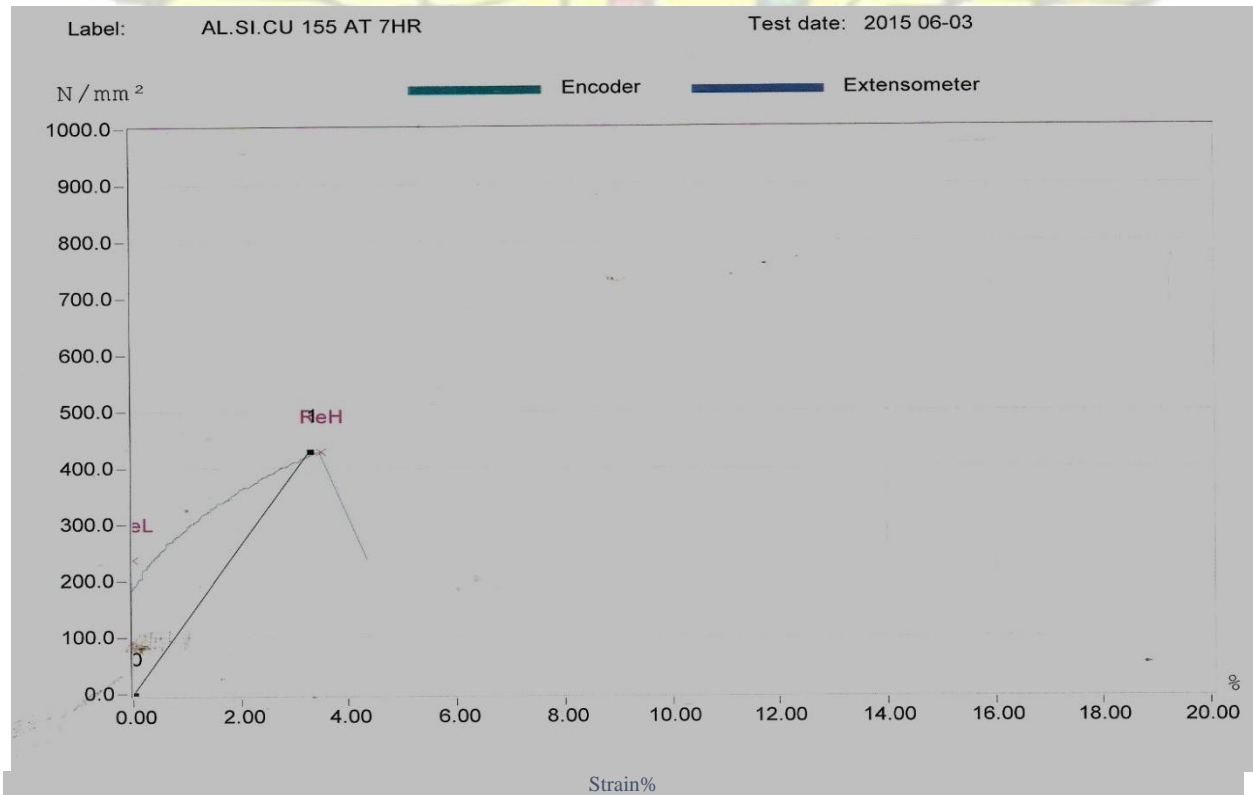


Figure 4-38 Stress-strain graphs for Al-Si-Cu alloy at 155 °C artificially aged for 7 hours

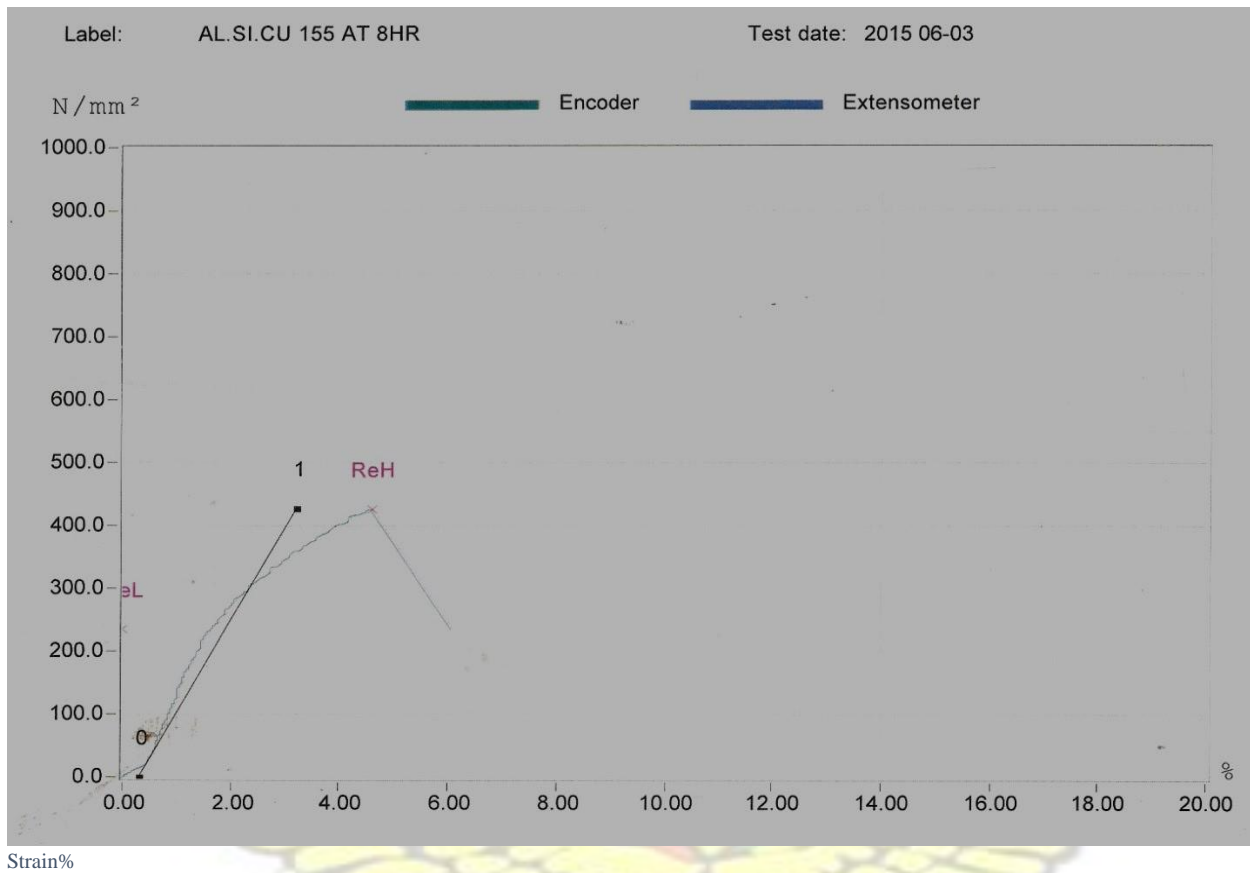


Figure 4-39 Stress-strain graphs for Al-Si-Cu alloy at 155 °C artificially aged for 8 hours

It is observed from Figure 4-36 to Figure 4-39, that the stress increased gradually from the first hour and the second hour with a reduction in elongation as well. But the stress started increasing at the 4th hour and at the 7th and 8th hour high stresses were recorded. The highest stress was recorded at the 7th hour of artificial ageing for the artificial ageing temperature of 155 °C as compared to the 6th hour in the alloy artificially age at 165 °C.

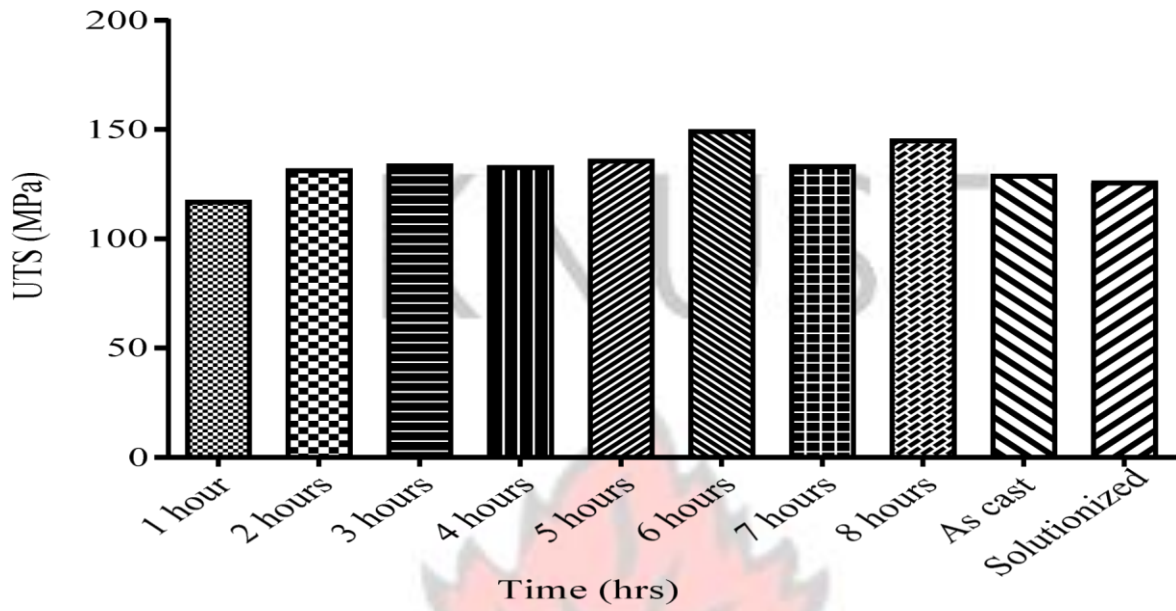


Figure 4-40 Composite bar charts of UTS of as cast, solutionized and ageing time between 1 and 8 hours for Al-Si-Cu alloy at 165 °C.

Figure 4-40 above depicts composite ultimate tensile strengths for the cast, solutionized sample and artificial ageing time used in the work. This bar chart helped in understanding how the T6 heat treatment enhanced the UTS of the alloy at 165 °C.

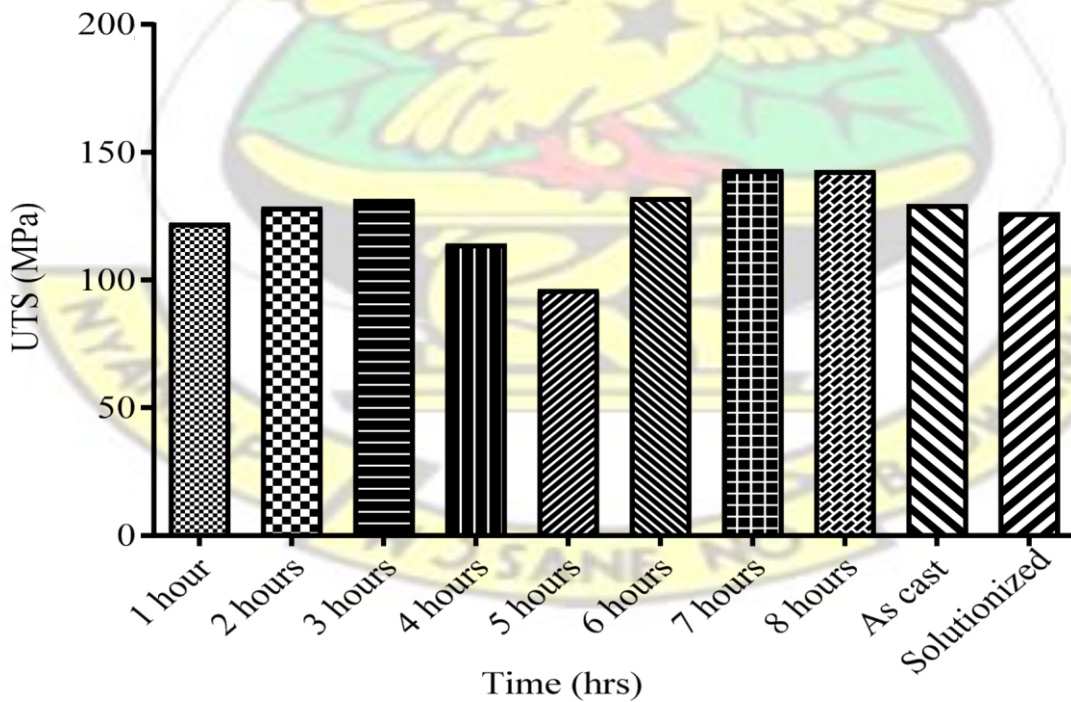


Figure 4-41 Composite bar charts of UTS of as cast, solutionized and ageing time between 1 and 8 hours for Al-Si-Cu alloy at 155 °C.

Figure 4-41 depicts composite ultimate tensile strengths for the cast, solutionized sample and artificial ageing time used in the work. This bar chart helped in understanding how the T6 heat treatment enhanced the UTS of the material at 155 °C. It can be observed that the values for the tensile strengths at 155 °C were lesser than the 165 °C see Figure 4-40. The graphs shows that as ageing temperature are increased the UTS values also increased.

Table 4-6 below compares the values obtained for the solution heat treated, as cast, peak aged at 155 °C and 165 °C.

Table 4-6 Tensile properties of as cast, SHT, Peaked aged at 155 °C and 165 °C Al-Si-Cu alloys respectively

Alloy	Condition	Time(hrs)	UTS(MPa)
Al-14Si-2.66Cu	As cast		129.94
	SHT (480 °C)	6	126.72
	Peak Aged 155 °C	7	143.46
	Peak Aged 165 °C	6	150.70

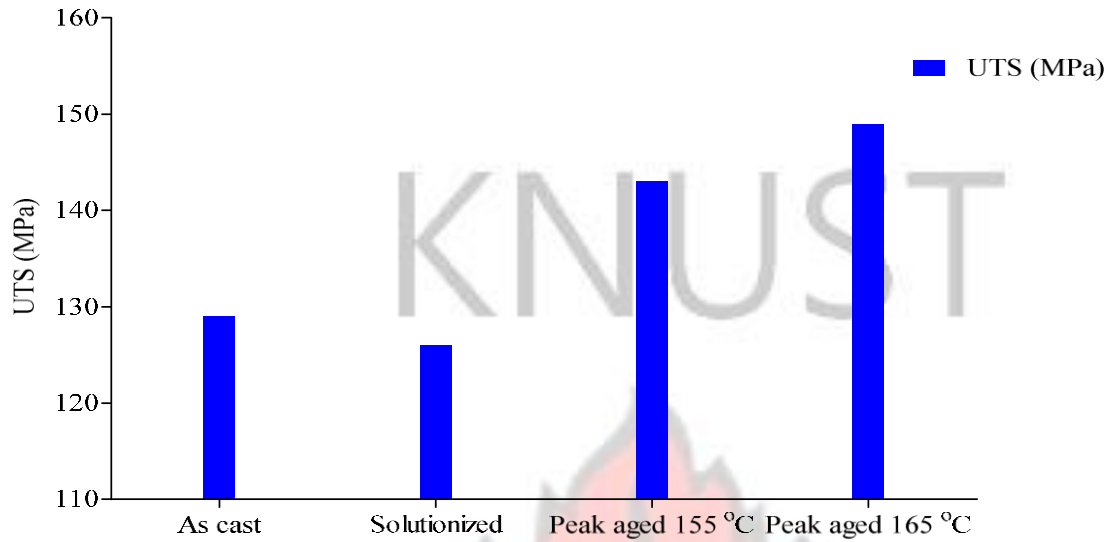


Figure 4-42 Tensile strengths of Al-14%Si-2.688Cu: as cast, solutionized, peak-aged at 155 °C for 7 hours and the same alloy peak-aged at 165 °C for 6 hours.

The graph above shows the results acquired for Al-Si-Cu alloy after T6 treatment. The UTS for the as cast was (129.94±0.66 MPa) while the solution treated sample at 480 °C was (126.72±0.50 MPa). It observed from Figure (4-42) that the UTS of the as cast structure is 2.54% more than the solutionized sample at 480 °C for 6 hours. This was attributed to slow cooling rate during quenching of the sample which caused particles to form at grain boundaries and this resulted in a decrease in the super saturation of solute atoms and resulting in reduction in ultimate tensile strength (Ishak et al., 2013). As expected when the samples were age at the two different temperatures, the ultimate tensile strength started increasing and the peak UTS was (143.46±0.32 MPa) and (150.70±1.20 MPa). Comparing these values to the as cast structure, there was a 10.4% increase in strength for the 155 °C and 15.97% increase for the temperature 165 °C. The ageing curves for the Al-14%Si-2.66Cu at temperature 155 °C and 165 °C at 8 hours of artificial heat treatment are represented below in Figure (4-43)

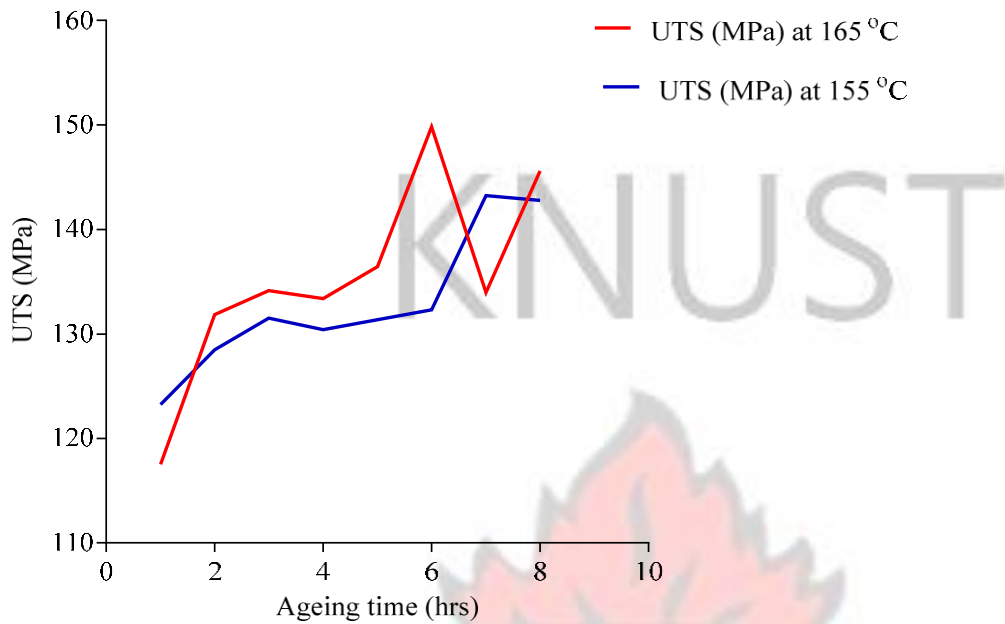


Figure 4-43 Composite curves for Al-14%Si-2.68Cu at temperatures of 155 °C and 165 °C

Results from ageing curve at 155 °C from Figure 4-43 above, shows the UTS value started to increase from (122.50±0.35 MPa) 1st hour to (132.02±0.72 MPa) at the 3rd hour and fluctuated up to 6th hour. This fluctuating in UTS value may be as a result of small increase in inter-particle spacing and precipitates coarsening. But after 6 hours, the UTS value increased up to (143.46±0.32 MPa) which was the peak UTS at time 7 hours and dropped after that. At the peak UTS the heat treatment has refined the strengthening phases and there is finely dispersed structures of the Al₂Cu and other strengthening phases in the microstructure which impedes dislocation movement thereby strengthening the alloy. Beyond this time the UTS value

decreased again which predicted the onset of over-ageing see Figure (4-43). The UTS value increased from (118.06±0.74 MPa) to (150.70±1.20 MPa) which was the peak UTS for 165 °C, this proved the fact that raising aging temperature improves mechanical property of Al-Si-Cu alloys. Increase in UTS value was due to the accelerated production of Al₂Cu and Al₅Mg₈Cu₂Si₆

phases and other intermetallic particles which are the strengthening phases. It's seen from Figure 4-43 that, the peak UTS value was recorded at time 6 hours which is lower than that of 155 °C. This shows that increasing ageing temperature also reduced the time taking to achieve peak mechanical properties. After this time the strength decreased and increased again describing the onset of over-ageing, which was due to the coarsening of the precipitates and increasing in interparticle spacing between strengthening phase. This confirms reports made by (Ma et al., 2010). The figure below shows the microstructures of the peak UTS values for 165 °C and 155 °C respectively.

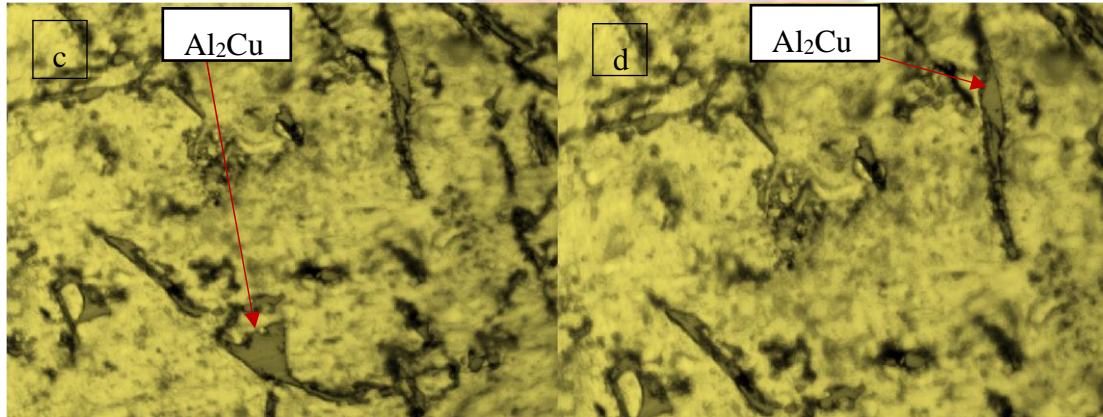


Figure 4-44 Microstructures of peak aged Al-14%Si-2.688Cu (c) at time 6 hours at 165 °C and (d) 155 °C at time 7 hours (x500).

The microstructures of these two temperatures are almost the same, and the phases that are contained in these microstructures are (Al₂Cu rich phases other intermetallic). This phases contributes to increase in strengthening or decrease in strengthening of the Al-Si-Cu alloy.

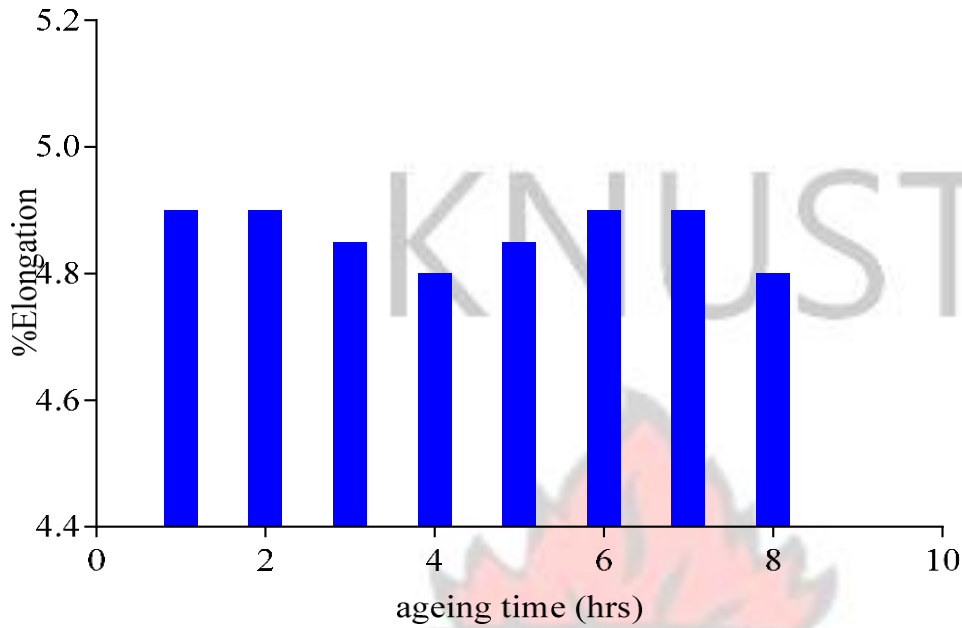


Figure 4-45 Bar charts of percentage elongation against ageing time at temperature 155 °C

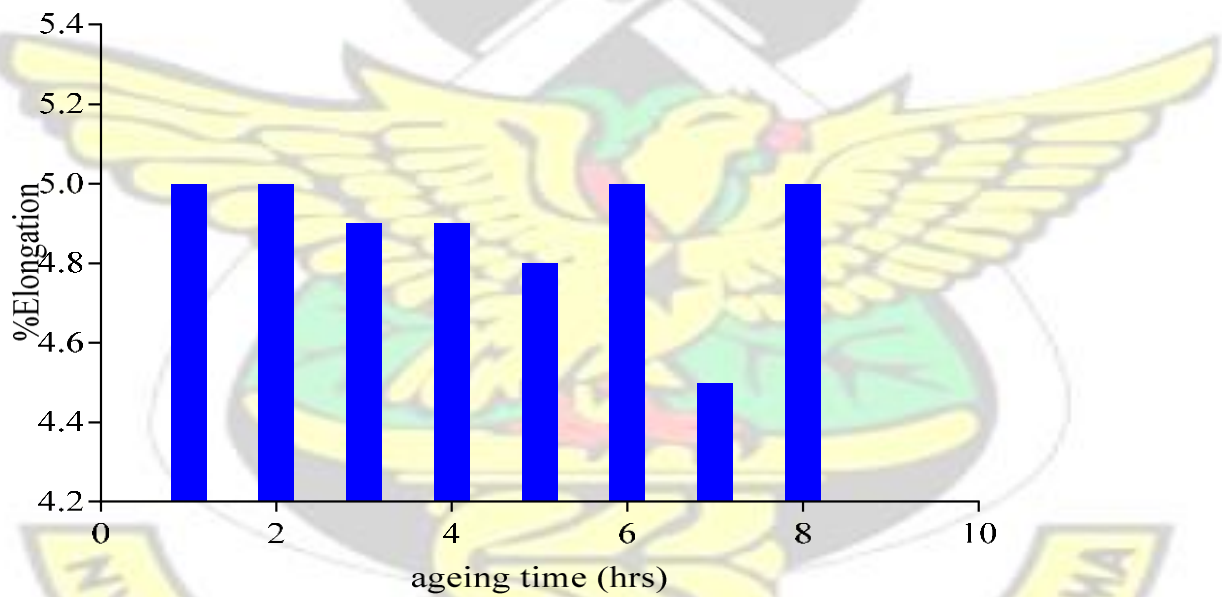


Figure 4-46 Bar charts of percentage elongation against ageing time at temperature 165 °C

Figure 4-45 and Figure 4-46 shows percentage elongation for Al-Si-Cu at ageing temperatures 155 °C and 165 °C. Figure 4-45 shows the percentage elongation being uniform from 1-2 hour and dropped from the 3rd hour and increased from 4th hour to the peak ageing time. Generally the

mechanical properties were good. Figure 4-46 also depicted an almost uniform percentage elongation up to the 4th hour and dropped at the 5th hour. Beyond this hour it fluctuated up to the last ageing time, 8 hours. Mechanical properties were generally good for these percentage elongations.

The table below shows the summary of strength values for the alloys containing copper artificially age at two different temperatures from 1 to 8 hours.

Table 4-7 Summary of ultimate tensile strength values for Al-Si-Cu alloys

Ageing time (hrs)	Ageing temp	
	155 °C UTS (MPa)	165 °C UTS (MPa)
1	122.25	118.06
2	128.46	131.85
3	131.51	134.17
4	114.14	133.38
5	96.26	136.43
6	132.30	150.70
7	143.46	133.94
8	142.77	145.60

4.3.4 Impact properties of Al-14%-2.688Cu alloys

The following graphs show the results from the heat treatment of Al-14%-2.688Cu.

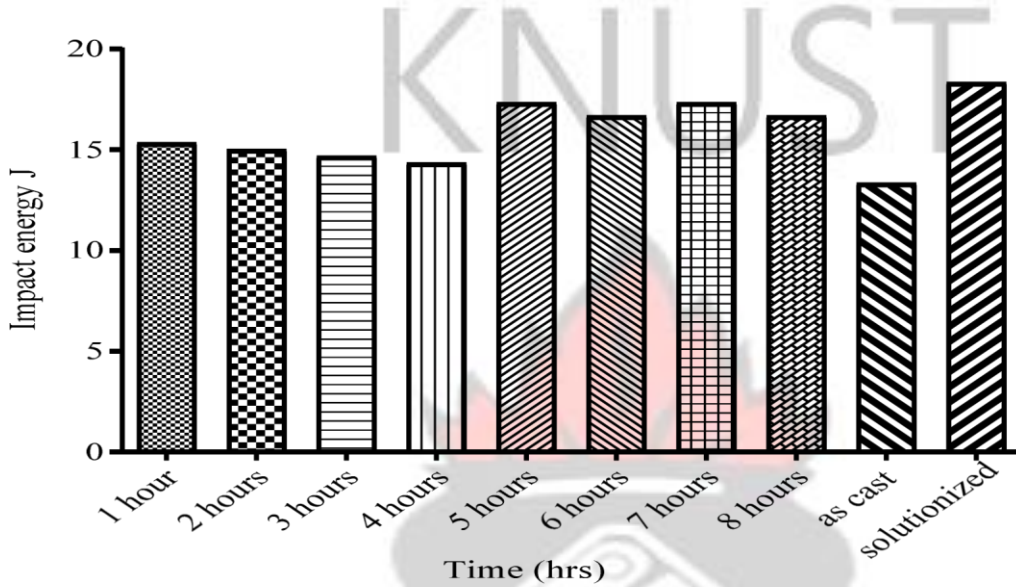


Figure 4-47 Bar charts of Impact energies at various times and conditions at 155 °C (Al-Si-Cu)

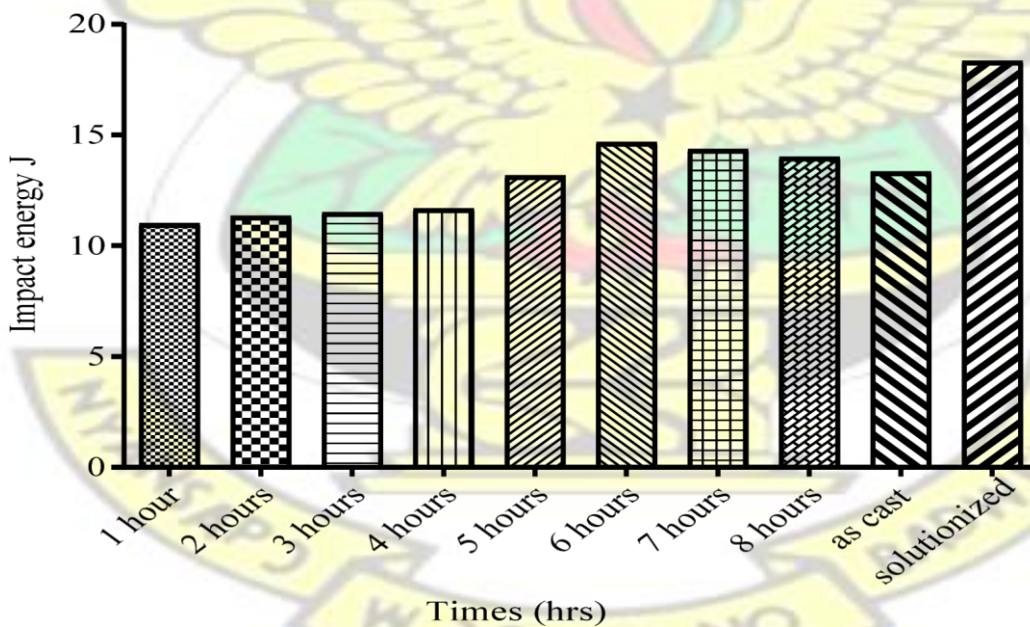


Figure 4-48 Bar charts of Impact energies at various times and conditions at 165 °C (Al-Si-Cu)

Graphs from Figure 4-47 and Figure 4-48, shows the impact energies of Al-Si-Cu alloys heat treated

at various ageing temperatures. It can be seen from the graph that the impact values of the artificial ageing temperature of 155 °C are more than that of 165 °C.

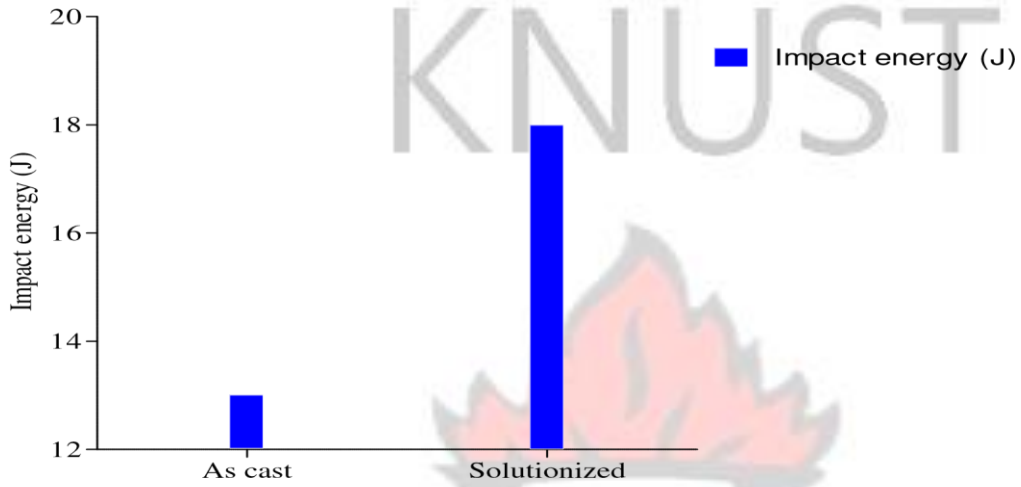


Figure 4-49 Impact energy of As-cast and Solutionized sample (temperature 480 °C at time 6 hours).

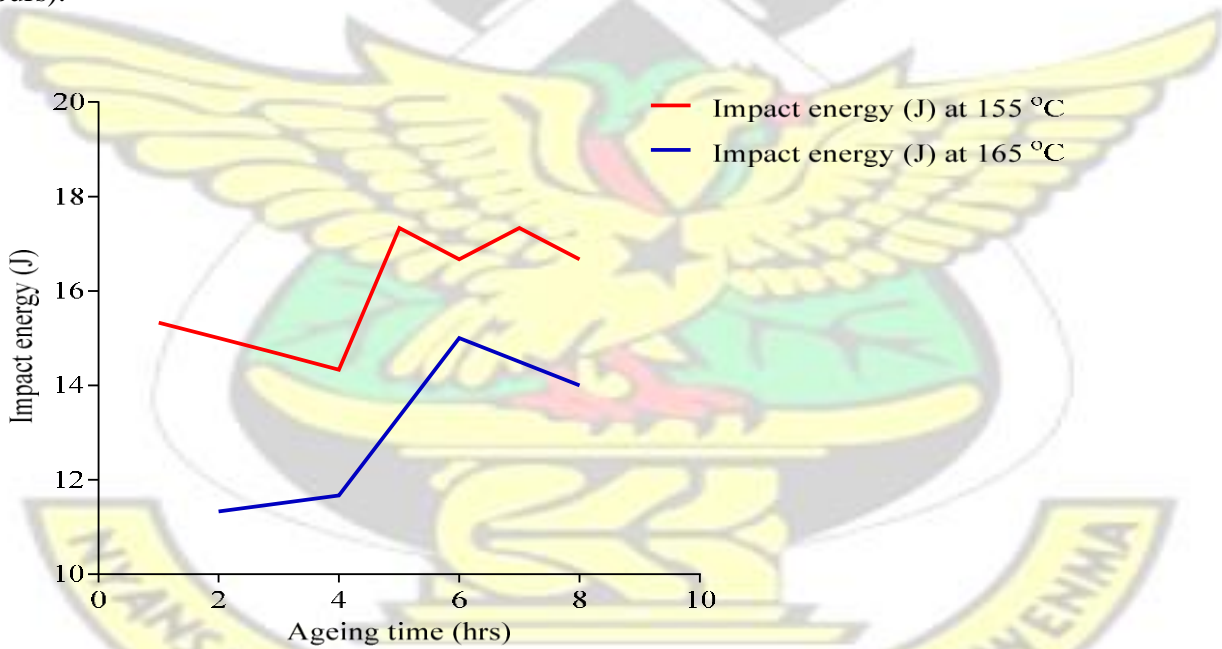


Figure 4-50 Composite curves of impact energy at 155 °C and 165 °C for Al-Si-Cu alloy

Figure 4-49, above shows impact energy of cast structure and solutionized sample. The cast structure was (13.33±1.15 joules) and the solutionized sample was (18.33±0.58 joules) indicating

37.5% increase in impact energy. This was due to the existence of countless weak microconstituents as well as acicular eutectic silicon particulates, Al_2Cu , $\beta\text{-AlFeSi}$ platelets which serve as crack commencement sites in the alloy matrix. Solution treating the as-cast structure produces Si particles of fibrous morphology which tends to reduce the amount of crack commencement sites and improve the alloy matrix opposition to crack commencement and transmission. After 2 hours of artificial ageing at $165\text{ }^\circ\text{C}$, there is a sharp decrease in impact energy to a value of $(11.33\pm 0.58\text{ joules})$ which corresponds to a decrease of 61.7% compared to the solutionized sample, Figure (4-50). This is the peak aging power of the alloy and this suggest an improvement of Al_2Cu phase and $\beta\text{-AlFeSi}$ phases in the microstructure, increasing the matrix strength at the expense of ductility. This means movements of dislocations are being restricted and dislocation bowing is difficult. After the 2 hours, the impact energy or fracture toughness tends to increase again up to $(15.00\pm 0.00\text{ joules})$ at 6 hours which is a positive effect. It then drops again at 8 hours Figure (4-50). This means to get a positive effect on sample impact energy, solution treatment and ageing it beyond 2 hours up to 6 hours might be enough.

When the temperature was decreased to $155\text{ }^\circ\text{C}$, there was a drop in impact energy or fracture toughness between the hours 2 and 4 before the impact energy increased again at time 5 hours, refer to Figure 4-50 above. Beyond this time there were fluctuations in the impact energy of the samples. It must be noted that the reduction in impact energy at this ageing time 2 and 4 hours corresponded to an increase in UTS in the samples at these same times under the same ageing temperature of $155\text{ }^\circ\text{C}$. Comparing impact energies of ageing temperatures $155\text{ }^\circ\text{C}$ and $165\text{ }^\circ\text{C}$, it is seen that, increasing aging temperature resulted in reduction of impact energy values which was a negative effects. In a product design using Al-Si-Cu alloy, where more impact energy is needed artificially ageing at $155\text{ }^\circ\text{C}$ will be enough.

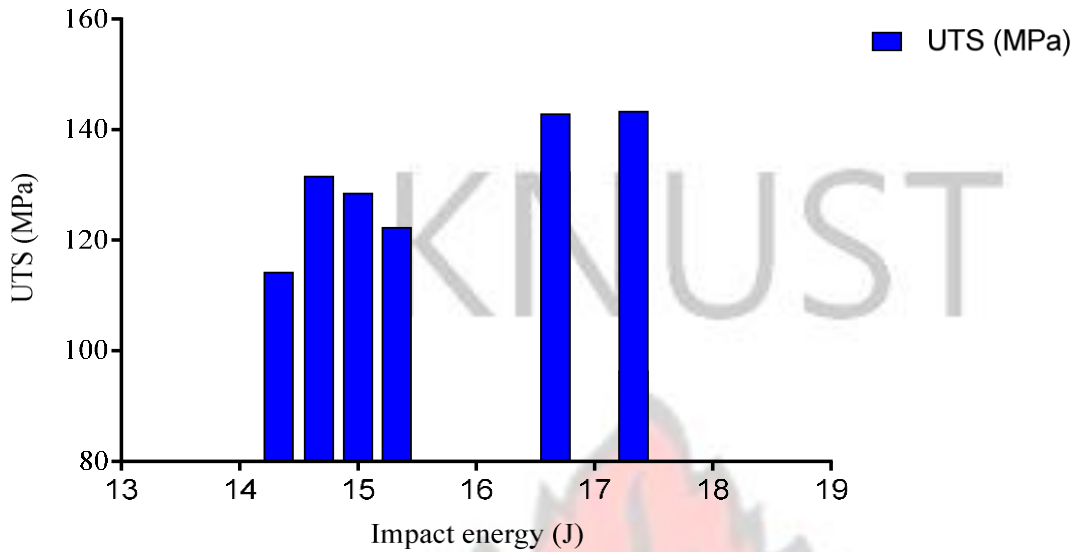


Figure 4-51 Bar charts of UTS against impact energies at ageing temperature of 155 °C (Al-SiCu alloys)

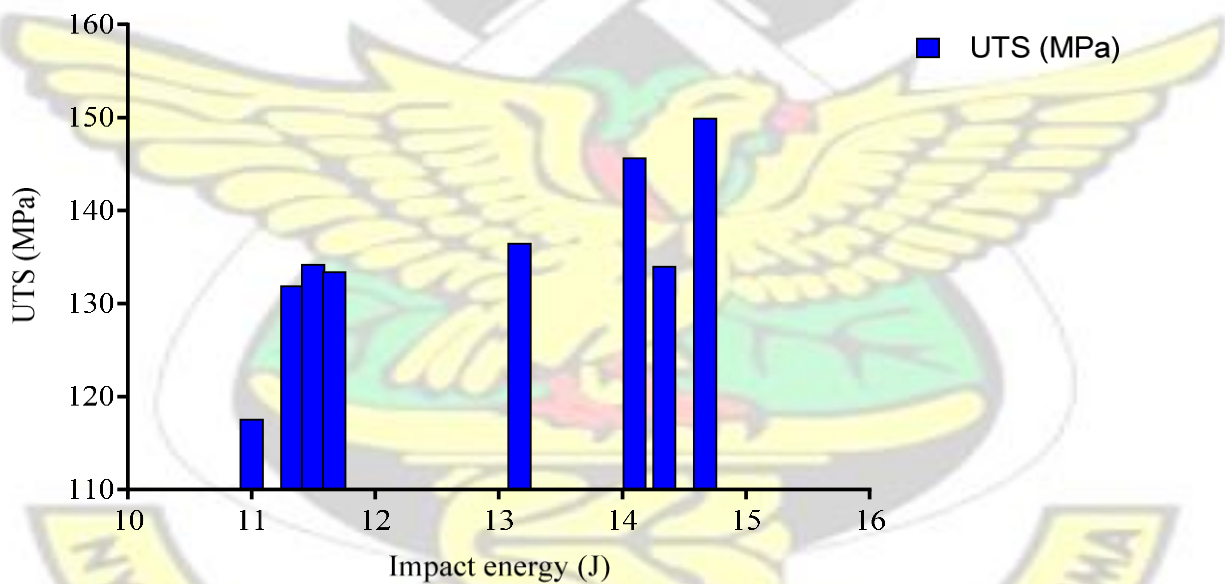


Figure 4-52 Bar charts of UTS against impact energies at ageing temperature of 165 °C (Al-SiCu alloys)

Figure 4-51 and Figure 4-52 shows that the relationship between the impact strength of the Al-SiCu alloys and their tensile strength were different from that of the Al-Si-Mg alloys in which an improvement in tensile strength resulted in a reduction of impact strength. Even though this

difference exists, products with balanced impact strength and ultimate tensile strengths are good for engineering applications.

The table below summarizes the tensile strengths and impact energies for the Al-Si alloy containing magnesium samples when heat treated in different conditions.

Table 4-8 Ultimate tensile strength values versus impact energy values of Al-Si-Cu alloys at 155 °C and 165 °C

Ageing time (hrs)	Ageing temp 165 °C UTS (MPa)	Ageing temp 155 °C UTS (MPa)	Ageing temp 165 °C Impact Energy J	Ageing temp 155 °C Impact Energy J
1	117.53	122.25	11.00	15.33
2	131.85	128.46	11.33	15.00
3	134.17	131.51	11.50	14.67
4	133.38	114.14	11.67	14.33
5	136.43	96.26	13.17	17.33
6	150.70	132.30	14.67	16.67
7	133.94	143.46	14.34	17.33
8	145.60	142.77	14.10	16.67

CHAPTER 5

CONCLUSIONS AND RECOMMENDATION

5.1 CONCLUSIONS

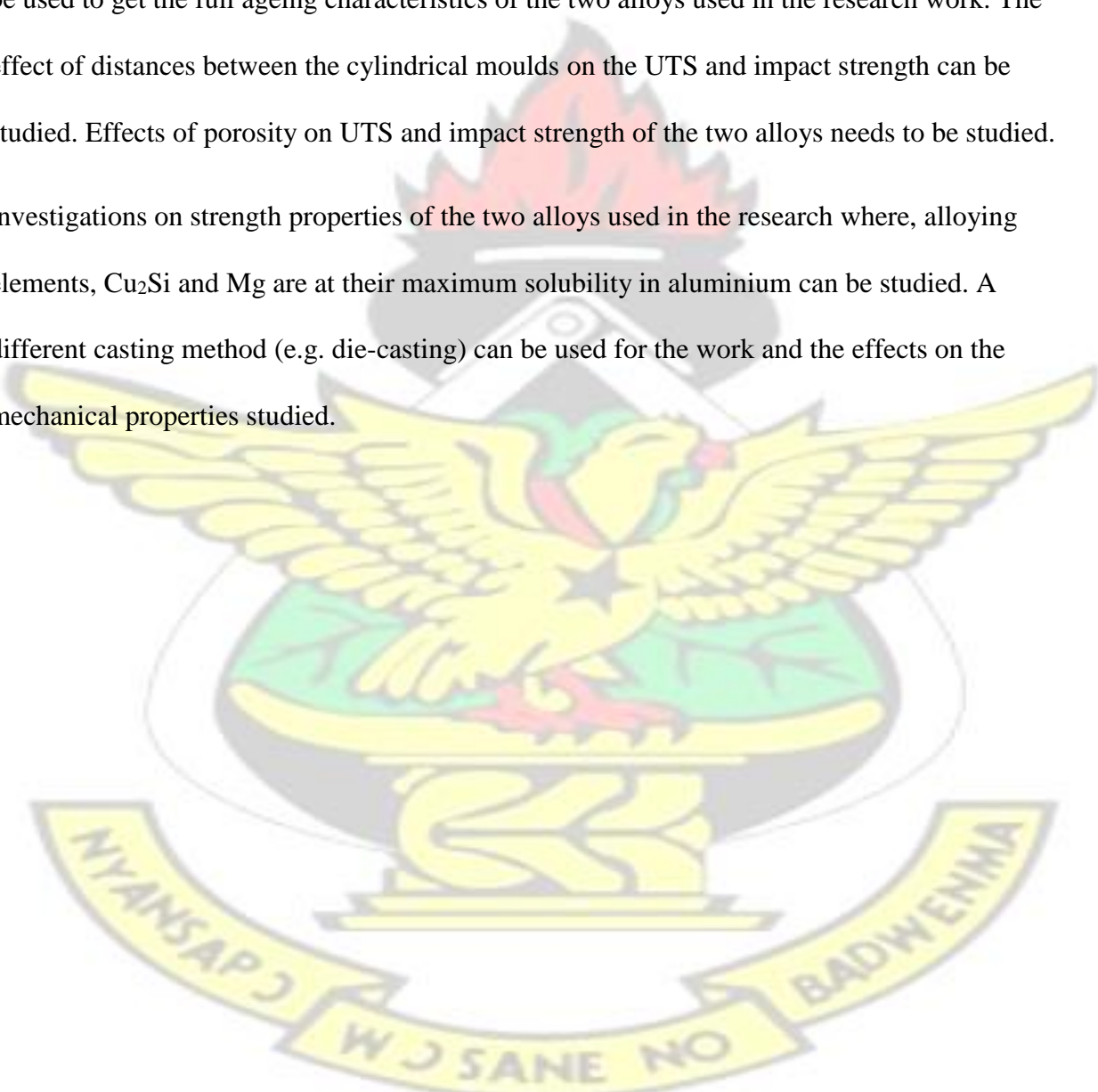
Effects of heat treatment on locally produced sand cast Al-14%-Si-0.288Mg and Al14%Si-2.688Cu has been conducted and the tensile, percentage elongation and impact strengths were measured and correlated to the microstructures. The following conclusions have been made from the research. Al-Si-Mg alloys respond very well to heat treatment more than Al-Si-Cu alloys. Rising temperature increases both rate of precipitation and the Ultimate tensile strength (UTS) of Al-Si-Cu and Al-Si-Mg alloys. The time taken to attain the highest strength was longer for Al-Si alloy containing copper, than Al-Si alloy containing magnesium. The lesser the aging temperature, the more the time needed to attain highest strength and the elevated the temperature the smaller the time needed to attain highest strength.). Lower temperature in artificial aging of Al-Si alloy containing copper produced UTS values at longer times. The ultimate tensile strength (UTS) recorded for both alloys were within the European standards for sand and chill cast aluminium alloys (ISO Al Si7Mg, ISO Al Si10Mg and ISO Al Si12Cu in the T6 conditions are 260, 260 and 170 MPa) respectively.

Some limitations encountered during the research were, erratic power supply in the country posed a big challenge during the heat treatment phase of the project. Secondly, the tensile machine at Standards Authority could not directly determine some key mechanical properties such yield strength and elastic modulus.

5.2 RECOMMENDATIONS

Other mechanical properties useful for automobile applications that may be measured are hardness, wear resistance and fatigue. The effects of dendritic arm spacing on the UTS and impact strength on the two alloys used in this study can be studied. Longer ageing times need to be used to get the full ageing characteristics of the two alloys used in the research work. The effect of distances between the cylindrical moulds on the UTS and impact strength can be studied. Effects of porosity on UTS and impact strength of the two alloys needs to be studied.

Investigations on strength properties of the two alloys used in the research where, alloying elements, Cu_2Si and Mg are at their maximum solubility in aluminium can be studied. A different casting method (e.g. die-casting) can be used for the work and the effects on the mechanical properties studied.



REFERENCES

- Abdulwahab, M., Madugu, I. A., Yaro, S. A., Hassan, S. B., and Popoola, A. P. I. (2011). Effects of multiple-step thermal ageing treatment on the hardness characteristics of A356.0-type AlSi-Mg alloy. *Materials and Design*, 32(3), 1159–1166.
<http://doi.org/10.1016/j.matdes.2010.10.028>
- Jones, D. R., and Ashby, M. F. (2005). *Engineering materials 2: an introduction to microstructures, processing and design*. Butterworth-Heinemann, 100-112
- Askeland, D. R., and Wright, W. J. (2009). *Essentials of materials science & engineering*. Cengage Learning, 225-438
- Basavakumar, K., Mukunda, P., and Chakraborty, M. (2008a). Impact toughness in Al–12Si and Al–12Si–3Cu cast alloys – Part 1: effect of process variables and microstructure. *International Journal of Impact Engineering*, 35, 199–205.
- Basavakumar, K., Mukunda, P., and Chakraborty, M. (2008b). Influence of grain refinement and modification on microstructure and mechanical properties of Al–7Si and Al–7Si–2.5Cu cast alloys. *Materials Characterization*, 59, 283–9.
- Bogdanoff, T., and Dahlström, J. (2009). *The influence of copper on an Al-Si-Mg alloy (A356) - Microstructure and mechanical properties The influence of Copper on an Al-Si-Mg alloy (A356) – Microstructure and Mechanical properties*. Jönköping University.
- Brown, J. R. (1999). *Non-Ferrous Foundryman's Handbook*. Butterworth-Heinemann, 23-45
- Callister, W. D., and Rethwisch, D. G. (2009). *Materials Science and Engineering: An Introduction*, 198-213
- Elahetia, S. M. (2013). *Effect of Short Cycle Heat Treatment and Cooling Rate on Microstructure and Mechanical Properties of Recycled Aluminium Sand Casting*.
- European Aluminium Association. (2002). Manufacturing – Casting methods. In *The Aluminium Automotive Manual*. Brickwall 1-20
- Fatai Olufemi, A. (2012). Ageing Characteristics of Sand Cast Al-Mg-Si (6063) Alloy. *International Journal of Metallurgical Engineering*, 1(6), 126–129.
<http://doi.org/10.5923/j.ijmee.20120106.06>

Groover, M.P. (2010). *Fundamental of Modern Manufacturing; Material, Processes and Systems*,225-237

Han, Y., Samuel, A. M., Doty, H. W., Valtierra, S., and Samuel, F. H. (2014). Optimizing the tensile properties of Al – Si – Cu – Mg 319-type alloys : Role of solution heat treatment.

Journal of Materials and Design,58(2014), 426–438.
<http://doi.org/10.1016/j.matdes.2014.01.060>

Hull, D., and Bacon, D. J. (2001). *Introduction to dislocations*. Butterworth-Heinemann.219-220

Hurtalová, L., Belan, J., Tillová, E., and Chalupová, M. (2012). Changes in structural characteristics of hypoeutectic Al-Si cast alloy after age hardening. *Medziagotyra*, 18(3), 228–233. <http://doi.org/10.5755/j01.ms.18.3.2430>

Ishak, M., Amir, a, and Hadi, a. (2013). Effect of Solution Treatment Temperature on Microstructure and Mechanical Properties of a356 Alloy, (July), 1–3.

Kaufman, J. G. (2000). *Introduction to Aluminium Alloys and Tempers*. ASM International,10-76

Kaufman, J. G., and Rooy, E. L. (2004). *Aluminum Alloy Castings: Properties, Processes, and Applications*. Retrieved from
<http://books.google.com/books?id=JM0u1vwrS5UC&pgis=1,1-6>

Ma, Z., Samuel, E., Mohamed, a. M. a, Samuel, a. M., Samuel, F. H., and Doty, H. W. (2010). Influence of aging treatments and alloying additives on the hardness of Al-11Si-2.5Cu-Mg alloys. *Materials and Design*, 31(8), 3791–3803.
<http://doi.org/10.1016/j.matdes.2010.03.026>

Mohamed, A. M. A., and Samuel, F. H. (2012). A review on the heat treatment of Al-Si-Cu/Mg casting alloys. *Heat Treatment: Conventional and Novel Applications; InTech: Rijeka, Croatia*.

Paray, F., Kulunk, B., and Gruzleski, J. (2000). Impact properties of Al–Si foundry alloys. *International Journal of Cast Metals Research*, 13, 17–37.

Prillhofer, R., Rank, G., Berneder, J., Antrekowitsch, H., Uggowitzner, P. J., and Pogatscher, S. (2014). Property criteria for automotive Al-Mg-Si sheet alloys. *Materials*, 7(7), 5047–5068.
<http://doi.org/10.3390/ma7075047>

Rodríguez, A., Torres, R., Talamantes-Silva, J., Velasco, E., Valtierra, S., and Colás, R. (2012).

Metallographic study of a cast Al-Si-Cu alloy by means of a novel etchant. *Materials Characterization*, 68, 110–116. <http://doi.org/10.1016/j.matchar.2012.03.012>

Seifeddine, S. (2006). Characteristics of cast aluminium-silicon alloys – Microstructures and mechanical properties.

Sjölander, E., and Seifeddine, S. (2010). The heat treatment of Al–Si–Cu–Mg casting alloys. *Journal of Materials Processing Technology*, 210(10), 1249–1259. <http://doi.org/10.1016/j.jmatprotec.2010.03.020>

Taylor, J. A., St John, D. H., Barresi, J., and Couper, M. J. (2000). An empirical analysis of trends in mechanical properties of T6 heat treated Al-Si-Mg casting alloys. *International Journal of Cast Metals Research*, 12(6), 419–430.

Zhang, D. L. (2002). Effect of a short solution treatment time on microstructure and mechanical properties of modified Al – 7wt .% Si – 0 . 3wt .% Mg alloy. *Journal of Light Metals*, 2, 27–36.



APPENDICES

Appendix A

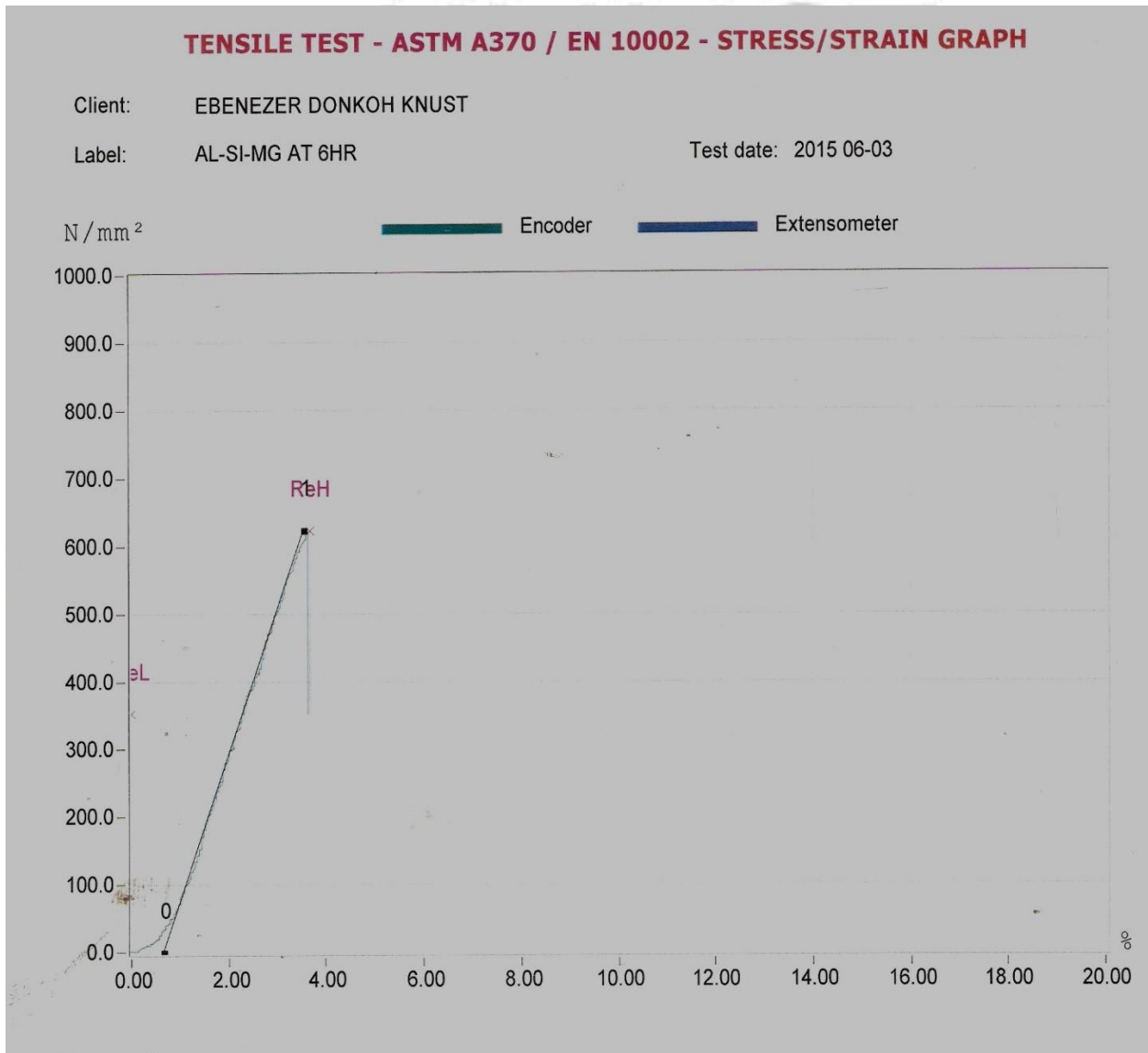


Figure 1 stress-strain curve for Al-Si-Mg alloy artificially aged for 6 hours at 170°C

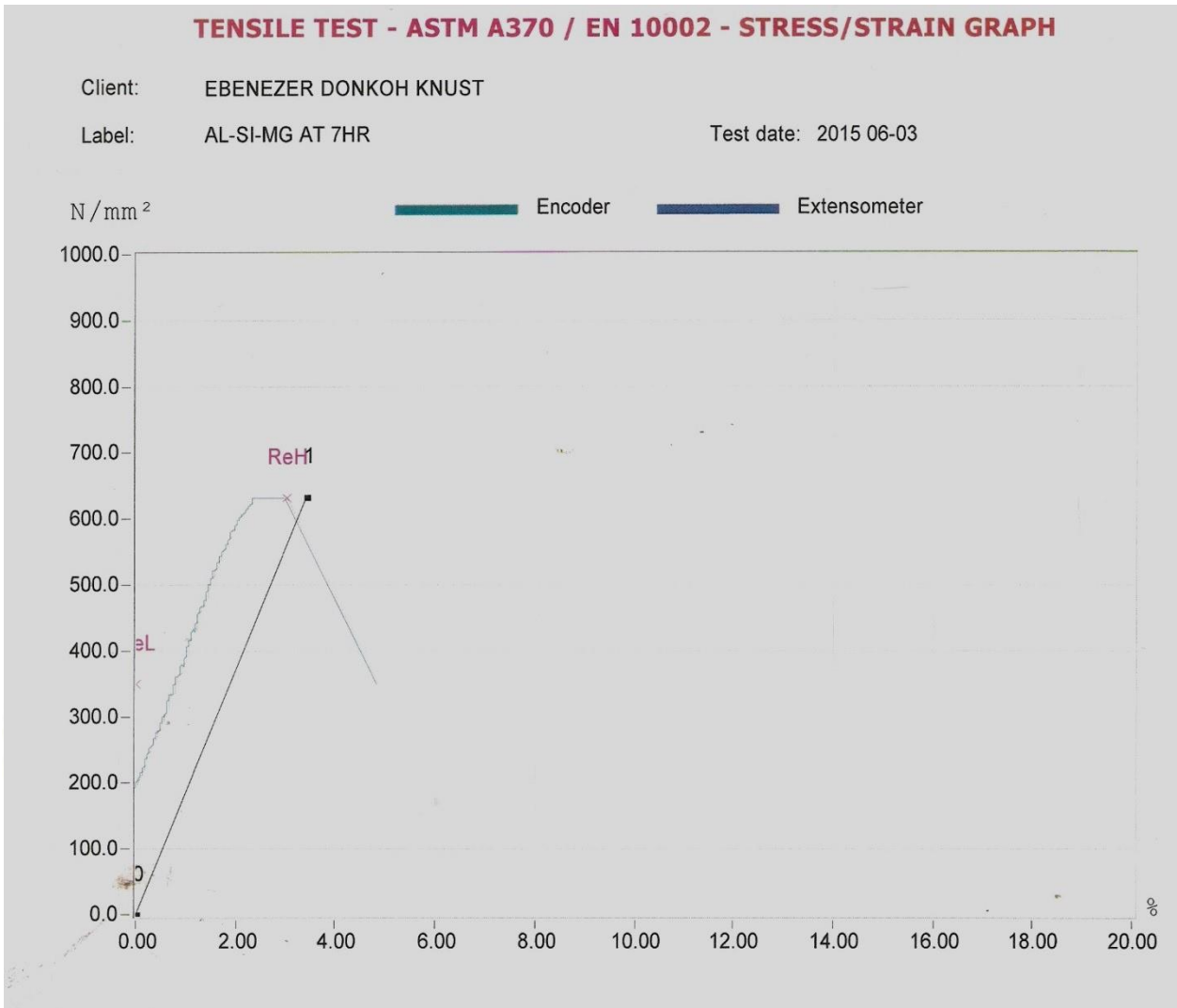


Figure 2 Stress-strain curve for Al-Si-Mg alloy artificially aged for 7 hours at 170°C



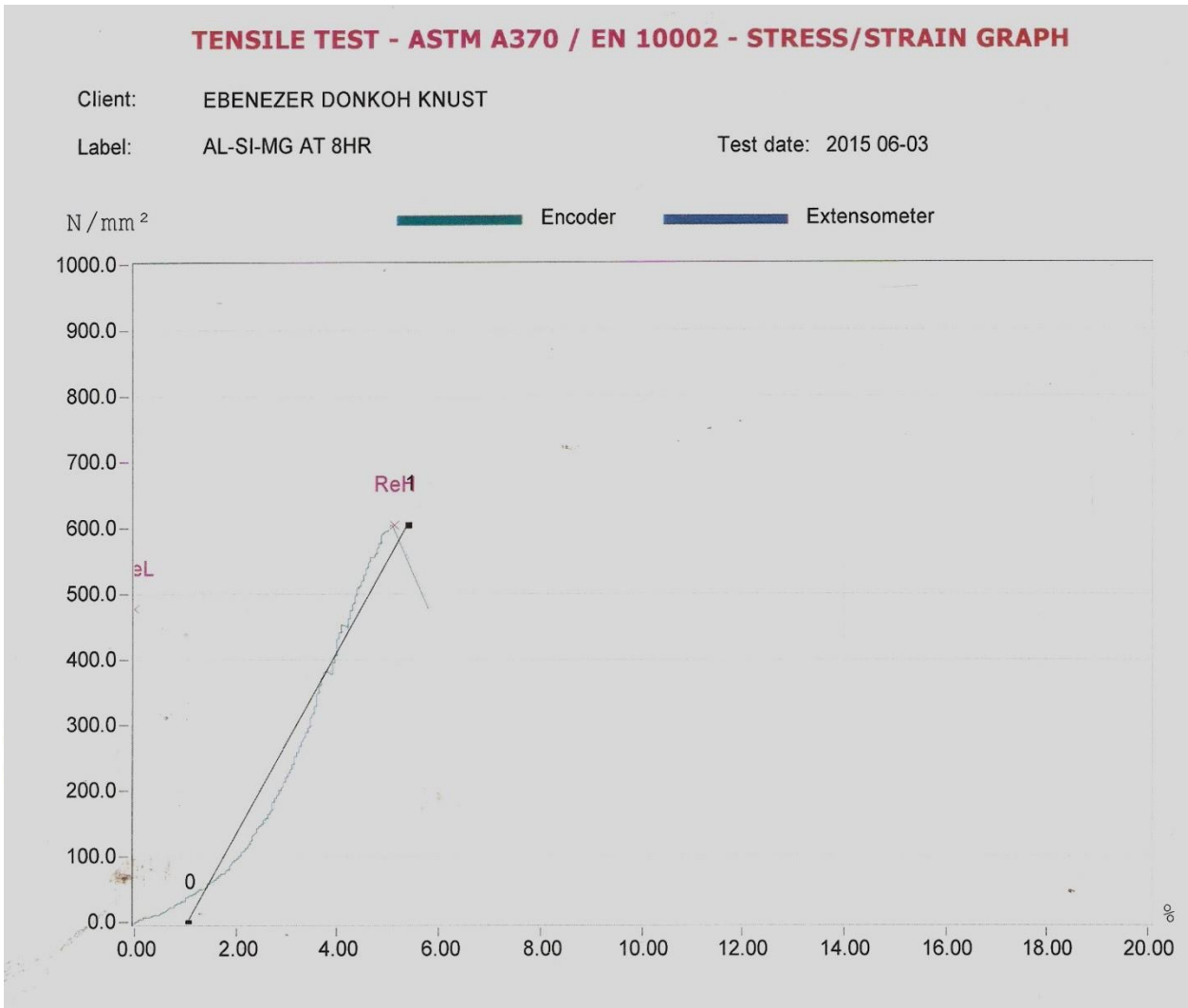


Figure 3 Stress-strain curve for Al-Si-Mg alloy artificially aged for 8 hours at 170°C



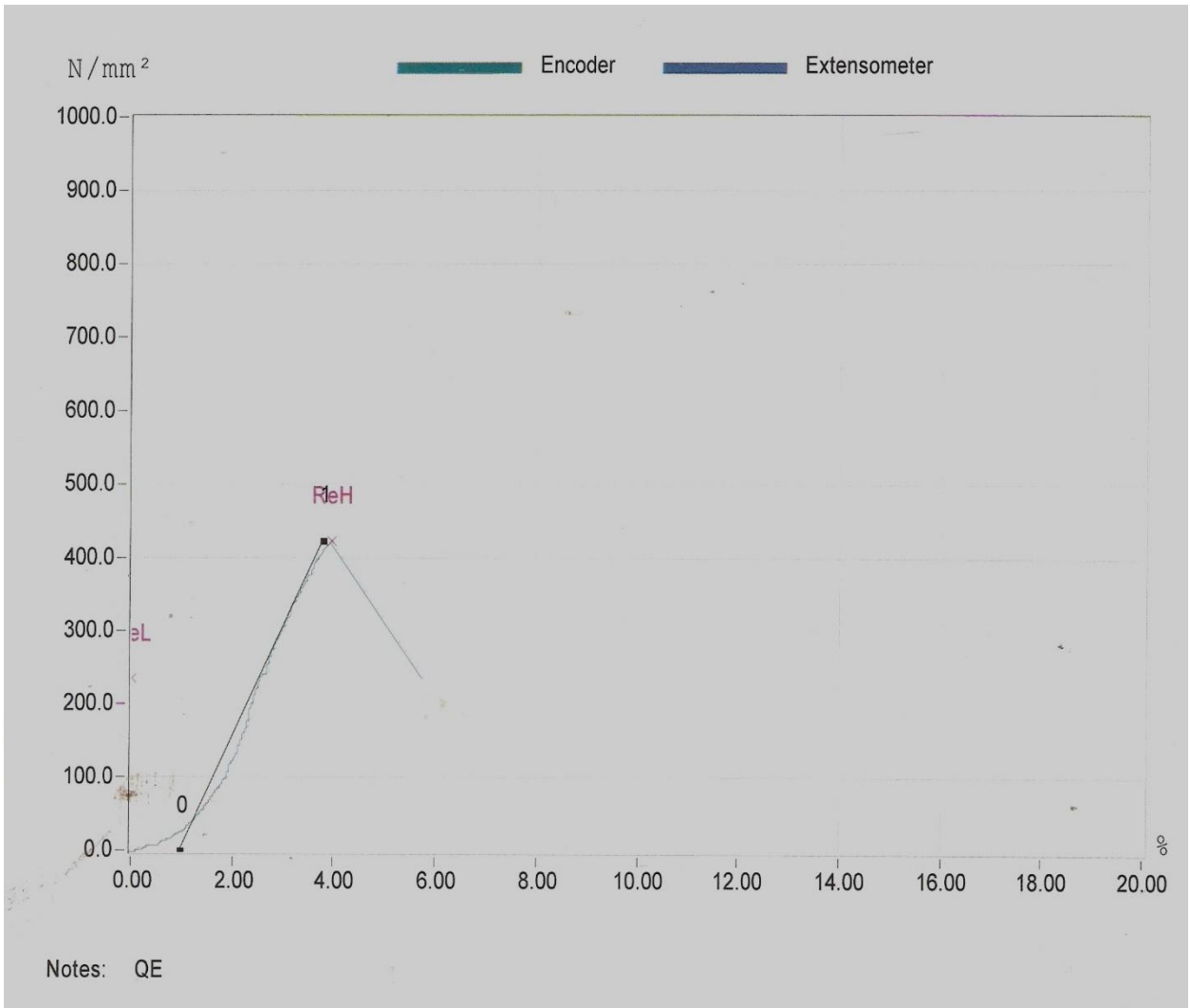


Figure 4 Stress-strain curve for Al-Si-Mg alloy artificially aged for 5 hours at 160°C



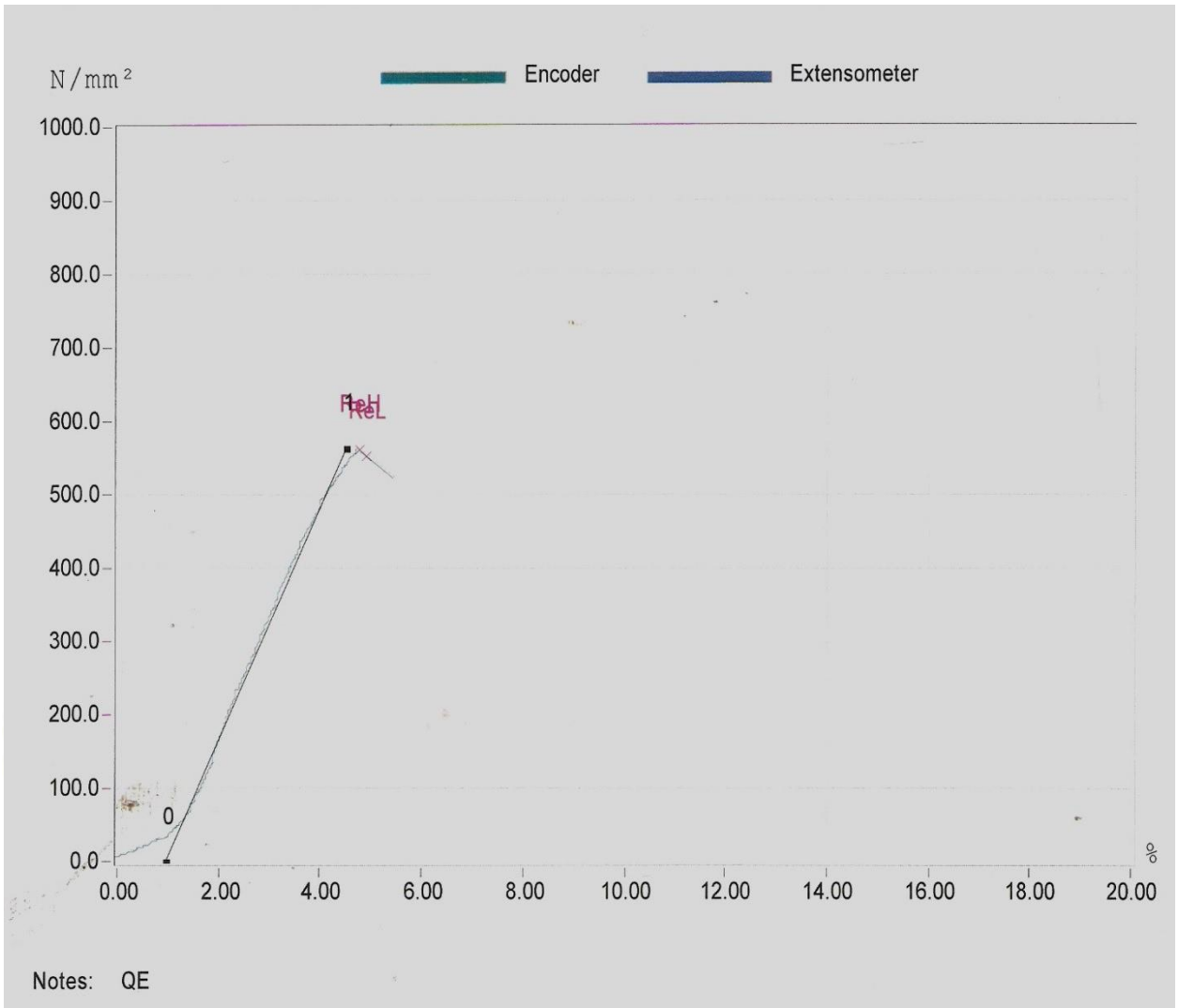


Figure 5 Stress-strain curve for Al-Si-Mg alloy artificially aged for 6 hours at 160°C



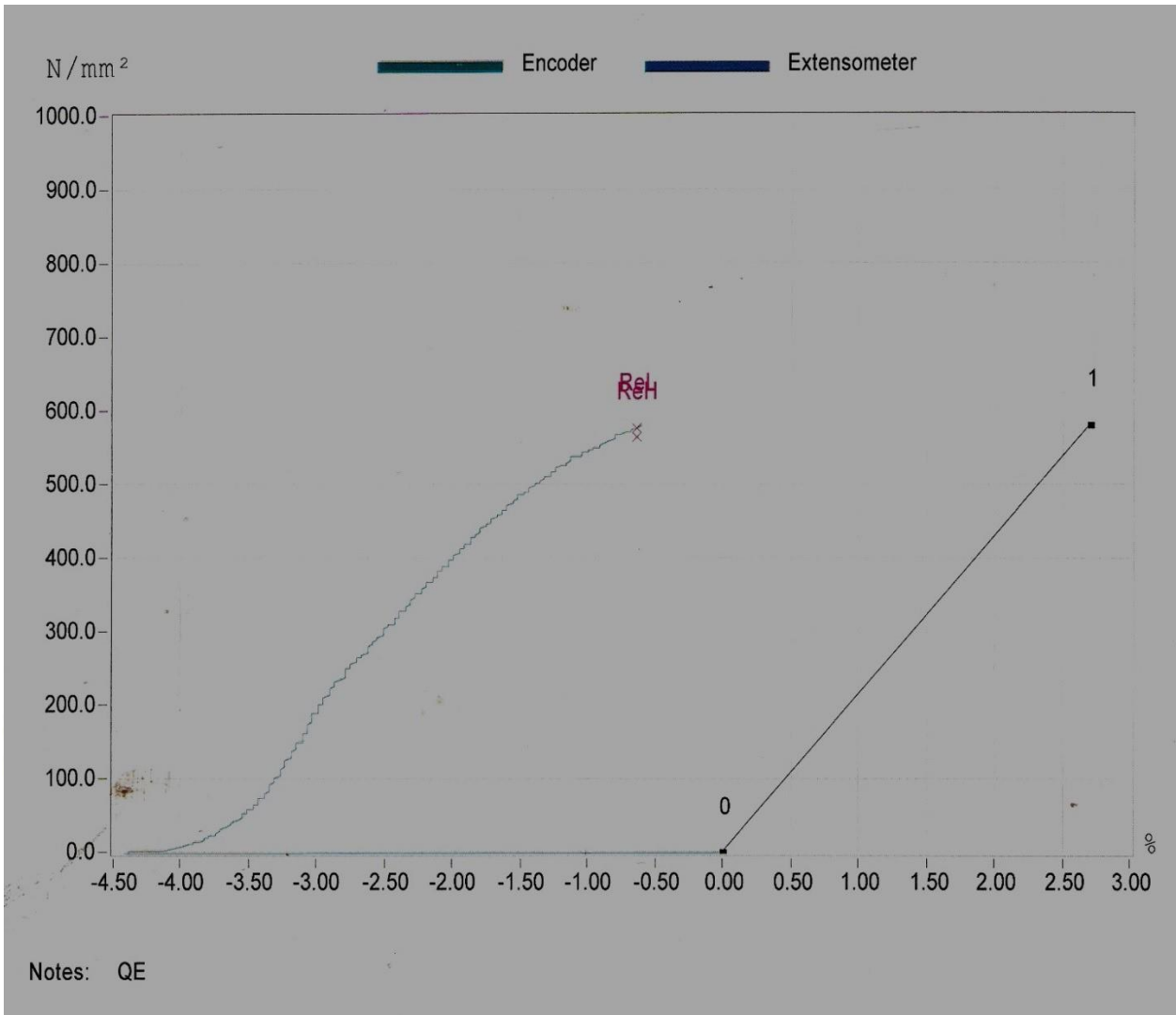
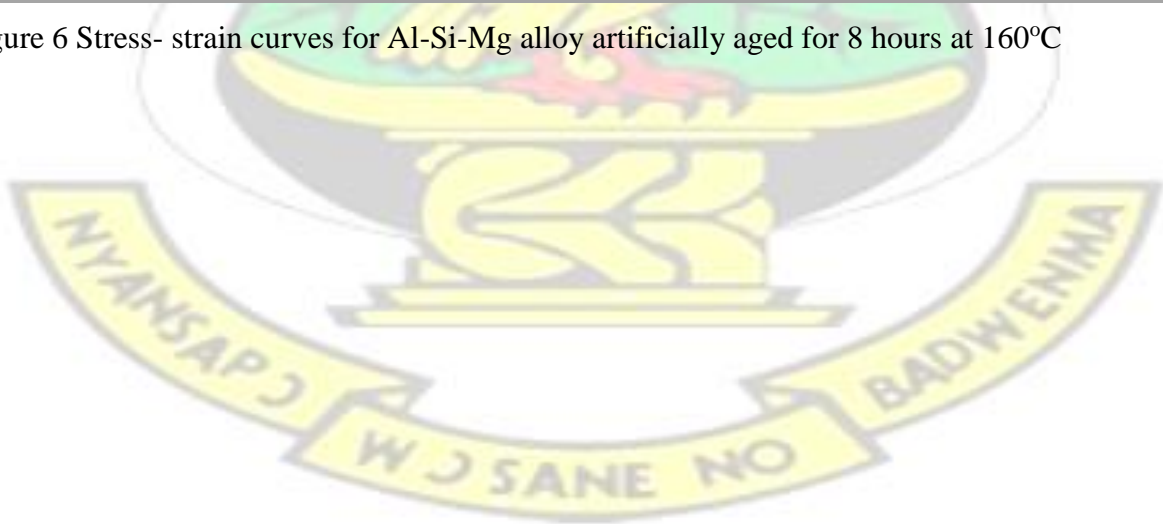


Figure 6 Stress- strain curves for Al-Si-Mg alloy artificially aged for 8 hours at 160°C



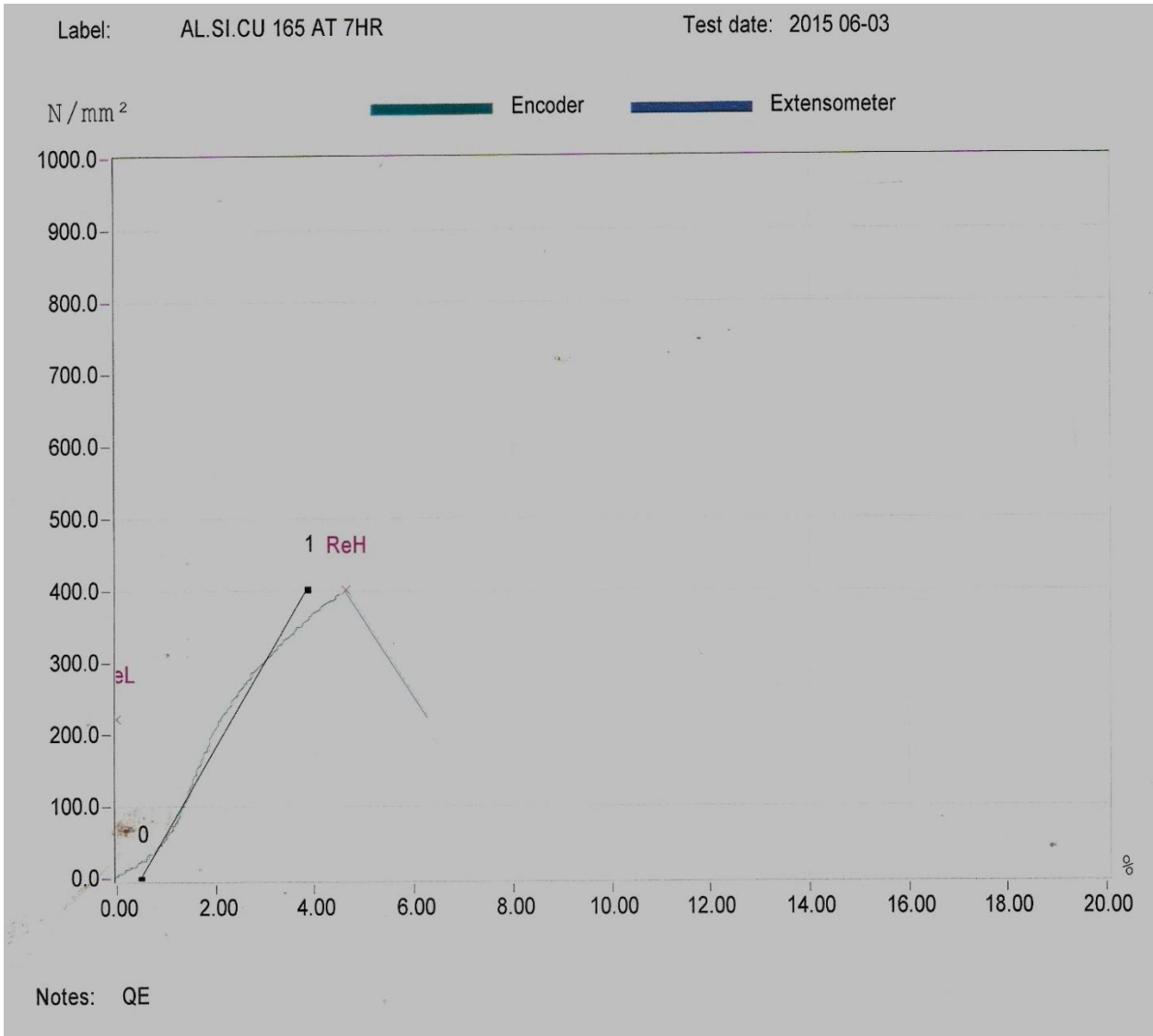
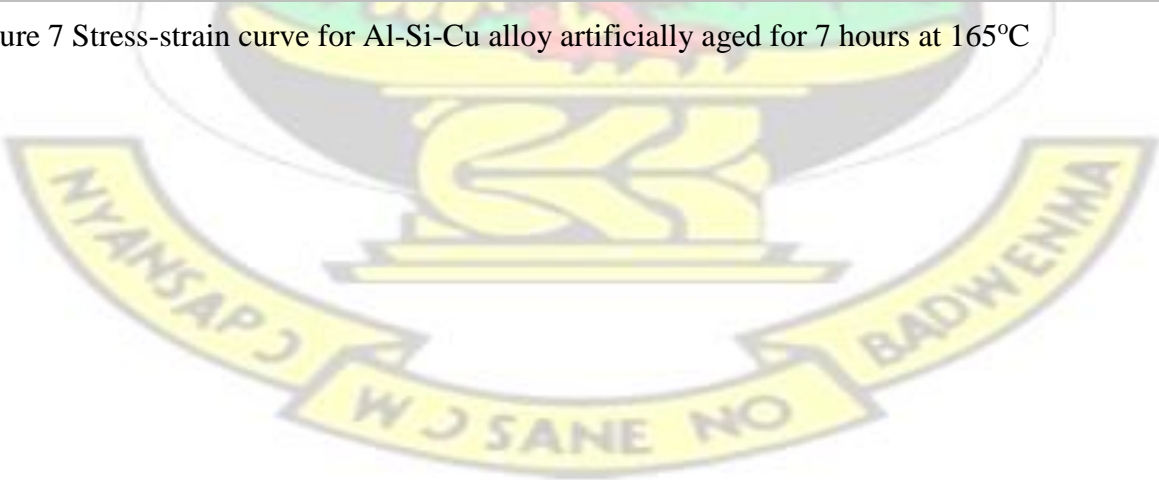


Figure 7 Stress-strain curve for Al-Si-Cu alloy artificially aged for 7 hours at 165°C



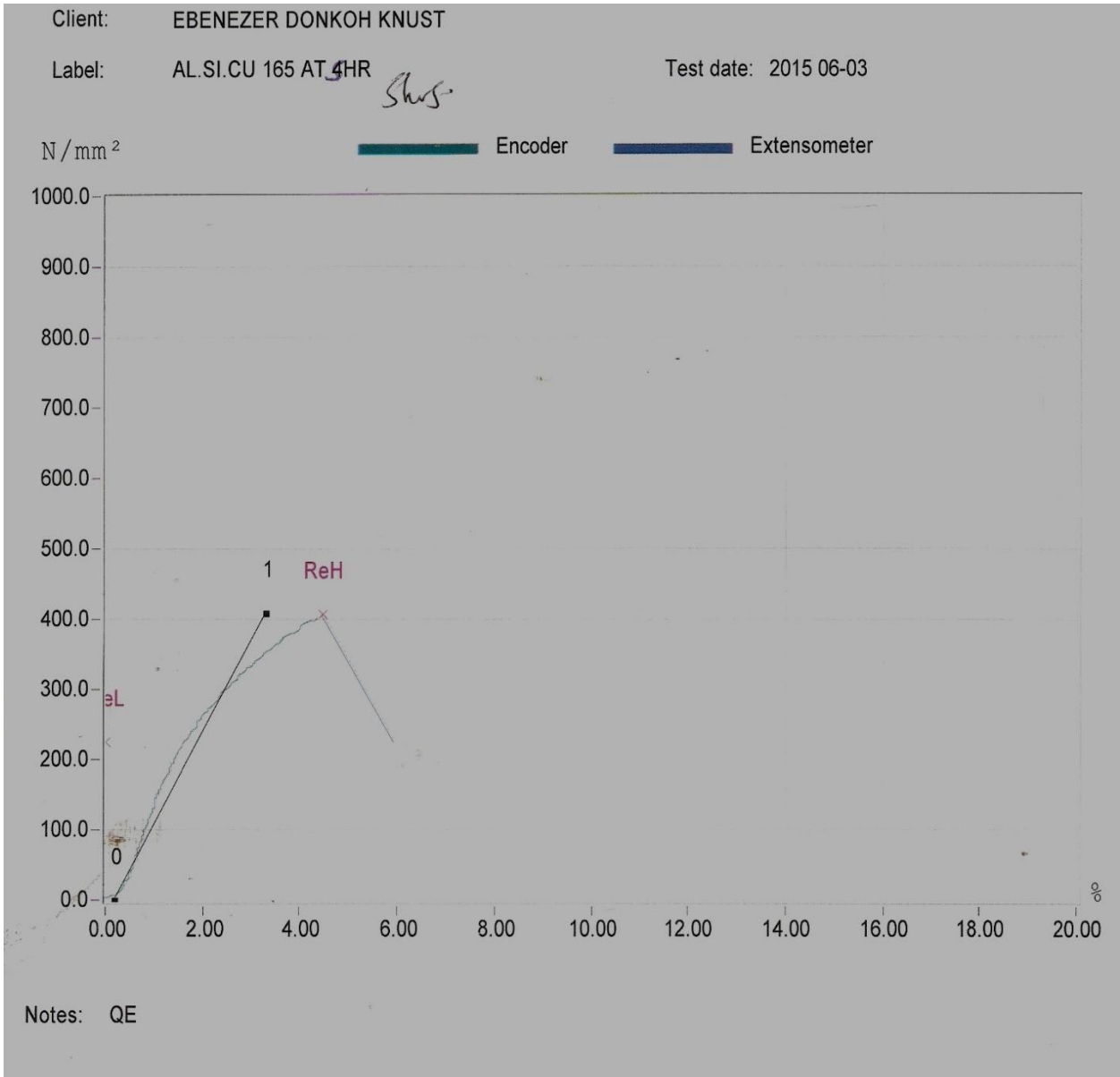
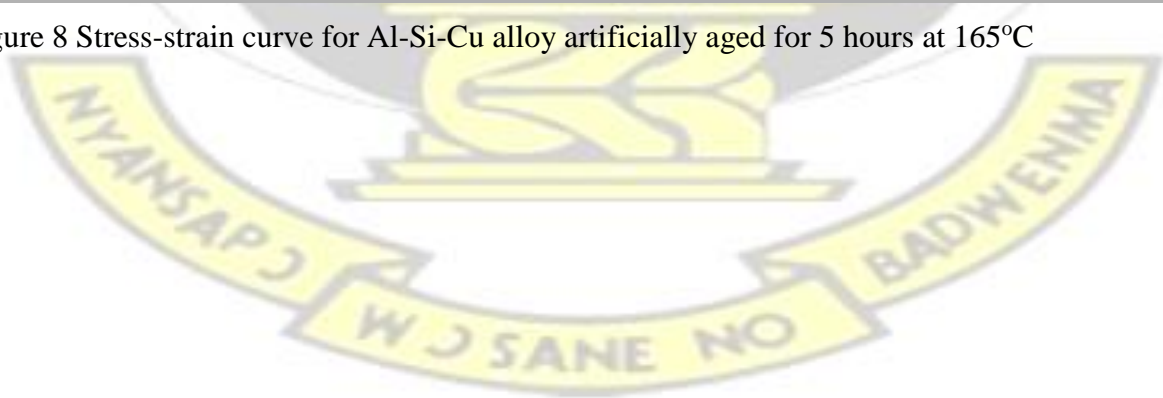


Figure 8 Stress-strain curve for Al-Si-Cu alloy artificially aged for 5 hours at 165°C



TENSILE TEST - ASTM A370 / EN 10002 - STRESS/STRAIN GRAPH

Client: EBENEZER DONKOH KNUST

Label: AL.SI.CU 165 AT 3HR

Test date: 2015 06-03

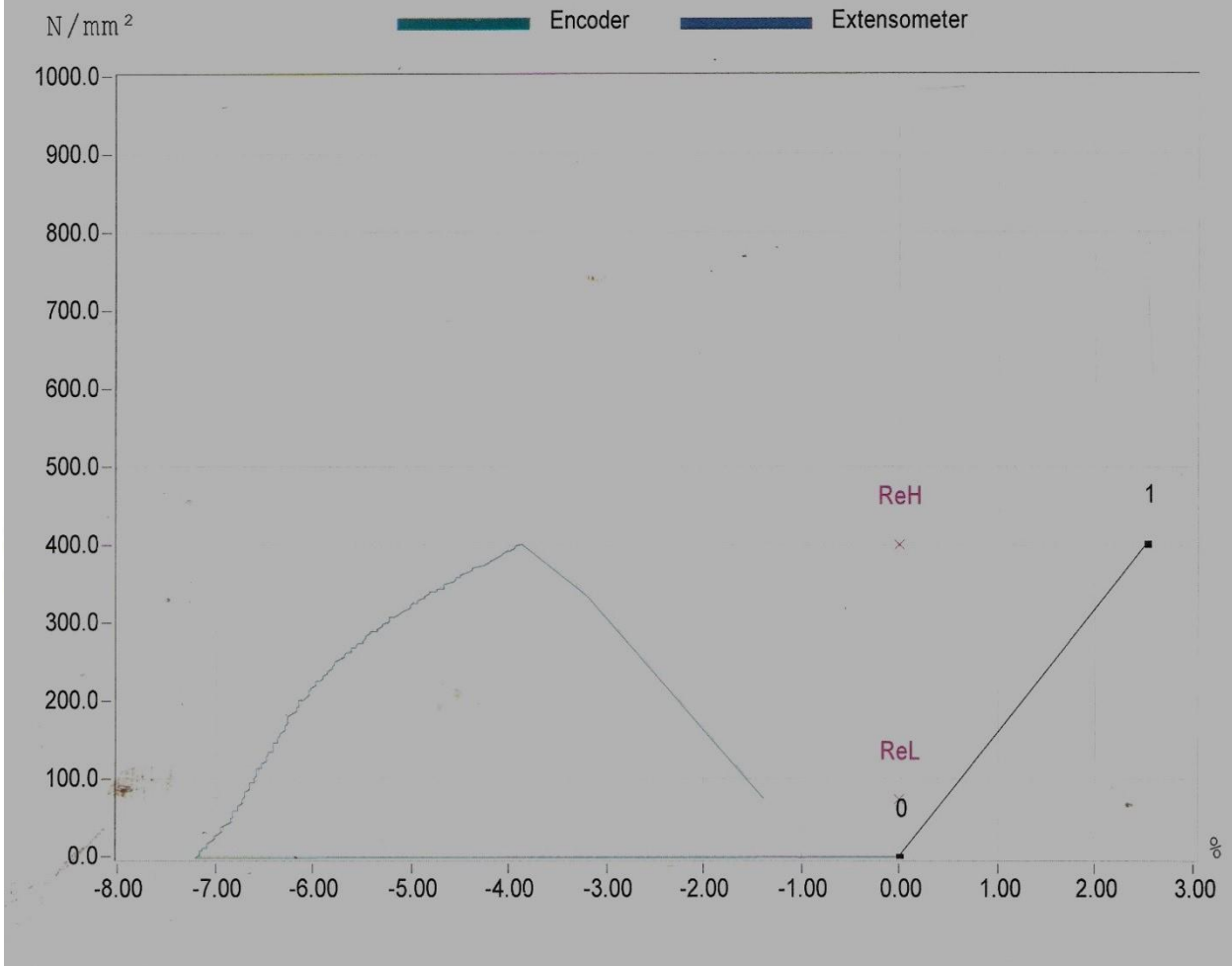


Figure 9 Stress-strain curve for Al-Si-Cu alloy artificially aged for 3 hours at 165°C

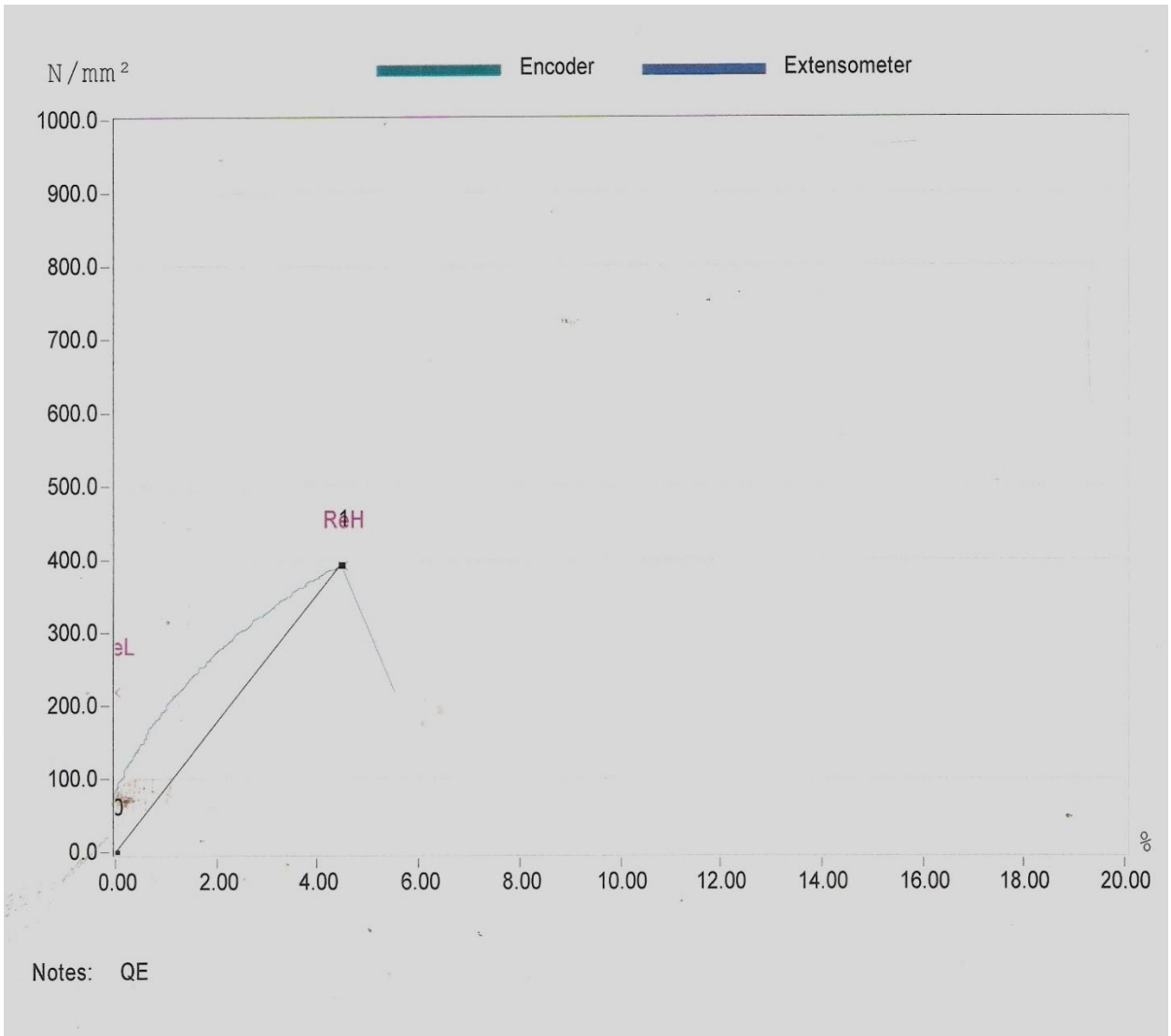


Figure 10 Stress-strain curve for Al-Si-Cu alloy artificially aged for 3 hours at 155°C



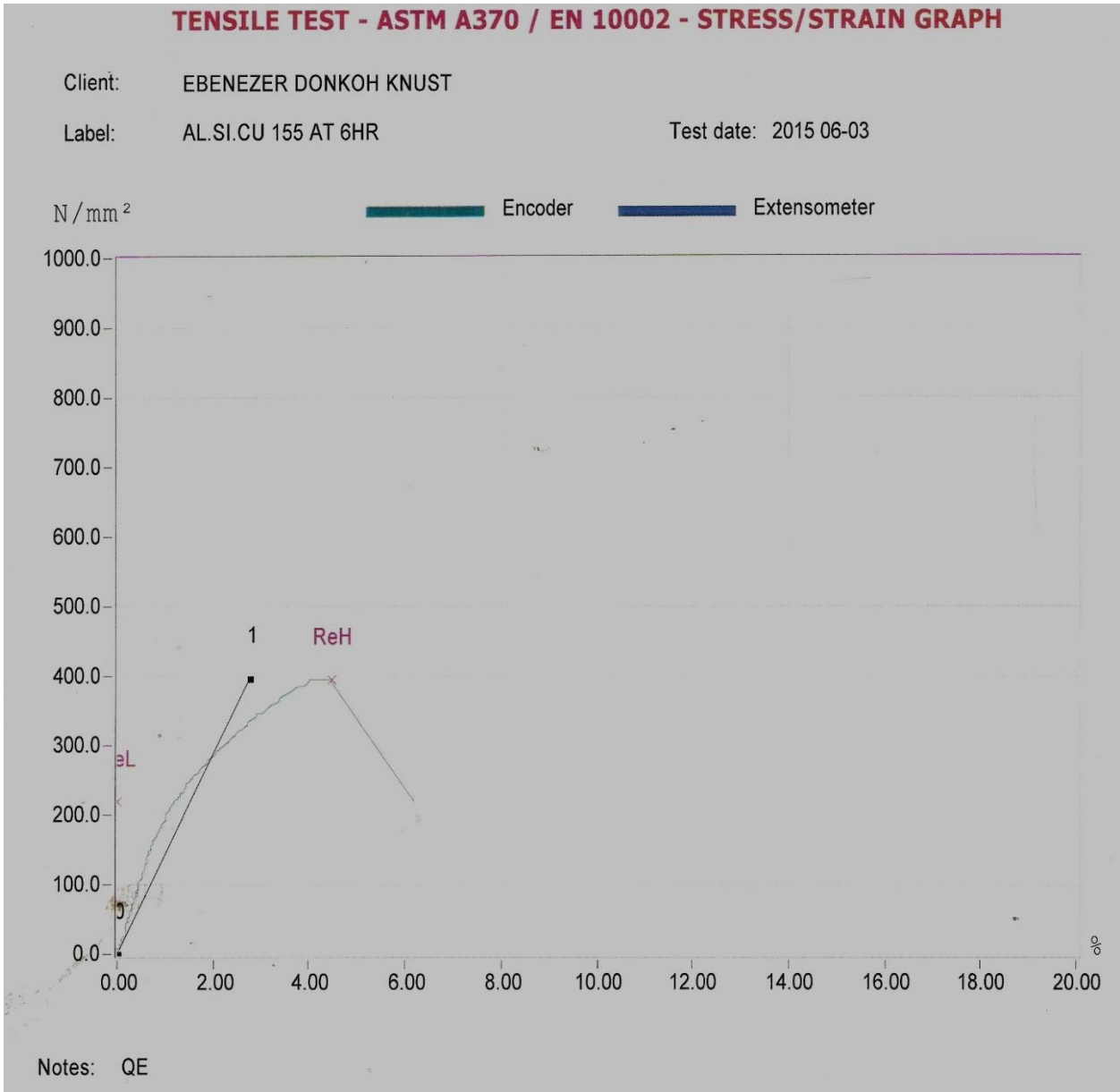
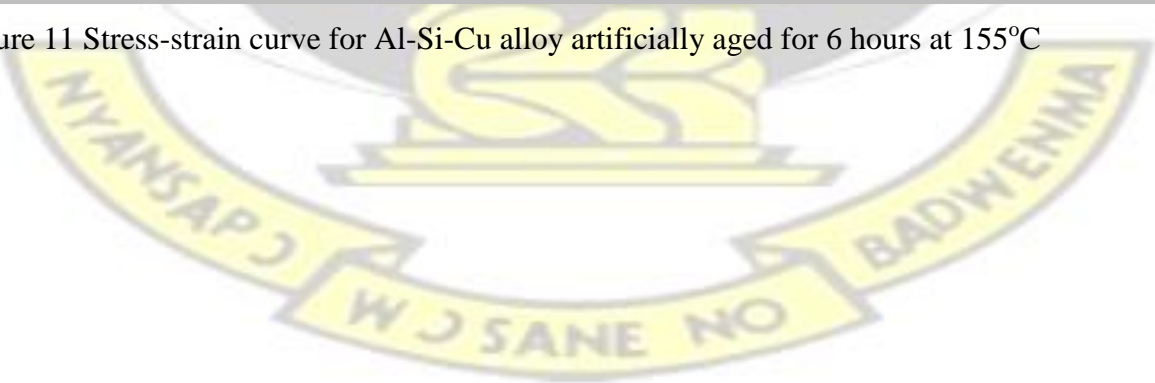


Figure 11 Stress-strain curve for Al-Si-Cu alloy artificially aged for 6 hours at 155°C



Appendix B
Pictures of Fractured Surfaces



(a)



(b)

Figure 12 (a) and (b) shows fractured surfaces of Al-Si-Mg and Al-Si-Cu samples



(c)



Appendix C

Error Analysis

The error in the ultimate tensile strength, impact strength and percentage elongation was calculated by using an in built formula in Microsoft excel. It first calculates the standard deviation followed by the standard error. Data for the error calculations were exported into excel to be used by the inbuilt formula. The inbuilt formula is

$$\sigma = \sqrt{\frac{1}{N} \sum_{i=1}^N (x_i - \bar{x})^2},$$

Where x_1, \dots, x_N are the N elements in the data set having a mean of \bar{x} .

The error, s, was calculated by the formula

$$s = \sigma/\sqrt{N}$$

